1987

A Study of the Temperature Dependence of Ion-Molecule Association Reactions. Halide Ion Addition to a Selected Group of Lewis Acids.

Charles Ray Herd
Louisiana State University and Agricultural & Mechanical College

Order Number 8719867

A study of the temperature dependence of ion-molecule association reactions. Halide ion addition to a selected group of Lewis acids

Herd, Charles Ray, Ph.D.

The Louisiana State University and Agricultural and Mechanical Col., 1987

U·M·I
300 N. Zeeb Rd.
Ann Arbor, MI 48106

PLEASE NOTE:

In all cases this material has been filmed in the best possible way from the available copy. Problems encountered with this document have been identified here with a check mark __✓__.

1. Glossy photographs or pages _____
2. Colored illustrations, paper or print _____
3. Photographs with dark background _____
4. Illustrations are poor copy _____
5. Pages with black marks, not original copy _____
6. Print shows through as there is text on both sides of page _____
7. Indistinct, broken or small print on several pages __✓__
8. Print exceeds margin requirements _____
9. Tightly bound copy with print lost in spine _____
10. Computer printout pages with indistinct print _____
11. Page(s) _____ lacking when material received, and not available from school or author.
12. Page(s) _____ seem to be missing in numbering only as text follows.
13. Two pages numbered _____. Text follows.
14. Curling and wrinkled pages _____
15. Dissertation contains pages with print at a slant, filmed as received _____
16. Other _____

_____

_____

University
Microfilms
International

A STUDY OF THE TEMPERATURE DEPENDENCE OF ION-MOLECULE ASSOCIATION REACTIONS. HALIDE ION ADDITION TO A SELECTED GROUP OF LEWIS ACIDS.

A Dissertation

Submitted to the Graduate Faculty of the
Louisiana State University and
Agricultural and Mechanical College
in partial fulfillment of the
requirements for the degree of
Doctor of Philosophy

in

The Department of Chemistry

by
Charles R. Herd
B. S., Louisiana State University of Shreveport, 1982
May 1987

ACKNOWLEDGEMENTS

I would first like to thank my major advisor, Dr. Lucia M. Babcock for her guidance throughout my graduate career and for her contributions to this research effort. Her eye for detail and knowledge of the scientific field have been invaluable in my education as a graduate student.

Certainly the people at the Air Force Geophysics Laboratory (AFGL), John Paulson, Al Viggiano, and Fred Dale deserve credit for the success of this research effort. Use of their facilities at AFGL along with their contributions and hospitality during our stay there are greatly appreciated.

Wolf Bergmann, Tim Fillingam, and Bill Taylor deserve mention as their friendship has made this experience more than simply academic. Gwendolyn Givens, my fiancee', has provided me with support and love during my last two years here at LSU for which I am very appreciative and greatly indebted. My parents, Ray and Elinor Herd, deserve most of the credit as their love and support and dedication to achievement of an education have made this all possible.

Finally I would like to thank Universal Energy Systems and the Air Force Office of Scientific Research for their sponsorship and support of the Graduate Student Summer Support Program. I would also like to thank the LSU Center for Energy Studies for their financial support for part of my graduate career.

TABLE OF CONTENTS

LIST OF TABLES

LIST OF FIGURES

ABSTRACT

Recent evidence has indicated that the ion-molecule association reaction $BF_3 + F^- \longrightarrow BF_4^-$ has both collisional stabilization and radiative stabilization pathways. Preliminary studies indicated that other boron trihalide systems ($BF_3 + Cl^-$, Br^-, and $BCl_3 + Cl^-$,Br^-) behave similarly. We have studied the temperature dependence of these systems in an effort to learn more about the individual rate coefficients that constitute the standard association mechanism modified to include a radiative stabilization pathway. In order to determine properties of a system which play an important role in the opening of a radiative stabilization channel, we extended our studies to include other halogen ion-Lewis acid addition reactions: $SiF_4 + F^-$, Cl^-, and Br^-; and $SF_4 + F^-$, Cl^-, and Br^-. These allow us to assess the role of number of degrees of freedom, exoergicity, and complex lifetime in influencing the association rate. These systems were studied using a selected-ion flow tube (SIFT) in the temperature region 219 to 408 K for pressures in the region 0.2 to 0.9 torr. Our results yield overall rates which have a negative dependence upon temperature ($k_{obs} = AT^{-n}$). This temperature dependence is consistent with a theoretical model in which rotation and vibration are included for calculation of n, the magnitude of the temperature dependence. The magnitude of n ranges from

1.8 for the $BF_3 + F^-$ system to 3.3 for the $SiF_4 + Cl^-$ system. In addition all of the boron systems radiate with the possible exception of $BF_3 + Br^-$ where the unimolecular decomposition back to reactants is very fast. The SiF_4 and SF_4 systems appear not to possess a radiative stabilization pathway.

CHAPTER 1

INTRODUCTION

The general field of ion-neutral reactions or ion-molecule reactions as it is better known, has experienced tremendous growth throughout the last twenty-five years, with investigators all over the world conducting research in the various areas which comprise the field of ion-molecule reactions. Research on cluster ions in the solid, liquid and gas phase is important in such areas as surface development, solvation effects, combustion processes, biochemistry, atmospheric and interstellar chemistry, along with such fundamental processes as energy transfer and redistribution.[1] All of the work contained in this dissertation pertains to gas phase ion-molecule reactions, or, more specifically, to the large subfield of gas phase ion-molecule association reactions. The generally accepted mechanism for gas phase ion-molecule association reactions, which will be discussed in detail later, is one in which the exchange of energy plays an important role. Thus, this study is one of energy transfer and redistribution and has important implications in the field of study of ion-molecule association reactions occurring in the interstellar medium.

A large portion of study in the field of ion-molecule (IM) association reactions is devoted to IM processes occurring in the interstellar medium, the earth's atmosphere, and other planetary atmospheres. The great need for quan-

titative rate coefficients of IM processes occurring in our atmosphere for the purposes of modeling, lead to the development of the very successful flowing afterglow (FA) technique by Ferguson, Fehsenfeld, and Schmeltekopf.[2] The FA is a fast flow gas reactor which operates at thermal energies in the range 0.01 to 0.08 eV (80 to 600 K). This one technique has been largely responsible for allowing the accumulation of a large amount of data on gas phase IM association reactions. Modifications of the FA technique such as the variable temperature FA (VT-FA), along with variations of the FA technique such as the selected-ion flow tube (SIFT) and the variable temperature SIFT (VT-SIFT) invented by Adams and Smith[3], have allowed researchers to gain a more thorough and detailed understanding of IM processes. Both FA and VT-SIFT instruments (experimental section for descriptions) were used to collect data on the IM systems studied for this dissertation.

The work contained herein was suggested by an initial FA study done by Babcock and Streit[4] in 1984. They chose to study the third-body effects on halide ion (F^- and Cl^-) addition to two different Lewis acids, BF_3 and BCl_3. These Lewis acids are trigonal planar in structure and add anions to form the tetrahedral anion complex shown below:

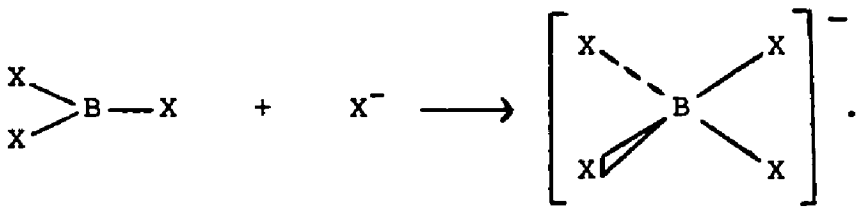

(1.1)

For some of the systems, evidence seemed to indicate the presence of a radiative stabilization pathway which is seldom seen in IM systems, although its presence has been inferred for several IM systems in the interstellar medium.[5] Therefore we chose to investigate these systems further and to extend the work to include new systems by studying the temperature and pressure dependence of halide ion addition to a selected group of Lewis acids. The halide ions implemented in this study were F^-, Cl^-, and Br^-, and the neutral systems implemented were BF_3, BCl_3, SiF_4, and SF_4. The goals in investigating the temperature and pressure dependence of these systems were threefold:

(1) to obtain information on the temperature dependence (TD) of these systems and on IM reactions in general, since the TD of IM association reactions generally behaves oppositely from that of neutral-neutral systems (i.e. the overall rate coefficient, k_{obs}, increases as temperature decreases), and is an area of much experimental and theoretical investigation;

(2) to study several different Lewis acids in order to determine what properties of a system, such as bond strength and number and magnitude of internal degrees of freedom, must be present for a system to be able to stabilize radiatively;

(3) lastly, to obtain information on the individual rates that contribute to the mechanism of our systems, which allows us to determine such parameters as the unimolecular

rate coefficient, k_d, the radiative rate coefficient, k_r (if present), and to determine what type (i.e. infrared or electronic) of radiative transition is occurring.

In order to be able to evaluate our data to achieve the above listed goals, an overview of the physical nature of IM reactions, along with mechanistic behavior, and the pressure and temperature dependent behavior in IM processes must be considered. A general discussion of each of these topics follows.

I. IM Collision Theory

Gas phase IM reactions differ from most neutral-neutral reactions in that long-range attractive forces play a dominant role in determining their behavior. The basis for the long-range attractive force is an ion-induced dipole interaction for ion-nonpolar systems, and an ion-dipole interaction for ion-polar systems. The result is a potential energy surface dominated by a purely attractive component; the short range repulsive part of the expression for the potential is often not considered. There are no appreciable barriers to reaction except for a small centrifugal barrier which arises from the angular momentum of the nascent orbiting complex. In neutral-neutral systems, the simplest collision theory for calculation of bimolecular rate coefficients, hard sphere collision theory, assumes that no attractive force is present and that collision between two "hard spheres" results in reaction. For

instance, for the neutral system of A + B $\longrightarrow$ C + D as treated by hard sphere collision theory, the maximum radius of collision would be the sum of the radius of A, r_a, and the radius of B, r_b. This results in a geometric reaction cross section, σ_c, at a given relative velocity v, given by:

$$\sigma_c(v) = \pi (r_a + r_b)^2(v) \quad , \qquad (1.2)$$

which is the area of the circle around A with radius of r_a + r_b. The distance of closest approach is known as the impact parameter, b_c. For the hard sphere collision of A and B, the impact parameter is simply r_A + r_B and equation (1.2) becomes:

$$\sigma_c(v) = \pi b_c^2(v) \quad . \qquad (1.3)$$

Equation 1.3 is also true for IM association reactions, but the impact parameter, b_c, is not simply the sum of the radii of the two "hard spheres", but rather now is defined as the maximum distance at which a capture collision will occur. A larger cross section results, of course, because of the attractive potential arising from the ion-dipole or ion-induced dipole interaction.

The hard sphere collision theory is crude and does not in general accurately predict rate coefficients. As a result, more realistic potentials such as the Lennard-Jones and Morse potentials, which take into account intermolecular forces (both attractive and repulsive) between reactant molecules, were developed. The Lennard-Jones attractive

potential varies as r^{-6}, where r is the distance between reactants A and B. For IM reactions, on the other hand, a pure polarization theory is used. The potential is purely attractive and varies as r^{-4} for an ion-induced dipole and r^{-2} for an ion-dipole system. Therefore, in the case of an ion-neutral interaction, the attractive force is more prevalent at longer separations than in the corresponding neutral-neutral interaction.

This clearly demonstrates the principal difference between neutral-neutral and IM association reactions; IM potentials have a dominant long-range attractive force which gives rise to the many of the unique properties of IM association reactions. For example, this strong, long-range attractive force diminishes the importance of any activation energy barrier, often yielding an overall apparent bimolecular rate coefficient for IM association with an inverse dependence upon temperature.

In 1905 Langevin[6] developed a model describing the mobilities of ions in the gas phase. In 1958, Gioumousis and Stevenson[7] expanded on Langevin's model and derived an expression for a bimolecular rate coefficient under thermal conditions for reactions between ions and polarizable neutrals with no permanent dipole moment occurring in a mass spectrometer. The expression derived was:

$$k = 2\pi q(\alpha/\mu)^{1/2} \quad , \qquad (1.4)$$

where q is the charge on the ion, α is the polarizability

of the neutral, and μ is the reduced mass of the colliding IM pair. This rate is commonly known as the Langevin rate. It is also the collision rate, and is usually considered to be an upper limit to the rate of reaction for ion-nonpolar systems. The units are in cm^3 $molec^{-1}$ s^{-1}, as is appropriate for a second-order process. Note also that the Langevin rate as given in equation (1.4) is temperature independent. The Langevin theory underestimates the rate for IM association reactions in which the neutral possesses a permanent dipole moment. Several theories have been formulated to deal with these types of systems; a recent review has been written by Su and Bowers.[8] The most convenient theory for calculation of binary rate coefficients for ion-polar molecules is the average dipole orientation (ADO) theory. The expression for the rate coefficient is given by:

$$k_{ADO} = \frac{2\pi q}{\mu^{1/2}}\left[\alpha^{1/2} + cu_D\left(\frac{2}{\pi kT}\right)^{1/2}\right], \qquad (1.5)$$

where again q is the charge on the ion, μ is the reduced mass of the IM pair, α is the polarizability of the polar neutral, u_D is the permanent dipole moment of the polar neutral, and c is an empirically determined locking constant which ranges in value from 0 to 1. This locking constant is a temperature dependent term and is a measure of how well the ion "locks in" on the dipole as the col-

liding pair approach one another. Values for c have been determined over the temperature range from 150 to 500 K at 50 K intervals and also at 650 K,[9,10] and decrease as the temperature increases. Note that expression (1.5) for the ADO rate coefficient contains a term which has an inverse dependence upon temperature. This added term resulting from the permanent dipole moment gives a collision rate as much as 50 to 100% larger than the Langevin rate at room temperature[9], and imparts a small temperature dependence to k_{ADO}.

Both of these theories, Langevin and ADO, and modifications thereof, are used to describe the collision rate or the upper limit at which an IM association reaction can occur. This rate is called the rate of association, k_a, and the Langevin or ADO calculated rates are often used as the best approximation for the values of k_a. However, not all gas phase IM association reactions proceed at the collision rate, and it becomes necessary to consider what is occurring mechanistically as discussed below.

II. The IM Association Mechanism

The general mechanism for IM association reactions is similar to the energy transfer mechanism as proposed by Rabinovitch in 1937 for atom-atom recombinations.[11] This mechanism as applied to the IM association reaction of $A^+ + B \longrightarrow AB^+$ is given by:

$$A^+ + B \underset{k_d}{\overset{k_a}{\rightleftharpoons}} (AB^+)^* \qquad (1.6)$$

$$(AB^+)^* \xrightarrow{k_s(M)} AB^+ \quad , \qquad (1.7)$$

where k_a (cm^3 $molec^{-1}$ s^{-1}) is the rate of association or formation of the excited complex $(AB^+)^*$ which is formed by chemical activation, k_d (s^{-1}) is the rate of dissociation of $(AB^+)^*$ back to reactants, k_s (cm^3 $molec^{-1}$ s^{-1}) is the rate of stabilization of $(AB^+)^*$ by collision with the inert third-body M, and (M) (molec cm^{-3}) is the number density of the third-body, M. If the steady state approximation is applied to $(AB^+)^*$, an expression for the overall binary rate coefficient for the above mechanism can be derived, and is given by:

$$k_{obs} = \frac{k_a \ \beta k_s(M)}{k_d \ + \beta k_s(M)} \quad . \qquad (1.8)$$

The term β introduced above is a collisional efficiency factor and is discussed later. If another route for stabilization of the excited complex is included in the mechanism, radiative stabilization for example, as given below:

$$(AB^+)^* \xrightarrow{k_r} AB^+ + h\upsilon \quad , \qquad (1.9)$$

the expression for k_{obs} becomes:

$$k_{obs} = \frac{k_a(\beta k_s(M) + k_r)}{k_d \ + \beta k_s(M) + k_r} \quad . \qquad (1.10)$$

The above individual rate coefficients making up expression (1.10) can be estimated in various ways for analysis of data. As explained earlier, the rate of association, k_a, can be estimated by the ADO or Langevin rate depending upon whether the neutral does or does not possess a permanent dipole moment. The rate coefficient for collisional stabilization of $(AB^+)^*$, k_s, again can be estimated by ADO or Langevin theory, (the colliding IM couple is now the excited complex $(AB^+)^*$ and the inert third-body M) modified by β , the collisional efficiency factor which is a measure of how efficient the inert third-body, M, is in collisionally deactivating or stabilizing the excited (usually internal excitation i.e., vibrational and rotational modes) $(AB^+)^*$ complex. The collisional deactivation of $(AB^+)^*$ involves the transfer of energy from the excited complex to the inert third-body M. Several models have been proposed to explain how this transfer of energy might occur, and thus why some third-bodies are more efficient stabilizers than others.[12-16] Basically these models fall in to two categories: (1) those that involve formation of a collision complex in which the excess energy from the excited complex is removed through the new vibrational or transitional modes formed from the loss of translational and rotational degrees of freedom of the separated species, or (2) those that involve collisions between the excited complex and inert third-body where V-V and/or V-R energy transfer occur.

The values of β , the collisional efficiency, range from 0 to 1. A value of 1 represents unit collisional efficiency with every collision resulting in stabilization. Only a few systematic studies of the collisional efficiencies of third-bodies for a large number of different third-bodies (> 20) have been carried out.[14,16] In general, all the studies are qualitatively the same. That is, monatomic third-bodies such as He, Ne, Ar, Kr, and Xe, all have about the same collisional efficiency. The values of β for these gases typically range from 0.2 to 0.3. Values as low as 0.1 to 0.03 have been reported.[17,18] As one might expect, as molecular complexity of the third-body increases so does its collisional efficiency, with the order of efficiency generally proceeding as such: polyatomics > triatomics > diatomics > monatomics. Typical values of β for diatomics are in the range 0.2 to 0.5, for triatomics 0.5 to 0.8, and for polyatomics 0.5 to 1.0.

The collisional efficiency β is postulated to possess a slight pressure and temperature dependence.[17] The temperature dependence of β has sometimes been expressed as $T^{-\delta}$, where δ has been found to range from 0 to -1 for most systems[18,19] while exceptions where $\delta > 1$ have been reported.[20] Herbst[15] has developed a sophisticated theory for calculation of δ and has found the results to be in good accord with experimental δ values found by Adams and Smith.[19]

In summary, absolute values of β are difficult to

measure and the different results have generated various models for the energy transfer. While one model seems appropriate for certain IM systems, it seems not to work for others. Overall, β seems to be rather nebulous in its behavior and in the validity of its interpretation, with one author, D.R Bates,[15] even suggesting that β might simply be a "catch all" for any processes that might be occurring other than those explicitly stated in the IM association mechanism (expressions (1.6) and (1.7)). Nevertheless, β is an often-utilized parameter, and although exact values may not be known, reasonable estimates can be made.

Another parameter which is difficult to evaluate but is very important in the mechanism, is the rate of unimolecular decay of the excited complex $(AB^+)^*$. Knowledge of k_d is important because: (1) it controls how much of $(AB^+)^*$ can continue to product formation, (2) most of the temperature dependence of k_{obs} lies in this process (in our data analysis we assume all of the temperature dependence lies in this step), and (3) valuable information on the lifetime of the excited complex can be determined from the relation:

$$k_d = 1 / \tau_{avg} \quad , \qquad (1.11)$$

where τ_{avg} is the average lifetime of the excited complexes and the unimolecular decay rate, k_d is itself an average value. Although as mentioned above quantitative information about k_d is one of the most valuable pieces of

information one could obtain, calculations of k_d are not trivial. Sophisticated statistical theories[23-27] have been used for the calculation of k_d and the prediction of the pressure and temperature dependence of the overall third-order rate coefficient. Generally these theories are based on the RRKM formalism[23] which assumes complete randomization of the internal energy of the excited complex, and often requires detailed information about the excited complex which is usually not reliably known.

The rate of unimolecular decomposition, k_d, is both pressure and temperature dependent. The pressure dependence has no simple functional form, while the temperature dependence of k_d is often expressed as $k_d = AT^n$, where n denotes the magnitude of the temperature dependence. The value of n has been found to range from 0 to 8 but common values are in the range 0 to 4. The pressure dependence of k_d arises because k_d is a function of energy, and the energy distribution of the excited complexes is pressure dependent; thus k_d should display a pressure dependence.[24] At a "high" pressure where the time between collisions is short, the average lifetime of the complexes that can dissociate before being stabilized is short (the high energy complexes), thus k_d ($= 1/\tau_{avg}$) becomes larger. By contrast, in the low pressure case the time between collisions is longer, and the average lifetime of the excited complexes that can dissociate before being stabilized is longer (the lower energy complexes), and thus k_d becomes

smaller.[24] Of course the changes in magnitude of k_d with pressure and temperature will vary from system to system. The fact that k_d changes with both pressure and temperature has made theoretical calculations of k_d over wide pressure and temperature ranges difficult, but certainly not impossible. It is, however, often possible to determine k_d from experimental data of k_{obs} as a function (M) as will be disscused later.

The last rate coefficient to be discussed, k_r, the rate of radiative stabilization, is seldom invoked as important in the mechanistic scheme for stabilization in IM association reactions at "high" pressure. Usually at accessible pressures used in the laboratory for the study of IM association reactions, collisional stabilization, as opposed to stabilization by emission of a photon, is the dominant stabilization process, i.e., $k_s(M) >> k_r$. As such, radiative stabilization usually becomes important only at low pressures or low number densities, where collisional stabilization is difficult and radiative stabilization can effectively compete; k_r is not known to possess a temperature dependence. One such area of very low pressure is the interstellar medium where the number density ranges from 10 to 10^7 molec cm^{-3}. [29] It has been postulated that radiative association plays an important role in the interstellar medium,[30-32] and therefore it has been included in models of the chemistry occurring there.[33,34]

The calculation of k_r again is not a trivial proced-

ure. Woodin and Beauchamp[34] have utilized the method of Dunbar,[35] and Herbst[36,37] has developed a theory for calculation of k_r for infrared emission from vibrationally excited molecular ions. In general, these theories predict that k_r for infrared emission lies in the range of 10 to 10^3 s^{-1}, with k_r being directly proportional to vibrational excitation energy.[38] Recently Bates[38] has discussed the possibility that his earlier predictions of k_r could have been an order of magnitude too low, and has indicated that k_r may be as high as 3×10^4 s^{-1} for the infrared emission rate of the excited complex from the addition of CH^+_3 to H_2, as studied by Barlow, Dunn, and Schauer.[39]

In conclusion, theoretical calculations tell us that radiative emission rate coefficients, k_r, could range from 10 to as high as 10^4 s^{-1} for infrared emission. Electronic emission rates are generally > 10^5 s^{-1}.[40] In addition, k_r can be obtained from experimental data if an appropriate IM system in which radiative stabilization can compete with collisional stabilization is found. To date, our systems are the only ones to our knowledge where this is possible, and the determination of k_r in our work is a focal point of this dissertation. The evaluation of k_r from experimental data is discussed later in the data analysis section of the dissertation.

In summary, the individual terms in the mechanism can be estimated in the following manner: k_a and k_s can be approximated by the Langevin or ADO collision rates; β can

be estimated by noting the complexity of the inert third-body and choosing an appropriate value characteristic thereof; k_d and k_r can be calculated from sophisticated theory[23-27,35-37] or obtained from experimental data as in this work.

III. Pressure Dependence of IM Association Reactions

The pressure dependence of IM association reactions is well documented and is often a valuable tool in gaining mechanistic information. It aids in the understanding of fundamental processes such as stabilization and unimolecular decomposition of the excited complex occurring in IM association reactions as discussed above. The pressure dependence of IM association reactions is best described by a pressure dependence curve as shown in figure (1.1). The general shape of this curve is described mathematically by expression (1.8). Figure (1.2) shows the resulting pressure dependence curve when expression (1.10) in which a radiative stabilization pathway has been included is considered. Note the nonzero intercept that results from the radiative bimolecular component of k_{obs} at (M) = 0. The pressure dependence curve follows the general trend as predicted by the mechanism of IM association reactions, with the first observance of a complete pressure dependence curve generated experimentally being seen by Bohme et al.[41] in 1968. This was important in that it showed that the generally accepted mechanism for IM association reactions

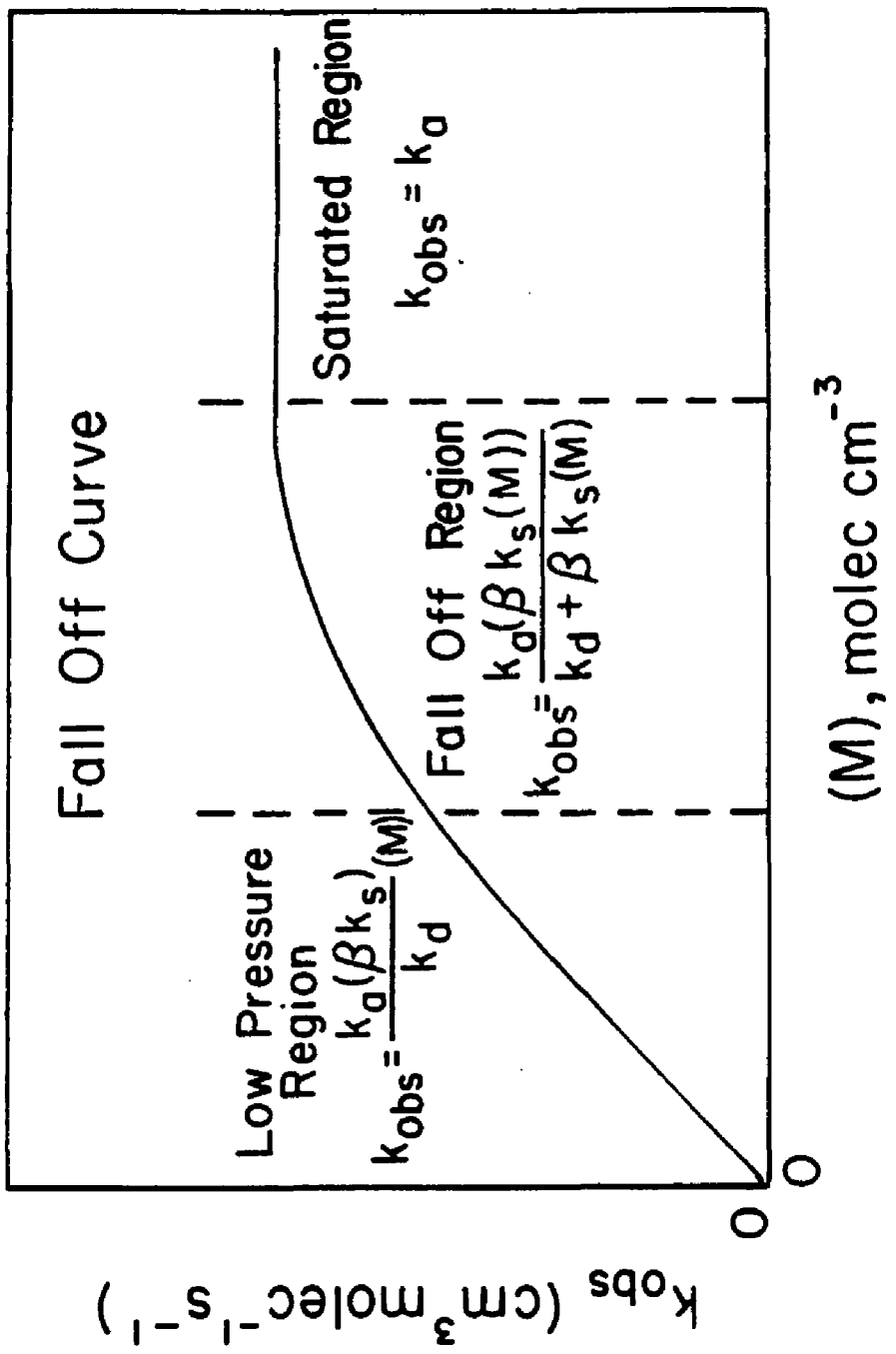

Figure 1.1. Pressure dependence curve for k_{obs}.

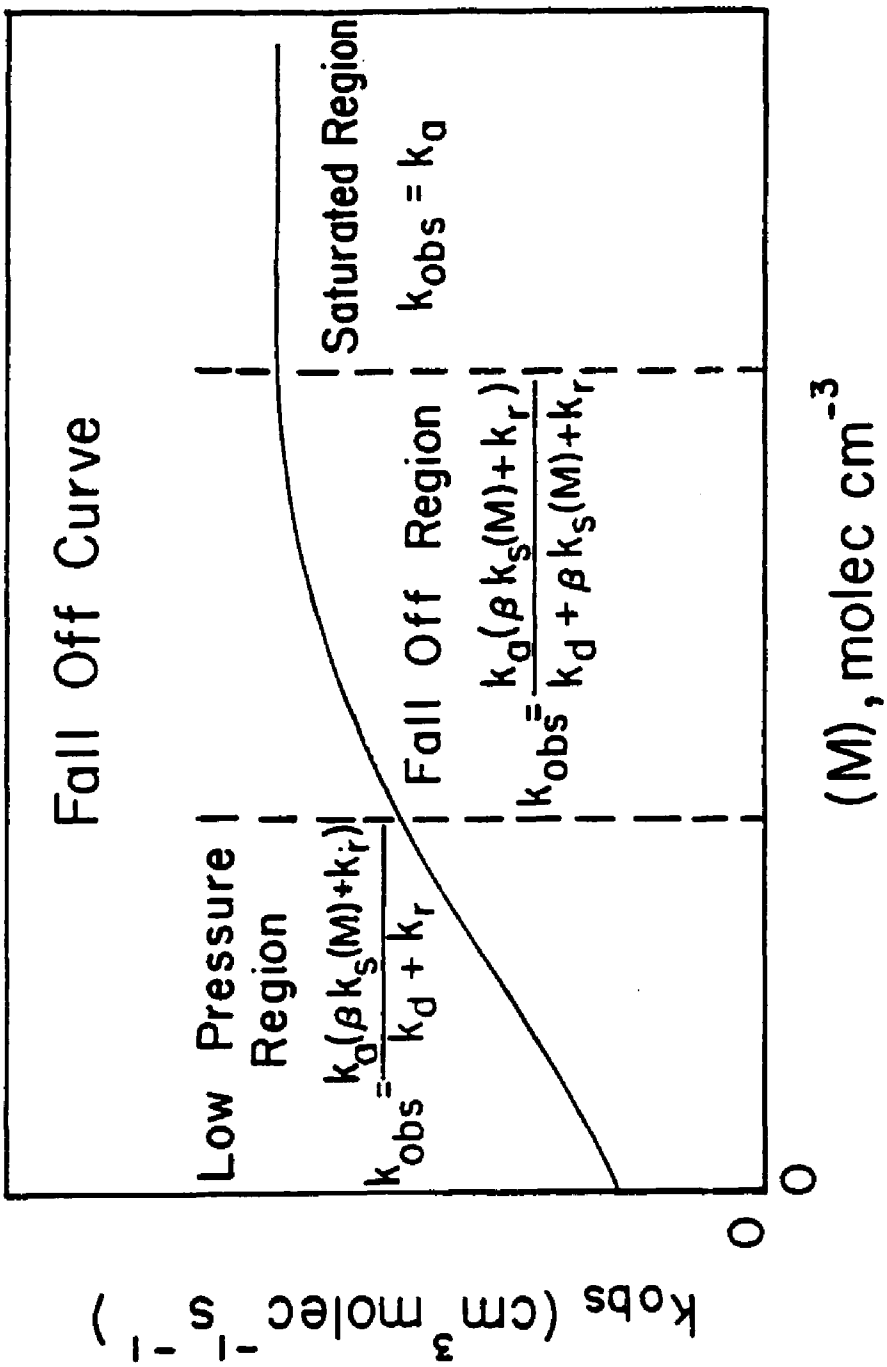

Figure 1.2. Pressure dependence curve for k_{obs} including radiative stabilization.

was indeed at least qualitatively correct. The pressure dependence is best evaluated by dividing the pressure dependence curve into three separate regions: (1) the high pressure or saturated region, (2) the intermediate or "fall-off" region, and (3) the low pressure or unsaturated region. A discussion of each region follows.

(a). High Pressure Region

The high pressure region, or saturated region as it is also known, is characterized by a flat line in a plot of k_{obs} versus pressure, i.e., k_{obs} displays no pressure dependence in this region. This can be seen by considering the expression for k_{obs} as given by:

$$k_{obs} = \frac{k_a(\ \beta k_s(M))}{k_d\ + \beta k_s(M)} \quad . \qquad (1.12)$$

In the high pressure region $k_s(M) >> k_d$, and the above expression reduces to:

$$k_{obs} = k_a \quad . \qquad (1.13)$$

Note that equation (1.12) does not include a radiative term. However, the expression for k_{obs} including a k_r term, equation (1.10), also reduces to (1.13) in the high pressure limit. Here second-order kinetics apply and we can approximate k_a by the Langevin or ADO collision rate. Usually the assumption $\beta = 1$ is valid in this region. For some IM systems the overall rate, k_{obs}, levels off well

below the Langevin or ADO collision rate. In a study done by Neilson et al.[42] this occurred. One explanation they proposed that might have caused this effect was "prompt back dissociation" to reactants on the order of a vibrational period (10^{-13} s) upon capture collision of B and A^+. This means every collision does not result in the formation of an excited complex which could be stabilized with unit efficiency and thus $k_{obs} < k_a$ if k_a is taken as the Langevin or ADO rate.

(b). Intermediate Pressure Region

Here in the "fall-off" region, $k_s(M) \simeq k_d$, and the entire expression for k_{obs} must be considered (expression (1.8) or (1.10)). The transition from second-order kinetics (high-pressure region) to third-order kinetics (low pressure region) occurs here. An indication that one is in the "fall-off" region would be the presence of curvature in a plot of k_{obs} versus pressure. But if the "fall-off" region is broad and the accessible pressure range narrow, (less than one order of magnitude) then the plot of k_{obs} versus pressure may appear linear. It then may be tempting to assume one is in the low pressure region and to attempt extrapolation outside of the pressure region studied. This could possibly lead to erroneous results and faulty conclusions. Extrapolation outside of the pressure region actually studied can be dangerous and must be carefully considered as will be shown below.

(c). Low Pressure Region

In this region $k_s(M) << k_d$; subsequently the complications of the contribution from $k_s(M)$ to the denominator of the expression for k_{obs} are removed, and data analysis becomes easier in this region as compared to the "fall-off" region. Expression (1.12) reduces to:

$$k_{obs} = \frac{k_a \beta k_s(M)}{k_d} \quad , \qquad (1.14)$$

or with a radiative stabilization pathway:

$$k_{obs} = \frac{k_a(\beta k_s(M) + k_r)}{k_d + k_r} \quad . \qquad (1.15)$$

A plot of k_{obs} vs. pressure for expression (1.14) should yield a straight line with a slope of $k_a \beta k_s/k_d$ and an intercept of zero, while a plot of k_{obs} vs. pressure for expression (1.15), should yield a straight line with a slope of $k_a \beta k_s/(k_d + k_r)$, and a nonzero intercept of $k_a k_r/(k_d + k_r)$. A zero intercept or a slightly nonzero intercept resulting from extrapolation is an indication that one is in the low pressure limit of the pressure dependence curve. Although, as van Koppen et al.[28] have demonstrated, to truly be in the low pressure limit one must be at very low pressures, probably $< 10^{-3}$ torr, or small errors may result in the determination of the third-order rate coefficient ($k_{obs}/(M)$) and thus in n, the magnitude of the TD. Third-order kinetics apply here as

the overall bimolecular rate coefficient, k_{obs}, shows a definite linear dependence upon pressure.

The low pressure region has the advantage that data analysis is easier because of the simplifying assumption that $k_s(M) << k_d$. Determination of k_d, β, and n can be done rather straightforwardly. For example, if expression (1.14) is considered, then the overall third-order rate coefficient, $k^{(3)}$ is given by:

$$k^{(3)} = \frac{k_{obs}}{(M)} = \frac{k_a \beta k_s}{k_d} \quad . \qquad (1.16)$$

Here $k^{(3)}$ is the slope of the line for a plot of k_{obs} vs. (M) as mentioned above. Once $k^{(3)}$ is known, a value for k_d can be calculated by estimating k_a and k_s to be equal to either the Langevin or ADO collision rate, whichever is appropriate; an estimation of β can be made from the complexity of the inert third-body M, as mentioned before. Expression (1.15), the low pressure limit with $k_r \neq 0$, can be rewritten as:

$$k_{obs} = \frac{k_a \beta k_s}{k_d + k_r}(M) + \frac{k_a k_r}{k_d + k_r} \quad , \qquad (1.17)$$

or:

$$k_{obs} = k^{(3)}(M) + k^{(2)} \quad , \qquad (1.18)$$

where $k^{(3)}$ is the overall third-order rate coefficient as given in (1.17), and $k^{(2)}$ is the overall second-order rate coefficient for the bimolecular contribution of the radia-

tive process. Even when the simplifying low pressure assumption is made, the inclusion of a radiative process leaves three unknowns: k_d, k_r, and β . With measurement of only the slope, $k^{(3)}$, and intercept, $k^{(2)}$, the three unknowns cannot be explicitly determined. However, if β is estimated, then the values for the other two unknowns can be obtained. For the work contained herein however, we are unable to make the low pressure assumption, equation (1.18), and we must use the entire expression for k_{obs} as given in equation (1.10). This is discussed in detail in the data analysis section.

Finally, in the truly low pressure limit as $(M) \rightarrow 0$, "true" values of n, the magnitude of the TD for IM association reactions, can be determined from plots of log $k^{(3)}$ vs. log T where $k_r = 0$.

In conclusion, in the low pressure region because of the simplifying assumption that $k_s(M) << k_d$, analysis of data becomes easier and more straightforward unless radiative stabilization must be considered. Direct evaluation of k_d and n in the experimental range studied are possible.

IV. Temperature Dependence of IM Association Reactions

Along with the pressure dependence of IM association reactions, the study of the temperature dependence of this class of reactions has also contributed greatly to the understanding of the fundamental mechanistic processes. As

mentioned, IM association reactions are important in many different areas, with the temperature variation of these areas ranging from as low as 10 - 50 K in the interstellar medium[43] to as high as 1500 - 2000 K in the upper regions of our atmosphere during maximum sunspot activity.[44] Thus it becomes apparent that a knowledge and understanding of the temperature dependence of IM association reactions is also important in understanding the various processes occurring in the gaseous medium surrounding us.

One of the first studies of the TD of an IM association reaction was that of $He^+ + 2He \longrightarrow He^+_2 + He$ over the temperature range of 77 K to 449 K, done by Niles and Robertson[45] in 1964. Since then this field of study has intensified with many different IM association reactions being studied. The first TD studies utilizing a flowing afterglow were done in 1968 by Dunkin et al.[46] For recent reviews see Meot-ner[47] and Adams and Smith[48].

Perhaps the most striking feature of the TD of these reactions is their inverse dependence upon temperature, a "non-Arrhenius" type behavior. Typically, for most gas phase and liquid phase neutral-neutral reactions, the temperature dependence of the overall rate coefficient follows the Arrhenius equation, given by:

$$k = Ae^{(-E_a/RT)} \quad , \qquad (1.19)$$

where A is the preexponential factor and E_a is the activation energy. Both of these terms are constants for a given

reaction, and, for the Arrhenius equation, assumed to be independent of temperature. As a rough estimate, k doubles or triples for a 10 °C rise in temperature for typical reactions in solution. The important point here though, is that as the temperature increases, so does the overall rate. In comparison, the overall rate for IM association reactions decreases with increasing temperature. This is mainly a result of this class of reaction possessing little or no activation energy as well as the fact that the main temperature-dependent rate coefficient, k_d, which has a strong positive dependence upon temperature appears in the denominator of the expression for k_{obs}.

This inverse dependence of k_{obs} upon temperature can be rationalized by considering classical RRK theory which predicts $k_d \propto T^{s-1}$, where s is the effective number of oscillators in the excited complex. In reality this model is too crude because s must be adjusted (usually lowered) for k_{calc} to coincide with experimental data.[49] Recent thermal models proposed by Bates[19,50] and Herbst[27,51-52] designed for IM association reactions and couched in the RRKM formalism in which the ratio of the partition functions of the excited complex to the reactants is considered, are preferred for predicting the TD. These models are derived with the assumption that one is in the low pressure limit, and they are used to predict the third-order rate coefficient, $k^{(3)}$, as given in expression (1.16), along with the magnitude of the TD, n. The form of the expres-

sion relating $k^{(3)}$ to temperature as given by these models is:

$$k^{(3)} \propto T^{-(\ell/2 + \delta)} \quad , \qquad (1.20)$$

where ℓ is the total number of rotational degrees of freedom of the reactants, and δ , whose value usually lies between 0 and 1, is the temperature dependence of the collisional stabilization efficiency term, β . Expression (1.20) can be rewritten in the form $k^{(3)} \propto T^{-n}$. For an IM association reaction between two linear species, n should range from 2 to 3, while for two non-linear species, n should range from 3 to 4. This formula has been found to yield good results for several different IM systems,[53-55,43] while for many other systems it has failed.[56-58] To obtain expression (1.20) it was assumed that the reactants were in their ground electronic and vibrational states i.e., $h\nu >> kT$, and only rotational partition functions were employed. Viggiano[56] has modified the above thermal model by omitting the assumption $h\nu >> kT$ i.e., by assuming that vibrational modes may be active and could contribute to the TD of the reacting system. This means the vibrational partition functions must be considered, yielding an expression relating $k^{(3)}$ to temperature in the low-pressure limit:

$$k^{(3)} \propto T^{-(\ell/2 + \delta)} \prod_i (1 - e^{(-h\nu_i/kT)}) \quad . \qquad (1.21)$$

Each vibrational mode for which $h\nu \approx kt$ is used in evalu-

ating the vibrational partition function. This expression yields a TD which changes depending upon the temperature range of interest due to the contribution of the various vibrational modes. It was found that this model could accurately describe the TD of certain IM systems having a temperature dependence of k_{obs} as high as $T^{-7.25}$.[56] Clearly this could not be explained by taking only the rotational contributions into account unless a value of $\delta > 6$ was used. This is certainly unreasonable; as Patrick and Golden[59] have pointed out, the value of δ should never be > 1 if it is only a result of the TD of the stabilization efficiency factor, β . We have successfully applied Viggiano's model[56] to the IM systems studied in this dissertation, and have found good agreement between it and the TD of k_d that we determine experimentally. (See Results and Discussion Section.)

V. Summary of Behavior of IM Association Reactions

In summary, IM association reactions in general are different from neutral-neutral reactions due to the presence of a long range range attractive force which plays a dominant role in determining the properties of these systems. The generally accepted mechanism for ion-molecule association reactions is shown to involve the redistribution and transfer of energy; the ion and molecule associate to form an excited complex that can then unimolecularly decay, or be stabilized through collision with an inert

third-body M or by emission of a photon. The individual rates k_a and k_s can be estimated by Langevin or ADO theory using equations (1.4) and (1.5) respectively, the stabilization efficiency factor, β , can be estimated by noting the molecular complexity of the inert third-body M, and k_d and k_r can be determined from theory with difficulty or from experiment. The expression for the overall bimolecular rate coefficient, k_{obs}, derived by assuming a steady state concentration of the excited complex, shows k_{obs} to possess a positive pressure dependence: i.e. k_{obs} increases as one passes from the low pressure region, through the "fall-off" region, and into the saturated or high pressure region. This behavior is readily seen by examination of the the pressure dependence curve generated from plots of k_{obs} vs. (M); recall figures (1.1) and (1.2). Also, the mechanism predicts that k_{obs} possesses a negative dependence upon temperature i.e., $k_{obs} \simeq AT^{-n}$ where $n > 0$, mainly due to the TD of k_d. Several theories have been developed for prediction of n. While experimental determination of n is possible, caution is advised when extrapolation outside of a given pressure and temperature range is performed. It is often necessary to extrapolate outside of a given range when trying to obtain information for processes that occur at very low temperatures which are not accessible experimentally, (for example those that occur in interstellar media), or for processes that occur at very high temperatures (such as those occurring in our atmos-

phere or during combustion). It is apparent, however, that such extrapolation outside of limited pressure and temperature ranges accessible in experiment entails risks, and care must be exercised unless clear evidence indicates low pressure conditions are applicable, or that extrapolation does not introduce significant error.

CHAPTER 2

EXPERIMENTAL

I. Introduction

All of the work contained in this dissertation was done on the selected-ion flow tube (SIFT) at the Air Force Geophysics Laboratory (AFGL), Hanscom AFB, MA. A SIFT is a variation of the flowing afterglow (FA) apparatus, and differs mainly in the respect that a quadrupole mass filter is placed in tandem with the ion source to allow for selection of the reactant ion. Other differences of a SIFT are that: (1) it does not operate under plasma conditions as does the FA, (2) it does not operate over as wide a pressure range as the FA, and (3) it is limited in the number of different carrier gases that can be used as compared to a FA. Overall, a SIFT and a FA share the same basic principles, and a description of the flowing afterglow apparatus and technique will serve well to familiarize one with the general principles behind both. Therefore, in this section a discussion of the FA apparatus and technique will be presented first. Then the specific differences and advantages of a SIFT versus a FA will be discussed, and finally, a description of the SIFT used at AFGL along with the specific experimental parameters and operating conditions will be presented.

II. Description of FA Apparatus and Technique

The development of the FA technique was begun in 1963 by Ferguson, Fehsenfeld, and Schmeltekopf at the NOAA Laboratories in Boulder, Colorado, and it came about as a natural extension of a glass afterglow tube used for optical spectroscopy by H. P. Broida at NBS - Washington Laboratory.[2] Ferguson et al. saw that by placing a mass spectrometer at the end of the tube and then adding a neutral reactant at some point along the flow tube, it was possible to obtain quantitative rate coefficients for ion-molecule reactions. Neutrals had been studied for years in slow flowing systems but quantitative rate coefficients of ion-molecule reactions, especially those occurring in our atmosphere, were largely unknown at this time. It was this lack of detailed rate information about ionospheric reactions which served as the impetus for the development of the FA technique as applied to the study of ion-molecule reactions today.

A schematic of a typical FA apparatus is shown in figure (2.1). In general the way the apparatus works is that an inert carrier gas, usually helium, is injected into the end of the stainless steel flow tube (usually ~1 meter long with an internal diameter of ~8 cm). The typical flow range for the helium buffer gas is 4 to 8 standard liters per minute (slm). The carrier gas is continuously pumped along the flow tube at velocities of $\sim 10^4$ cm s^{-1} by a large capacity roots blower; the resulting flow is laminar and

has a parabolic flow profile as depicted in figure (2.1). The typical operating pressure range in the tube itself is from 0.1 to as much as 3 torr, the upper limit depending on the ability of the diffusion pumps to maintain the detection chamber (not shown in figure (2.1)) at a pressure < 10^{-5} torr (the maximum operating pressure of the quadrupole mass filter) and also on the ability to maintain a suitable ion density for detection purposes. A heated filament which emits energetic electrons, is located a short distance downstream from the point of injection of the carrier gas. This filament is used to produce a plasma condition in the flow tube by electron bombardment of the carrier gas. This plasma condition produces electrons, carrier gas metastables and positive ions, with a resulting afterglow, into which a source gas is introduced to produce the reactant or primary ion(s). Positive ions can be produced by charge exchange with carrier gas positive ions or by direct electron bombardment, while negative ions can be produced by thermal electron attachment. The ionized species make up only a small fraction (< 1%) of the gases flowing downstream, the remainder is neutral carrier gas. The electrons, excited metastables, and ionized carrier and source gases, are then carried downstream and thermalized by collision with the neutral carrier gas after traveling a short distance down the flow tube. The presence of these oppositely charged particles makes ambipolar diffusion important as a loss mechanism of the reactant and product ions.

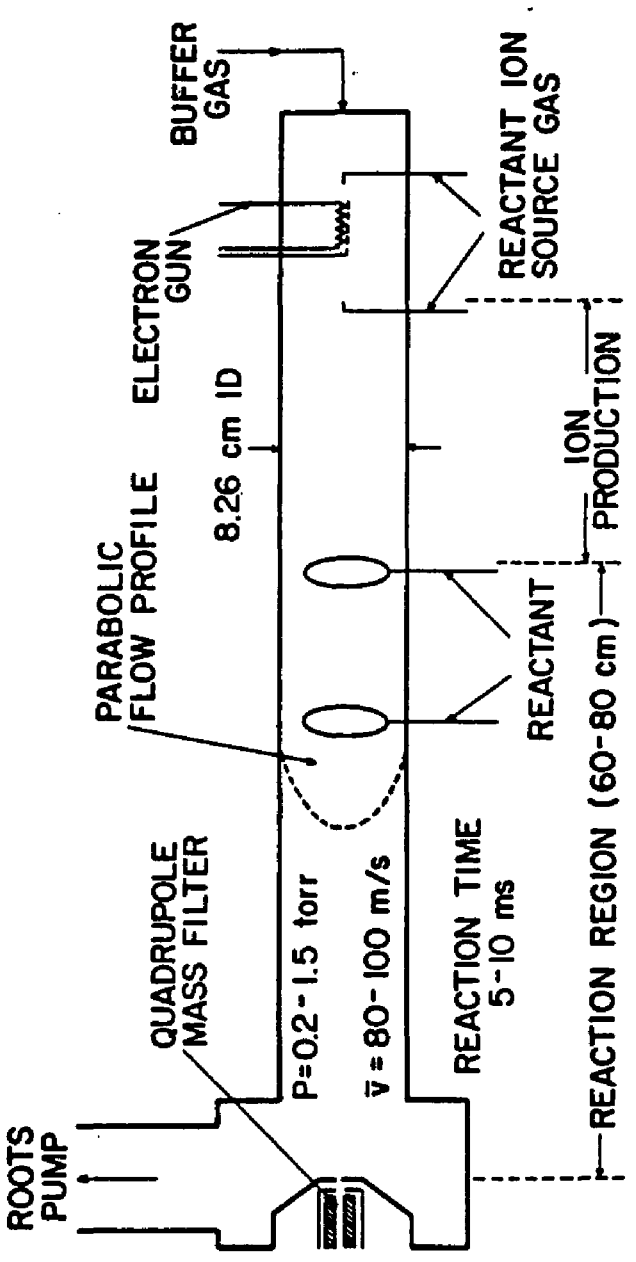

Figure 2.1. A schematic diagram of a flowing afterglow instrument.

A SIFT does not operate under plasma conditions (as will be explained in section IV) since the ionization source is remote from the flow tube and thus bombardment of the carrier gas by energetic electrons does not occur. Therefore oppositely charged particles are not present and only free diffusion of the ions serves as a loss mechanism. Approximately two-thirds of the way down the flow tube, a neutral reactant gas is introduced. Reaction then occurs from this point to the sampling orifice. Typical neutral flow rates range from 1 to 200 standard cubic centimeters per minute (sccm). The concentration of the neutral reactant ($\sim 10^{12}$ molec cm^{-3}) is in large excess as compared to the concentration of the primary ion ($\sim 10^{8}$ ions cm^{-3}) [60] and so psuedo first-order kinetic conditions hold. Typical reaction lengths, which are measured from the neutral gas injector to the nose cone sampling orifice, range from 30 to 85 cm. At the end of the reaction zone a small portion of the reactant mixture, including the remaining primary ions and resulting product ions, is sampled through a small orifice (0.1 to 1.5 mm in diameter) in a molybdenum plate mounted on a truncated nose cone. Molybdenum is used because it has been shown to be inert and give constant ion signals.[2] The primary and product ions are then mass selected by passing them through a quadrupole mass filter, then detected and counted by a Channeltron electron multiplier/ion counting system. The electron multiplier is placed off-axis from the center of the flow tube to mini-

mize photons and stray electrons from the afterglow impinging upon the electron multiplier resulting in a high background count rate.

In general, to obtain a rate coefficient using a FA or a SIFT apparatus, one sets the flow rate of the carrier gas and pressure of the flow tube at a desired level, produces a primary ion from the appropriate source gases, injects the chosen neutral downstream, and monitors the loss of the primary ion as a function of the flow rate (i.e. concentration) of the neutral. From this a rate coefficient can be obtained. Binary rate coefficients ranging from 10^{-9} to 10^{-13} cm^3 $molec^{-1}$ s^{-1} can be measured typically within an accuracy of $\pm$15%. A typical plot showing the primary ion signal versus the neutral flow rate is shown in figure (2.2) (this is from a SIFT experiment). The methodology and equations used to obtain a rate coefficient is discussed below.

III. Determination of the Rate Coefficient

If one considers the reaction of the ion A^+ with some neutral B,

$$A^+ + B \longrightarrow C^+ + D \quad , \qquad (2.1)$$

the rate of reaction of A^+ with B can be described as follows:

$$\frac{d(A^+)}{dt} = -k(A^+)(B) \quad , \qquad (2.2)$$

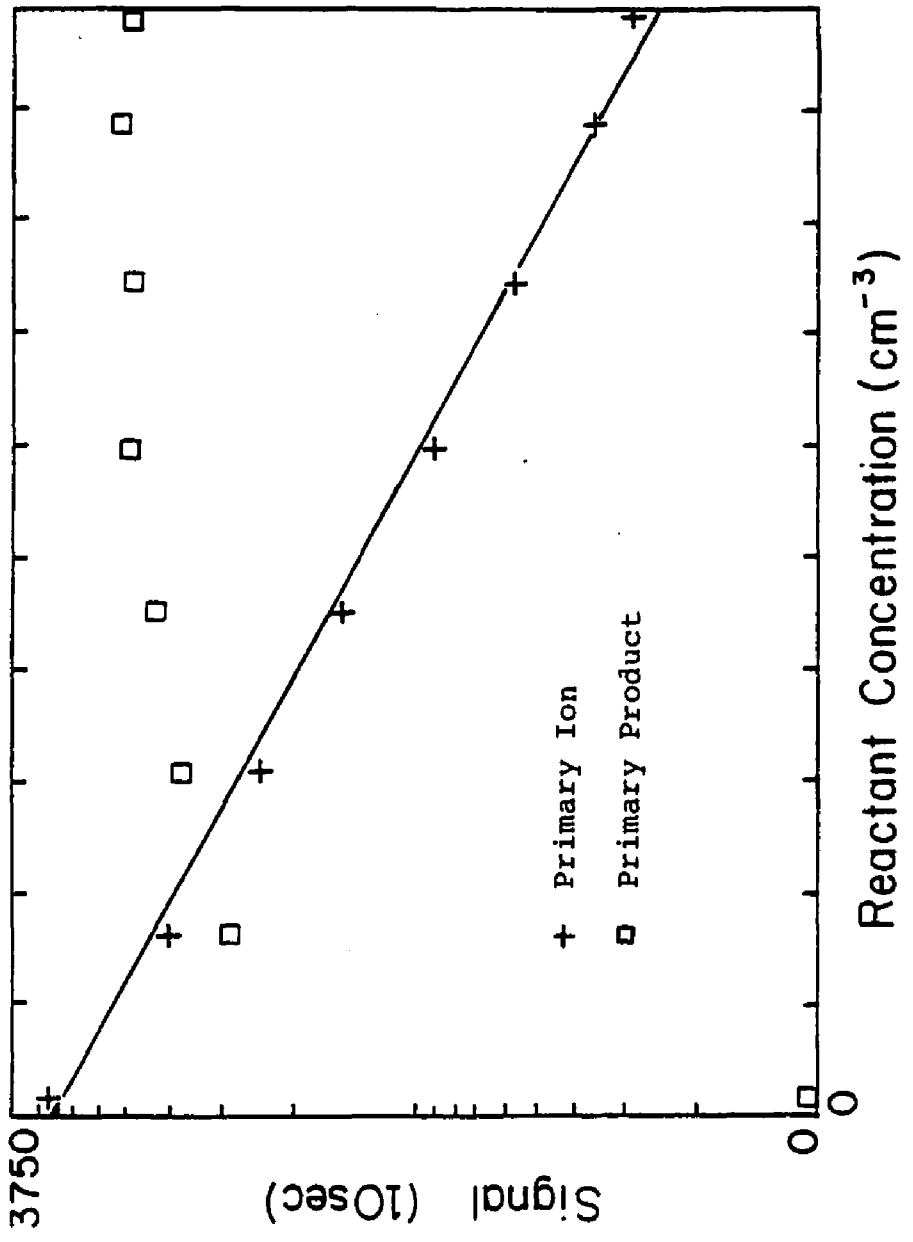

Figure 2.2. Plot of primary ion signal vs. neutral flow rate.

where k is the bimolecular reaction rate coefficient and (A^+) and (B) are the concentrations of A^+ and B. Rearrangement of (2.2) yields:

$$\frac{d(A^+)}{(A^+)} = -k(B)dt \quad . \tag{2.3}$$

In this expression the change in concentration of (A^+) is given as a function of time. In the FA and SIFT however, it is easier to consider the change of (A^+) with distance rather than time because distance is an easier variable to measure on a FA or SIFT. Also we can easily calculate the average bulk flow velocity, $\bar{v}$, of the carrier gas from the carrier gas flow and the pressure; a change in variable is appropriate, and we thus let $dt = dz / \bar{v}$, where z is the reaction length from the neutral injection port to the nose cone. Substituting this into equation (2.3) we obtain:

$$\frac{d(A^+)}{(A^+)} = \frac{-k(B)}{\bar{v}}dz \quad . \tag{2.4}$$

Upon integration and rearrangement of both sides, equation (2.4) now becomes:

$$\ln(A^+)_1 = \ln(A^+)_o - \frac{kz(B)}{\bar{v}} \quad , \tag{2.5}$$

or,

$$(A^+)_1 = (A^+)_o \exp -\frac{kz(B)}{\bar{v}} \quad . \tag{2.6}$$

This equation is a simplified model for monitoring the loss

of A^+ in that it only takes into account reactive loss of A^+ with a neutral B. There are also radial and axial diffusive losses of A^+ ions in the flow tube which have not been accounted for explicitly in (2.6). While the reaction mixture is flowing down the flow tube, ions are constantly diffusing and recombining at the walls. The axial diffusive loss is small enough to be omitted from a more complete equation taking into account not only loss of (A^+) to reaction, but also loss of (A^+) by radial diffusion. This more complete equation is given by:

$$[A^+]_x = [A^+]_o \exp - \left(\frac{\Delta D_a}{a^2} + \Gamma k[B]\right)\frac{z}{\bar{v}} \quad , \qquad (2.7)$$

where $[A^+]_x$ is the ion density of A^+ at the nose cone sampling orifice and $[A^+]_o$ is the ion density of A^+ just before the neutral injection port. The term D_a is the ambipolar diffusion coefficient used in describing the diffusion of A^+ in the FA since positive ions and electrons (or negative ions) diffuse together. For a SIFT however, D_a is replaced by $D_{+,-}$, the free diffusion coefficient since there are no electrons or ions of opposite charge as compared to the reactant ion present in the flow tube of a SIFT. The term a is the radius of the reaction zone and Δ and Γ are related to a slip coefficient and are pressure dependent terms. But, since the diffusive loss of A^+ ions is constant for a given run (i.e. constant pressure, $\bar{v}$, and z), the diffusion terms cancel for successive points and we

are left with the simple equation:

$$\frac{[\ln(A^+)_2 - \ln(A^+)_1]}{[(B)_2 - (B)_1]} = \frac{-kz}{\alpha \bar{v}} \quad . \qquad (2.8)$$

The term α introduced in the above equation is used to correct for the parabolic profile of the carrier gas. The result of this parabolic profile is that the ions, whose number density is greatest at the center of the flow tube, appear to move down the flow tube faster than the bulk flow velocity. The $\bar{v}$ used in the equation is the bulk flow velocity, but it is the ions which are detected and v_{ion} appears to be greater than the bulk flow velocity $\bar{v}$. Therefore, the velocity must be corrected and typical values of α range from 1.2 to 1.6.

Referring to equation (2.5), note that to obtain the rate coefficient, k, the reaction length, neutral flow, or bulk flow velocity could be varied while holding the other two parameters constant and monitoring (A^+). It is common to vary the neutral flow and use a set reaction length and bulk flow velocity (although for low vapor pressure neutrals it is often necessary to maintain (B) constant and use a movable injector). For fixed $\bar{v}$ and z, letting (B) vary we obtain:

$$\frac{[\ln(A^+)_2 - \ln(A^+)_1]}{[(B)_2 - (B)_1]} = \frac{-kz}{\alpha \bar{v}} \qquad (2.9)$$

which is the same as equation (2.8) derived from the more

complete equation with the velocity term added. Upon rearrangement of (2.9) to solve for the rate coefficient k, we obtain:

$$k = \frac{-\left[\ \ln(A^+)_2 - \ln(A^+)_1\ \right]}{\left[\ (B)_2 - (B)_1\ \right]} \left(\frac{\bar{v}\,\alpha}{z}\right). \qquad (2.10)$$

Earlier it was mentioned that the method for obtaining a rate coefficient with a FA or a SIFT is to monitor the loss of the primary ion and plot the logarithm of the primary ion count rate versus the flow of the neutral reactant. From the slope, a rate coefficient can be obtained. Note that in equation (2.9) the term $[\ln(A^+)_2 - \ln(A^+)_1] / [(B)_2 - (B)_1]$ is the slope of such a plot. Therefore, to obtain the rate coefficient one must only multiply the slope by $\bar{v}\alpha/z$ along with appropriate conversion factors to obtain the rate coefficient in the proper units of $cm^3molec^{-1}s^{-1}$.

IV. Description of the SIFT

As the FA technique became well established and was applied to many different ion-molecule reacting systems, some of its limitations were realized. There was a desire to study more exotic species such as those that occur in the interstellar medium and planetary atmospheres.[61] Thus the SIFT was developed and exploited by Adams and Smith in 1976 at the University of Birmingham in Birmingham, England.[62] A schematic diagram of a variable temperature SIFT is shown in figure (2.3).

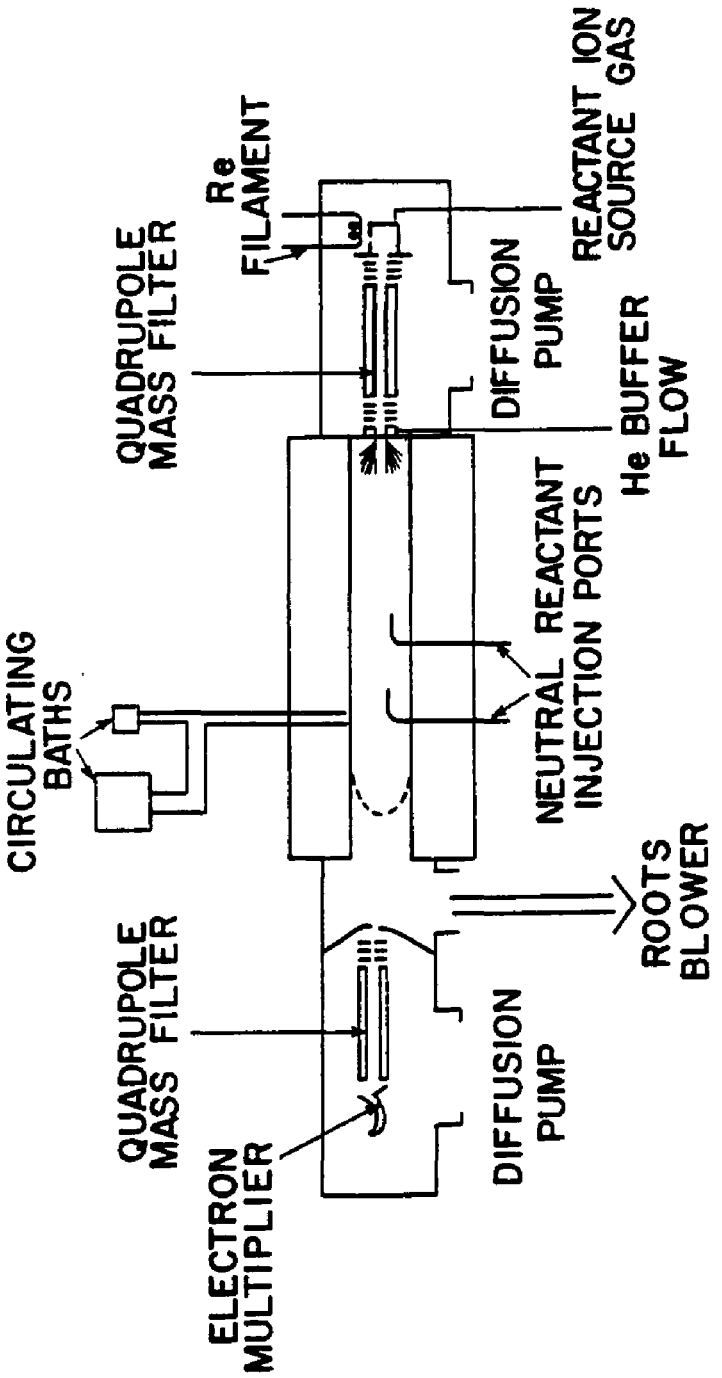

Figure 2.3. A schematic diagram of a variable temperature selected-ion flow tube.

In general, a SIFT operates by first introducing a source gas into a "high pressure" ionization chamber, (10^{-4} to 10^{-3} torr) where again a heated filament is used as an electron emitter to produce the primary ions; now, however, there is no carrier gas to form a plasma. Positive ions are produced by electron impact and negative ions are produced by electron attachment using appropriate source gases. The ions are directed into a quadrupole mass filter through which the desired primary ion is selected. Upon exiting the quadrupole mass filter, the primary ion is focused and accelerated through a set of electrostatic lenses and injected into the flow tube, which is maintained at pressures between 0.3 to 1.0 torr. Once the primary ion has been successfully injected, the general methodology of the SIFT is the same as the FA, viz. the selected ion is then thermalized by collision with the carrier gas, travels downstream, and is allowed to react with the desired neutral. The decline of the primary ion signal and subsequent growth of the product ion(s) are monitored as the neutral flow is varied. As in the flowing afterglow technique, ions are sampled through the small sampling orifice in the nose cone, mass filtered by a quadrupole, and finally detected and counted by an electron multiplier / ion counting system.

Clearly the general methodology behind the SIFT, and its physical dimensions and properties are all similar to those of the FA. The most obvious and perhaps most impor-

tant difference between a FA and a SIFT is that a SIFT has a quadrupole mass filter in tandem with the ion source to allow the injection of particular ion. This produces a cleaner reaction region since only the primary ion, carrier gas, and neutral reactant are present in the flow tube: this allows one to overcome some of the following problems inherent in a FA:[62]

(1) unionized source gas is present in the flow tube which can cause problems with product identification if it reacts with other ions present, or in a subsequent step with products produced from the reaction of interest;

(2) primary ions other than the one of interest can be present and if they react to produce ions of the same mass as the primary ion of interest, erroneously low rate coefficients will be obtained; again, product identification may become difficult because the mass spectrum is complicated by the presence of other ions;

(3) excited metastables may produce ions further downstream from the ion source by Penning ionization; if primary ions are produced, erroneously low rate coefficients will be obtained, and if any other ions are produced, the product identification may again be made difficult;

(4) positive primary ions may undergo dissociative attachment further downstream from the ion source with the electrons present in the flow tube; this would cause the primary ion signal to decay quicker and thus yield er-

roneuosly high rate coefficients; excited neutrals and ions can be destroyed by superelastic collisions with electrons making study of these species difficult; and

(5) photons from the afterglow may cause a high background count rate by impinging upon the electron multiplier; in a SIFT there is no afterglow.

Thus, using a SIFT for the study of ion-molecule reactions can be very advantageous because it allows one to eliminate the above problems. However, the disadvantages of the SIFT are that the primary ion counts are often one to two orders of magnitude less than those in the FA, the range of accessible pressures is generally narrower, and the number of different buffer gases which can be used is limited. The drop in primary ion signal occurs because the primary ions face a high backpressure at the point of injection since they must travel from the low pressure region ($<10^{-5}$ torr) of the quadrupole chamber, to the high pressure region (0.1 to 1 torr) of the flow tube. The problem of maintaining an acceptable primary ion signal has been partially overcome in two ways. First, in a SIFT, the electron multiplier can be placed directly in line with the center of the flow tube because the ion source is not in the flow tube itself and no afterglow is produced. Thus, the drop in ion count rate resulting from placement of the multiplier off axis can be eliminated. Second, Adams and Smith[61] have designed a method of carrier gas injection in which the carrier gas flows through a series of small

openings which are located around the ion injection point and which are parallel to the ion beam. The result is that an aspirator effect helps to pull the ions from the low pressure to the high pressure region, resulting in an enhanced primary ion count rate as more ions are injected initially. The working flow tube pressure range in the SIFT is limited to approximately 0.1 to 1 torr as compared to 0.1 to several torr in the FA. Again this range is determined by the ability of the diffusion pumps to keep the detection chamber at pressures $< 10^{-5}$ torr, the ability to maintain a sufficient ion density for detection purposes, and the difficulty of injecting the ions against a backpressure at the point of injection. Finally the injection energy of these ions must be kept at low energies (3 to 10 eV)[61] to prevent possible fragmentation of the ion upon collision with the inert carrier gas. If nitrogen or argon is used for the carrier gas instead of hydrogen or helium, the problem of fragmentation becomes more severe. Thus the different types of buffer gases which can be used in a SIFT is limited.

In summary, the SIFT is phenomenologically different from the FA in that a single reactant ion is injected into the flow tube. This provides a much cleaner reaction system and thus gives one the ability to overcome many of the potential problems associated with a FA, and also allows the opportunity to study exotic ions which could not be studied using a FA. Operating conditions are, however,

somewhat more limited.

V. AFGL SIFT and Experimental Conditions

The variable temperature selected-ion flow tube at AFGL used for all of this work has been described previously.[63] In summary, the stainless steel flow tube is 108 cm long with a 7.3 cm inside diameter. There are three available reaction lengths of 75.8, 45.9, and 30.3 cm. The reaction length of 45.9 cm was used for this work. A heated rhenium filament was used for an electron emitter. Rhenium was chosen because of its resistance to attack by halogens, halocarbons, and hydrogen halides. The ions F^-, Cl^-, and Br^- were produced in a high pressure ion source by dissociative electron attatchment to SF_6, CCl_4, and CH_3Br respectively.

The carrier gas used in all cases was helium, which was passed through molecular sieve at liquid nitrogen temperature to remove any impurities. The helium was brought to the temperature of the flow tube before injection by passing it through 0.125 in. stainless steel tubing which was clamped on to and ran the length of the flow tube. The helium flow range was typically 6 to 9 slm. All gas flows were measured and controlled by linear mass flow controllers. The flow controllers were calibrated for N_2 at 21 ^oC and flows of other gases were corrected for by multiplying the meter reading by the appropriate gas correction factor. This correction factor is determined by the method of heat

capacity ratios.[64] The accessible flow tube pressure range was 0.3 to 0.9 torr and pressure in the reaction zone was measured by a differential capacitance manometer. The accessible temperature range was 219 to 410 K and was measured by five Pt resistance thermometers placed along the flow tube. For temperatures > 353 K the flow tube was heated by five heaters clamped and spaced evenly along a copper jacket surrounding the flow tube. The control of the precision of the temperature was less than that of the circulating baths. For temperatures greater than room temperature but < 353 K, heated water was circulated through 0.25 in. copper tubing soldered to the copper jacket. A Neslab "Exocal" high temperature circulating bath was used for circulating the water and controlling the temperature to within $\pm$ 4 ^{o}C. For temperatures less than room temperature but > 219 K, chilled methanol was circulated through the copper tubing by a Neslab "Endocal" low temperature circulating bath which maintained the temperature at $\pm$ 4 ^{o}C.

The gases used for this work were BF_3, BCl_3, SF_4, SF_6, SiF_4, and CH_3Br. All of the above gases were obtained from Matheson with the exception of SF_4 which was obtained from Air Products Inc. No further purification of the gases was attempted. The BF_3, BCl_3, SiF_4, and SF_4 lecture bottles (the neutral reactants) were placed in a dry ice/methanol bath in an effort to condense any impurities before withdrawing the gas into the manifold. Reagent grade CCl_4,

the neutral source gas for Cl^- ions, was obtained from Fischer and was purified by the freeze/pump/thaw method.

Rate coefficients were determined from plots of the logarithm of the decay of the primary ion signal as a function of added neutral reactant as described earlier. An Apple II computer with an ISAAC interface was used to control the operation of the SIFT during an experiment, and to facilitate data collection and manipulation.

CHAPTER 3

DATA ANALYSIS

I. INTRODUCTION

The analysis of experimental data for determination of the magnitude of the temperature dependence, n, along with the individual parameters and rate coefficients such as β , k_d, and k_r constituting the mechanism, was done as described below.

II. Determination of the Magnitude of the TD, n.

The values of n were determined three different ways. (a). The first method involves use of the experimental data contained herein i.e., from k_{obs} at various (He) and different temperatures, one can utilize the following equation:

$$k_{obs} = AT^{-n} \quad . \qquad (3.1)$$

Upon taking the log of both sides the result is:

$$\log k_{obs} = \log A - n(\log T) \quad . \qquad (3.2)$$

From a plot of $\log k_{obs}$ vs. $\log T$ the value of n was determined from the slope of the line as found by a least squares fit. The log of the preexponential factor was of course the intercept as determined by the least squares fit. It should be noted that since the data was assumed to lie in the fall-off region, the entire expression for k_{obs} as given by expression (1.8) had to be considered. In

order to utilize equation (3.1), which as shown is only a function of temperature, only values of k_{obs} with the same (M) were chosen for the different temperatures. This must be done because k_{obs} is a function of pressure as well as temperature, therefore use of equation (3.1) for evaluation of n must be done at constant (M). Also, only those values of k_{obs} that had constant (M) for at least three different temperatures were chosen. It was felt that with three temperatures less error would be introduced in determination of n as opposed to using only two temperatures.
(b). Values of n were determined from the slope of a plot of log k_d vs. log T. Assuming the simple functional form for $k_d(T)$:

$$k_d(T) = AT^n \quad , \tag{3.3}$$

we used the same procedure as described above for k_{obs} to determine n and A. It should be noted that even though the functional form describing the temperature dependence of k_{obs} and $k_d(T)$ is the same, the preexponential factor, A, and the exponent, n, are not and should not be considered the same. The values for k_d, the unimolecular decay rate coefficient at the different temperatures implemented in this study, were determined by the method outlined below.
(c). Finally, n was determined theoretically using the modified thermal model in which vibrational contributions were considered active in the cases where $h\nu >> kT$, was <u>not</u> true. Expression (1.21) was utilized to evaluate "$k^{(3)}$"

(where "$k^{(3)}$" includes only the temperature terms in each partition function, and so it is not the actual low pressure third order rate coefficient, $k^{(3)}$, but rather some multiple of it) at 50 K intervals in the temperature range from 200 to 450 K. The value of n, the magnitude of the temperature dependence, was determined from the slope of a plot of log "$k^{(3)}$" vs. log T at each 50 K interval. Evaluation of n was done over the above temperature range with the number of active modes being varied from 0 to the maximum 3N - 6 possible modes for a non-linear molecule.

III. Determination of β, k_d, and k_r

As mentioned above, it was found that the low pressure assumption was not valid for our data and therefore the entire expression for k_{obs} was used for evaluation of β, k_d, and k_r. With this approach, potentially faulty conclusions resulting from extrapolation outside of our pressure and temperature range of study were avoided.

Recall expression (1.10) for the apparent bimolecular rate coefficient where a radiative stabilization pathway was included:

$$k_{obs} = \frac{k_a(\beta k_s(M) + k_r)}{k_d + \beta k_s(M) + k_r} \quad . \qquad (1.10)$$

The following assumptions were made for evaluation of β, k_d, and k_r:

(a) k_a and k_s were assumed to be equal to the Langevin or

ADO rate coefficients as appropriate, where k_a was evaluated as the collision rate between the ion and neutral molecule, and k_s was evaluated as the collision rate between the excited complex and the inert third body, M (see the Appendix for the neutral polarizabilities and calculated Langevin and ADO collision rates);

(b) β and k_r were assumed <u>not</u> to be functions of temperature over the narrow temperature and pressure range of this study (i.e. we assumed all of the temperature dependence of k_{obs} lies in k_d);

(c) k_d was assumed to be independent of pressure over our narrow pressure range of 0.2 to 0.8 torr. Although k_d is actually pressure dependent it has been shown that over a narrow pressure range as described above any changes in k_d due to pressure should be negligible.[25,28]

(d) lastly, the assumption was made that k_{obs} at (M) = 0 is given by $k_a k_r/(k_d + k_r)$. This last assumption is discussed in detail below.

In some of the systems studied ($BF_3 + F^-$, Cl^-, and $BCl_3 + Cl^-$) data from the previous study by Babcock and Streit[4], along with data from a low pressure technique[65] (Ion Cyclotron Resonance) was used to evaluate k_{obs} at room temperature at zero pressure, i.e. where $k_{obs} = k_a k_r/(k_d + k_r)$. By knowing the intercept at (M) = 0, and using $k_a = k_{Langevin}$, then k_r can be shown to equal some fraction of k_d as given by:

$$k_r = \frac{(k_{obs,\ 298}/k_a)}{(1 - k_{obs,\ 298}/k_a)}(k_{d,\ 298}) \quad , \qquad (3.4)$$

or, rewriting the above expression, one obtains:

$$k_r = Ck_{d,\ 298} \quad . \qquad (3.5)$$

By substituting $Ck_{d,\ 298}$ for k_r in expression (1.10), an expression for k_{obs} is then obtained with only two unknown parameters, β and k_d, as given below:

$$k_{obs} = \frac{k_a(\ \beta\ k_s(M) + Ck_d)}{k_d(1 + C) + \beta\ k_s(M)} \quad . \qquad (3.6)$$

The 298 subscripts were dropped for clarity, but k_{obs} and k_d at 298 K were used used for calculations. Using the above equation, the ratio k_d/β can be calculated again at 298 K. Since $k_r = Ck_{d,\ 298}$, and the ratio k_d/β can be determined, if k_d or k_r were known, the other two parameters could be determined. As mentioned, calculation of k_d and k_r from sophisticated theories is not trivial. Values of k_d/β were determined from equation (3.6) using data of k_{obs} at various pressures and 298 K for M = He and when available, for M = N_2, CO_2, CH_4, and CF_4. For the cases in which different buffer gases were employed the relative efficiencies of these gases were determined by assuming $\beta = 1$ for the polyatomic with the highest molecular weight. This places an upper limit on β_{He} which is used for further analysis of data in this work. For systems in which M = He only, an upper limit of β_{He} was set by comparison of

systems with similar molecular complexity and total molecular weight.

Once the upper limit for β_{He} was determined, $k_{d,\ 298}$ was calculated by multiplying the value of $k_d/\ \beta$ for He by the upper limit of β_{He} as evaluated from the relative efficiencies. Then from the expression of $k_r = Ck_{d,\ 298}$, a value of k_r was calculated. Once k_r and β were set, equation (3.6) was used to calculate an average k_d at the other temperatures using the experimental data of k_{obs} at various (He). The values of β_{He} were varied to investigate its effects upon k_d and thus k_r (since only their ratio is measured). The temperature dependence of k_d was determined as described in part (c) of section 1 above.

For systems where the radiative contribution appeared to be very small or nonexistent, the same general method as above was followed except that k_r was naturally set equal to zero.

Finally, once values for β, k_d, and k_r could be set at all temperatures, values of k_{obs} at various (He) were generated for different values of β_{He} to compare the experimental plots of k_{obs} vs. (He) with those generated from expression (1.10). A detailed example of this method is given in the results section for the system $BF_3 + F^-$.

In summary, the magnitude of the temperature dependence, n, of the rates ion-molecule association systems studied herein was determined three different ways: (1) from the slope of a plot of log k_{obs} vs. log T at constant

(He), (2) from calculations using a modified thermal theory which included vibrational contributions, and (3) from the slope of a plot of log k_d vs. log T where k_d was determined as described above. The values of β, k_d, and k_r were determined by considering the entire expression governing the fall-off region which avoided extrapolation outside of the pressure and temperature ranges studied. Lastly, plots of k_{obs} vs. (He) at various temperatures were generated using the values of β, k_d, and k_r determined from the above procedure, and these were compared to experimental results over the entire pressure and temperature range employed.

GENERAL INTRODUCTION TO CHAPTERS 4, 5, AND 6

The ion-molecule systems examined in this dissertation are:

$BF_3 + F^-$	$SiF_4 + F^-$
$BF_3 + Cl^-$	$SiF_4 + Cl^-$
$BF_3 + Br^-$	$SiF_4 + Br^-$
$BCl_3 + Cl^-$	$SF_4 + F^-$
$BCl_3 + Br^-$	$SF_4 + Cl^-$
	$SF_4 + Br^-$.

The ion-molecule system $BCl_3 + F^-$ was not studied because it has been shown that this reaction proceeds via an exothermic bimolecular pathway in which F^- displaces Cl^- which reacts further with BCl_3 to produce BCl_4^-; the neutral is presumed to be BCl_2F.[4] The above systems were studied over a pressure range from 0.2 to 0.8 torr and over a temperature range from 219 K to 410 K. In all cases the inert third body or buffer gas was He. Naturally, some of the pressure and temperature ranges were further limited depending upon the specific characteristics of the system. Each system displays the same general type of behavior in that k_{obs} increases with increasing pressure, although some systems display no pressure dependence; also k_{obs} generally increases with decreasing temperature as predicted for IM association reactions. This behavior is readily seen by examination of experimental plots of k_{obs} vs. (He) at

various temperatures: figures (4.1), (4.2), (4.4) - (4.9), (4.11) - (4.14), (4.16) - (4.18), (5.1) - (5.4), (5.6), (5.7), and (6.1) - (6.3).

In the Results section for each system the following is presented:

1.) plots of k_{obs} vs. (He) of the data (as represented by the symbols) along with computer generated lines for $k_{obs}(M,T)$ (as represented by lines), demonstrating the characteristics of each system;

2.) tables of k_d/β for various third-bodies, M, (where applicable) with corresponding relative collisional efficiencies, β ;

3.) tables of $k_{d,\ 298}$ with the corresponding values of k_r (where applicable) at various values of β ;

4.) tables of calculated average k_d's at the different temperatures studied for various values of β ;

5.) tables of n, the magnitude of the temperature dependence, as calculated by the three methods described in the Data Analysis section;

6.) and finally, plots of log k_{obs}, log k_d, and log "$k^{(3)}$" vs. log T.

Tables of k_{obs} vs. (He) data at each different temperature studied are located in Appendix (1) - Appendix (12). The Results and Discussion chapter is divided into four separate sections. The Results and Discussion of all the boron trihalide systems is presented first followed by separate Results and Discussion sections for the silicon

tetrafluoride and sulfur tetrafluoride systems. Lastly a general discussion of all the systems is presented in the Conclusions and Future Work chapter.

CHAPTER 4

RESULTS AND DISCUSSION OF THE HALIDE ION-BORON TRIHALIDE SYSTEMS

I. The Boron Trihalides

The boron trihalides, BF_3 and BCl_3 are trigonal planar molecules. Previous studies of the ion chemistry of these systems is not extensive, with the Lewis acidity properties[66] and the negative ion spectra of BF_3 and BCl_3[67,68] having been examined. The molecule BF_3 has been shown to possess multiple bonding[69,70] which results from the overlap of the empty p-orbital of boron with the p-orbitals of the three fluorine atoms. This bonding in BX_3 is thought to decrease as the halogen size increases because of less effective overlap of the p-orbitals.

Closed shell tetrahedral anions are formed when a negative ligand such as a halogen ion adds to BX_3 as shown below:

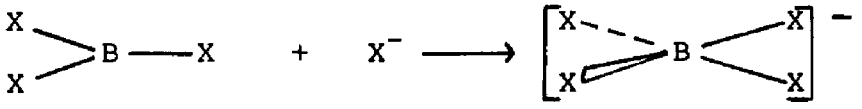

Because these systems form known chemical species which are thermodynamically more stable than the separated reactants, they are ideally suited for the study of ion-molecule association reactions as performed for this dissertation.

II. $BF_3 + F^-$ Results

(a). General Results

This system was studied over a pressure range from 0.3 to 0.8 torr and at five different temperatures: 409, 348, 298, 248, and 219 K. The only product observed was BF_4^- except at the two lowest temperatures, 248 and 219 K, where the cluster product $BF_4^- BF_3$ was also observed. The data of k_{obs} at various (He) at the five temperatures studied is given in Table (A1) in the appendix. Plots of experimental and calculated k_{obs}'s vs. (He) are shown in figures (4.1) and (4.2). Note the negative dependence of k_{obs} upon temperature and its positive dependence upon pressure.

(b). Results for the Calculation of β, k_d, and k_r.

The rate coefficients k_d and k_r and the collisional stabilization efficiency factor, β , were calculated as shown below.

For this system, $BF_3 + F^-$, we had two separate pieces of data that allowed us to determine k_{obs} at (M) = 0 (i.e., the intercept of a plot of k_{obs} vs. (M)). First, plots of k_{obs} vs. (M) where (M) = He, N_2, CH_4, and CF_4 over the pressure range 0.15 to 0.40 torr for all M except He where the pressure range was 0.15 to 1.0 torr, displayed a linear dependence upon (M) and all showed a common intercept of 9.0×10^{-10} cm^3 $molec^{-1}$ s^{-1}. [4] Second, from the low pressure ion-molecule technique Ion Cyclotron Resonance (ICR),

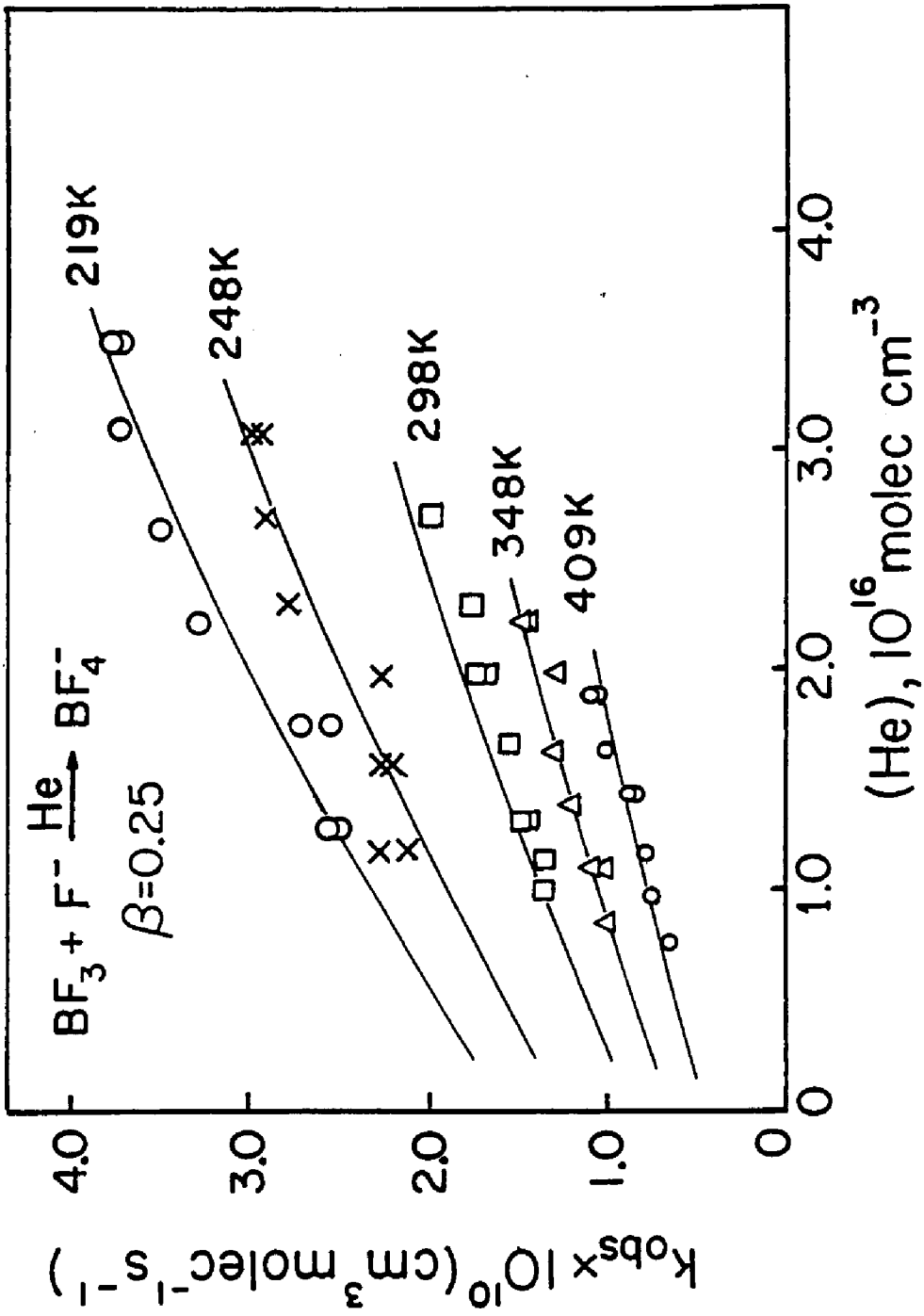

Figure 4.1. Pressure and temperature dependence of k_{obs} for halide ion addition.

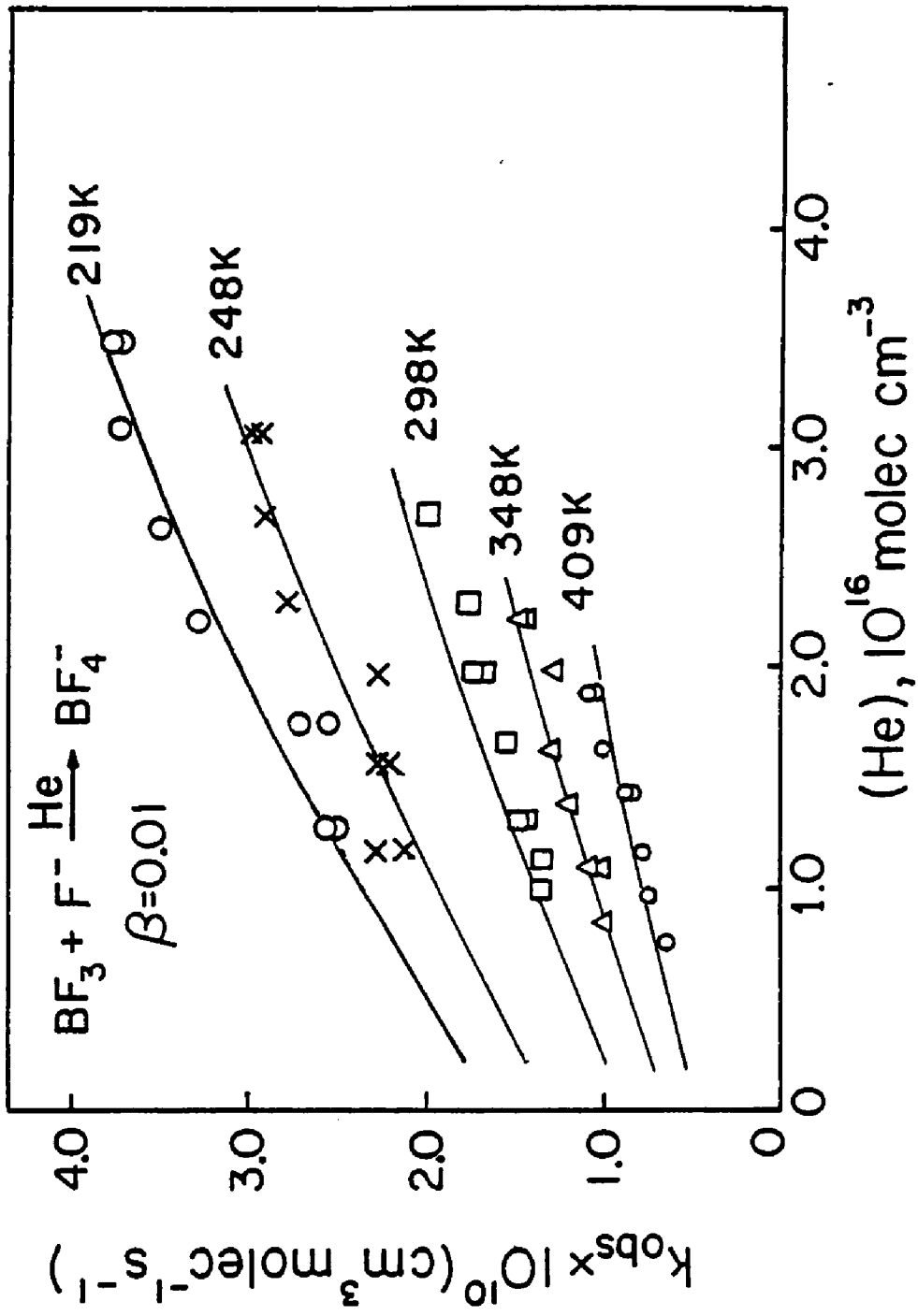

Figure 4.2. Pressure and temperature dependence of k_{obs} for halide ion addition.

k_{obs} was found to be on the order of 10^{-10} cm^3 $molec^{-1}$ s^{-1} at a pressure of 10^{-6} torr.[65] Since the ICR value is in agreement with the Flowing Afterglow value over a pressure range covering five orders of magnitude, we feel confident that the value for k_{obs} at (M) = 0 is good and does not contain significant error due to extrapolation outside of the experimental range of pressures. Using equation (1.10) with (M) =0 gives:

$$k_{obs} = \frac{k_a k_r}{k_d + k_r} \quad . \qquad (4.1)$$

Using the intercept data at 298 K, k_{obs} = 9.0 X 10^{-10} cm^3 $molec^{-1}$ s^{-1}, and using k_a = 1.11 X 10^{-10} cm^3 $molec^{-1}$ s^{-1} ($k_{Langevin}$ for $BF_3 + F^-$), we find that $k_r = 0.09k_{d,\ 298}$. Next, by substituting $0.09k_{d,\ 298}$ for k_r in eqution (1.10) along with k_a for $BF_3 + F^-$ and k_s for the BF_4^-/He couple, (where $k_a = k_{Langevin}$ and $\beta k_s = \beta k_L$) we obtain equation (4.2) which is:

$$k_{obs} = \frac{(1.11X10^{-9})(\ \beta\,(5.42\ X\ 10^{-10})(He) + 0.09k_d)}{1.09k_d + \quad \beta(5.42X10^{-10})(He)} \qquad (4.2)$$

The values of k_{obs} and k_d used are all at 298 K. The only unknown parameters are k_d and β , and by using the experimental values for k_{obs} at various (He) at 298 K an average k_d/β for He can be calculated. The data at 298 K was used because this is the temperature at which all the third-body data was taken and consequently where the ratio k_d/k_r was

determined. A short BASIC program was written to facilitate calculations. The same procedure was followed for the other third-bodies, N_2, CH_4, and CF_4, at 298 K. In this manner k_d/β for each third-body can be calculated and relative β's obtained. The most efficient third-body is expected to be CF_4, and if we set β for this gas equal to unity, we set k_d and thus β for the other third bodies as follows:

$$\left(\frac{k_d}{\beta}\right)_{CF_4} \Big/ \left(\frac{k_d}{\beta}\right)_M = (\beta)_M \quad . \tag{4.3}$$

With the assumption $\beta_{CF_4} = 1$, k_d was found to be 2.42×10^7 s^{-1}. The value of k_d/β_{He} determined from the data was found to be 9.65×10^7 s^{-1}. By substitution into equation (4.3) we obtain:

$$\frac{2.42 \times 10^7}{\beta_{He}} = 9.65 \times 10^7 \quad ; \tag{4.4}$$

the solution yields an upper limit of $\beta_{He} = 0.25$. This is an upper limit since $\beta_{CF_4} = 1$ is an upper limit (recall $0 \leq \beta \leq 1$). This same procedure was used to calculate for the other buffer gases. Average values of k_d/β along with the values of β relative to $\beta_{CF_4} = 1$ for these gases are shown in Table (I). The fact that β must be decreasing as the molecular comlexity of the third-body decreases is seen from the order of k_d/β_{He} for the various third-bodies. As the molecular complexity of the third-body decreases the value of k_d/β increases. Since k_d is

assumed to be independent of the identity of M, then must be decreasing for k_d/β to be increasing as M is varied. The values of β listed in Table (I) are upper limits, for if β_{CF_4} is actually somewhat less than unity then the other β's will also be lowered accordingly.

To calculate k_r, $k_{d,\ 298}$ was first determined by multiplying the k_d/β ratio for He by β_{He}. Once k_d is known, k_r is easily calculated since we know $k_r = 0.09k_{d,\ 298}$; k_r was found to be $2.17 \times 10^6\ s^{-1}$ for $\beta_{He} = 0.25$. Table (II) lists the values of $k_{d,\ 298}$ and k_r calculated for different values of β_{He}. Values of β_{He} were varied because as stated $\beta_{He} = 0.25$ is an upper limit. Also we wanted to examine the effect of smaller values of β_{He} since values of β_{He} as low as 0.1 and 0.03 have been reported.[17,18] In varying β_{He}, the absolute value of k_d changes because we measure the ratio of the two and since we also determine only the ratio k_d/k_r, the absolute value of k_r also changes.

After evaluation of β_{He}, k_d, and k_r is completed at 298, k_d can be determined at the other four temperatures studied for this system. Recall that we are assuming β_{He}, and k_r to be independent of temperature. Values of k_d were computed by using equation (1.10). Making the appropriate substitutions we obtain equation (4.5):

$$k_{obs} = \frac{(1.11\times10^{-9})[0.25(5.42\times10^{-10})(He) + 2.17\times10^{6}]}{k_d + (0.25)(5.42\times10^{-10})(He) + 2.17\times10^{6}}. \quad (4.5)$$

TABLE I

A Experimentally Determined Average Values of k_d/β at 298 K for $BF_3 + F^- \longrightarrow BF_4^-$

M	k_d/β , s^{-1}	β_{rel}
He	9.65×10^7	0.25
Ar	5.17×10^7	0.47
N_2	3.38×10^7	0.71
CH_4	4.23×10^7	0.57
CF_4	2.42×10^7	1.00

TABLE II

Radiative and Decomposition Rates Coefficients for $(BF_4^-)^*$ at 298 K Based on β_{He} Values

β_{He}	$k_{d,\,298}$, s^{-1}	k_r, s^{-1}
0.25	2.41×10^7	2.17×10^6
0.15	3.61×10^6	3.25×10^5
0.01	9.65×10^5	8.69×10^4

Note that a $\beta = 0.25$ and $k_r = 2.17 \times 10^6$ were chosen. An average k_d was evaluated by substituting the values of k_{obs} at various (He) at the different temperatures and solving for $k_d(T)$. A short BASIC program was written to facilitate these calculations. The change in k_d as (He) increased for a given T showed no detectable trend to within $\pm$ 15% of the average value, demonstrating that our assumption of k_d being independent of pressure over our narrow pressure range is justified. Again β_{He} was varied for investigative purposes. The average k_d's calculated at the five experimental temperatures and three different β's are shown in Table (III). As a check to see how well the calculated β's, k_d's, and k_r's reproduce our experimental data, values of k_{obs} at various (He) at the five different temperatures studied were generated. Again a short BASIC program was written to faciltate the above procedure. The solid lines shown in figures (4.1) and (4.2) are plots of the generated k_{obs} vs. (He) at two different β_{He}'s. The symbols are the actual experimental values of k_{obs} vs. (He). Note the good agreement.

(c). Results for the Magnitude of the TD, n.

As discussed in the Data Analysis section, the magnitude of the temperature dependence, n, was evaluated three ways: (1) from experimental data at constant (He), (2) from values of k_d as calculated at the five different temperatures from the method described above, and (3) from

TABLE III

Average Values of $k_d(T)$ for Different Values of β_{He} for BF_4^-

Temp., K	$^{a}k_d$, s^{-1}	$^{b}k_d$, s^{-1}	$^{c}k_d$, s^{-1}
409	4.66×10^7	2.79×10^7	1.87×10^6
348	3.43×10^7	2.05×10^7	1.37×10^6
298	2.70×10^7	1.62×10^7	1.06×10^6
248	1.68×10^7	1.01×10^7	6.72×10^5
219	1.33×10^7	7.96×10^6	5.31×10^5

a $\beta_{He} = 0.25$

b $\beta_{He} = 0.15$

c $\beta_{He} = 0.01$

a simple theory in which vibrational contributions are considered.

For the constant value (He) = 1.95 X 10^{16} molec cm^{-3}, k_{obs} was measured at 248, 298, and 348 K as shown in Table (IV). For this constant (He), a plot of log k_{obs} vs. log T yielded n = 1.6 as shown in Figure (4.3).

The change in k_d with temperature is given in Table (III). A plot of log k_d vs. log T yielded n = 2.0 as shown in Figure (4.3). Note that as β changes the value of n remains constant. Again as pointed out in the data analysis chapter, the values of n determined from k_{obs} and from k_d data should not be expected to yield the same results since k_{obs} is a complex function of temperature and pressure while k_d, at least over our narrow pressure range, is considered to be a function of temperature only.

The value of "$k^{(3)}$" as calculated from theory has no real meaning because its evaluation involved only the use of the temperature dependent portion of the partition functions, so "$k^{(3)}$" determined differs from the actual rate coefficient by some factor. Thus "$k^{(3)}$" was not tabulated. However, the values of n were tabulated and range from 1.79 in the region from 200 to 250 K with contribution from only one vibrational mode, to 2.77 in the range 400 to 450 K with all vibrations considered active. The change of n in which all vibrational modes are considered active is also plotted in Figure (4.3).

Recall that we are expressing the temperature depen-

TABLE IV

Values of k_{obs} at Constant (He) at Different Temperatures for BF_4^-

T, K	(He)	k_{obs}
348	1.95	1.35
298	1.95	1.70
248	1.95	2.28

(He) units: 10^{16} molec cm^{-3}

k_{obs} units: 10^{-10} cm^3 $molec^{-1}$ s^{-1}

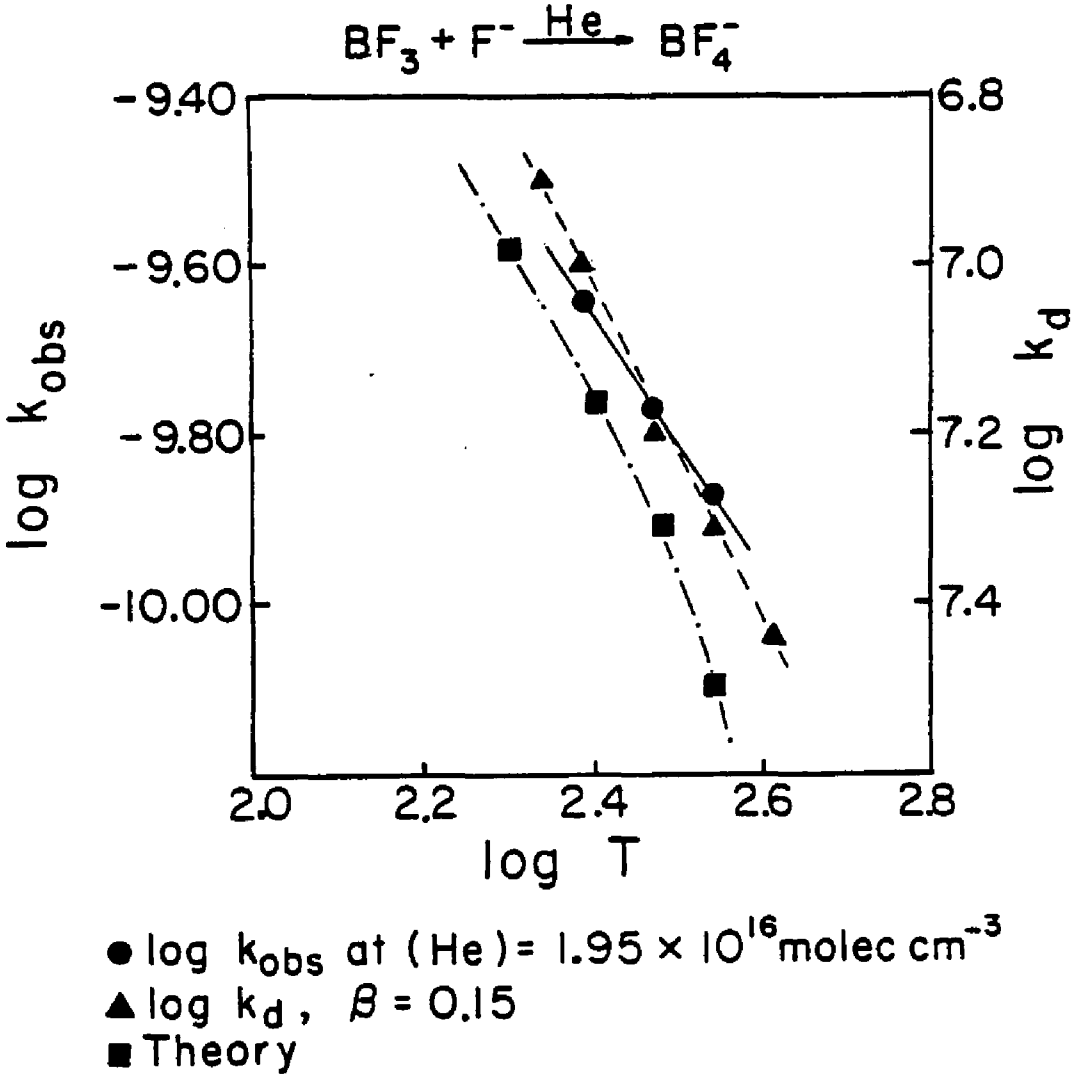

Figure 4.3. Temperature dependence of ion-molecule association reactions.

dence as some preexponential factor , A, multiplied by the temperature raised to some power, n. In Tables (V) and (VI) the values of the preexponential factor and n are listed for k_{obs} and $k_d(T)$ as calculated from equation (4.5). Table (VII) lists the values of n calculated over 50 K intervals with varying vibrational contributions as indicated.

TABLE V

Temperature Dependence of k_{obs} for BF_4^-

A	n
$10^{-5.97}$	1.5

TABLE VI

Temperature Dependence of k_d for BF_4^-

β_{He}	A	n
0.25	$10^{2.37}$	2.0
0.15	$10^{2.16}$	2.0
0.01	$10^{0.96}$	2.0

A units: cm^3 $molec^{-1}$ s^{-1}

TABLE VII

A Compilation of Calculated n Values Demonstrating Vibrational Contributions for $BF_3 + X^-$

Temp. Range, K	a_n	b_n	c_n	d_n
200-250	1.79	1.85	1.87	1.87
250-300	1.94	2.04	2.09	2.09
300-350	2.07	2.22	2.30	2.32
350-400	2.19	2.39	2.51	2.55
400-450	2.29	2.54	2.70	2.77

[a]Frequencies: 480(2) cm^{-1}

[b]Frequencies: 480(2), 691 cm^{-1}

[c]Frequencies: 480(2), 691, 888 cm^{-1}

[d]Frequencies: 480(2), 691, 888, 1446(2) cm^{-1}

Vibrational frequencies are from:

JANAF "Thermochemical Tables" 2nd ed. NSRDS-NBS 37 June 1971, Washington, D.C.

III. $BF_3 + Cl^-$ Results

(a). General Results

This system was studied over the pressure range from 0.2 to 0.8 torr and at four different temperatures: 348, 298, 248, and 219 K. The main association product produced was BF_3Cl^- with the cluster product, $BF_3Cl^- \cdot BF_3$, observed at 248 and 219 K. Another mass at~153 amu was also observed at these lower temperatures. It is thought to be the cluster product $BF_4^- \cdot BF_3$ resulting from a ligand exchange with the cluster $BF_4^- \cdot BF_2Cl$. This is elaborated on further in the discussion section. In any event, these cluster products are secondary products and do not affect the overall binary rate coefficient. Table (A2) in Appendix (2) lists k_{obs} at various (He) at the four different temperatures studied. Figures (4.4), (4.5), (4.6), (4.7), (4.8), and (4.9) present plots of the tabulated data along with k_{obs} calculated for various (He) by the method described in the data analysis section with and without a radiative stabilization pathway.

(b). Results for the Calculation of β , k_d, and k_r.

For this system, $BF_3 + Cl^-$, plots of k_{obs} vs. (M) done previously[4] where M = CO_2, N_2, and He over the pressure range from 0.15 to 0.4 torr for CO_2 and N_2 and 0.3 to 1.0 torr for He, gave an average intercept of 0.5 X 10^{-11} cm^3 $molec^{-1}$ s^{-1}. [4] Low pressure ICR data to corroborate our

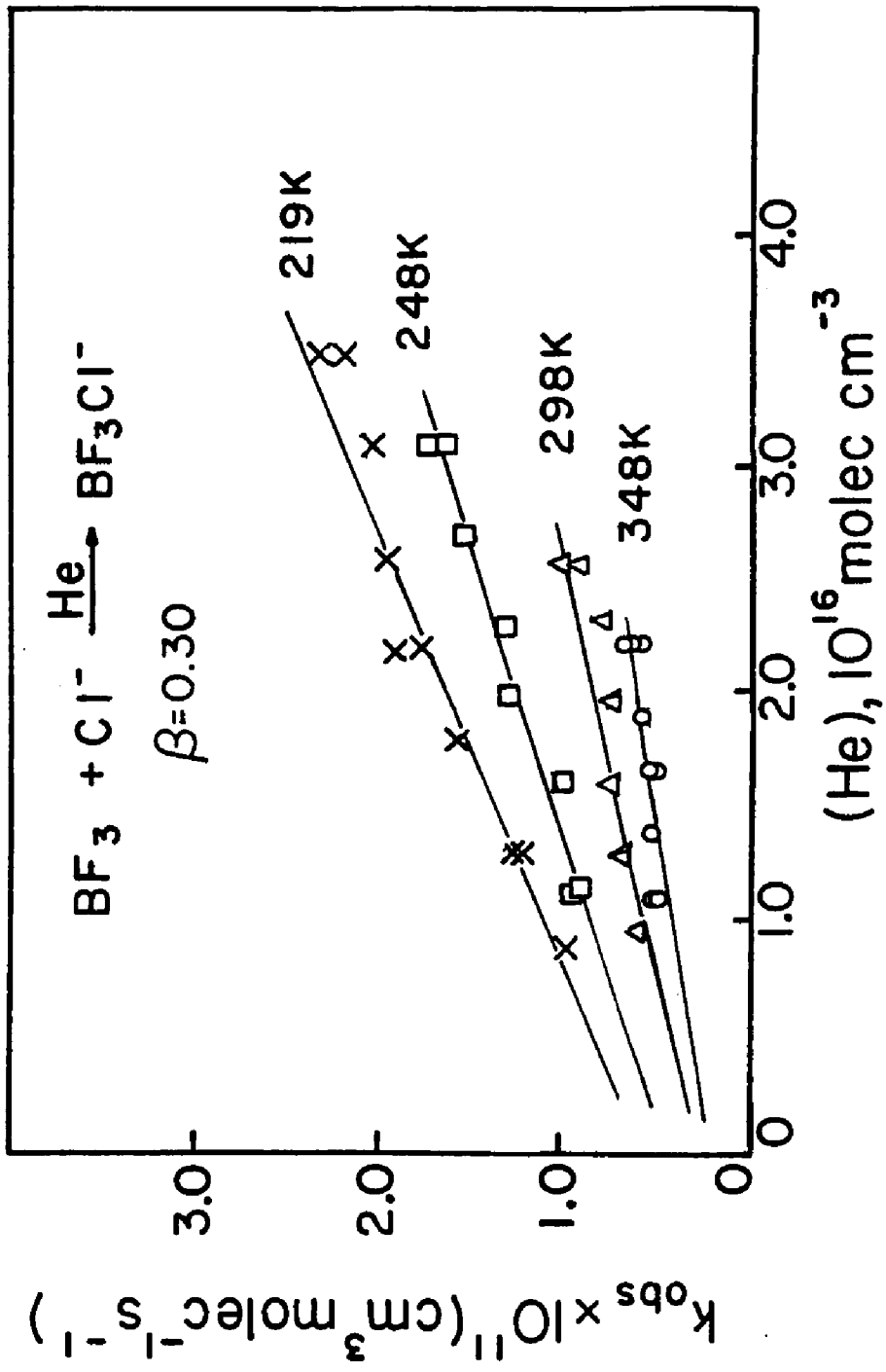

Figure 4.4. Pressure and temperature dependence of k_{obs} for halide ion addition.

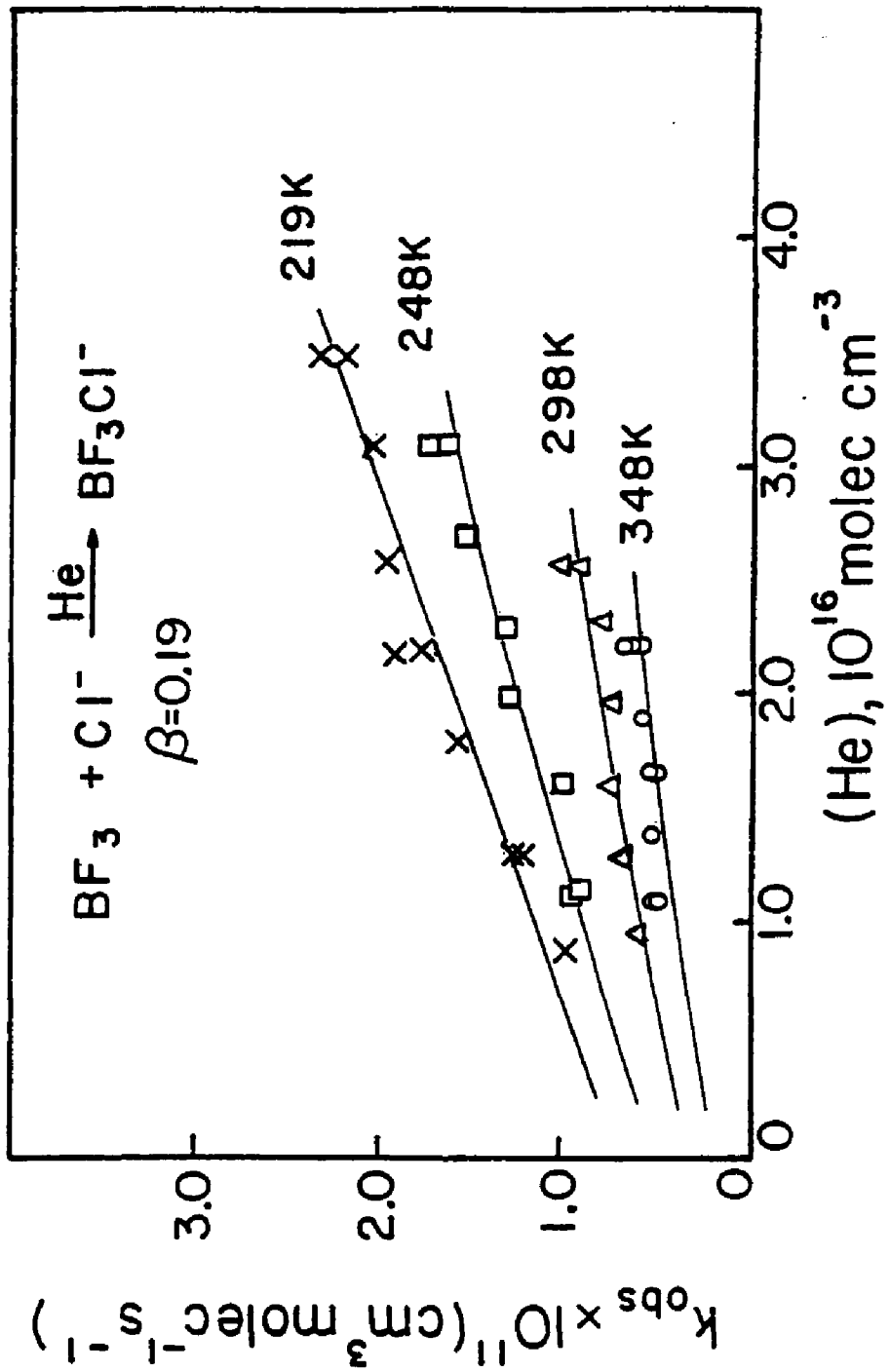

Figure 4.5. Pressure and temperature dependence of k_{obs} for halide ion addition.

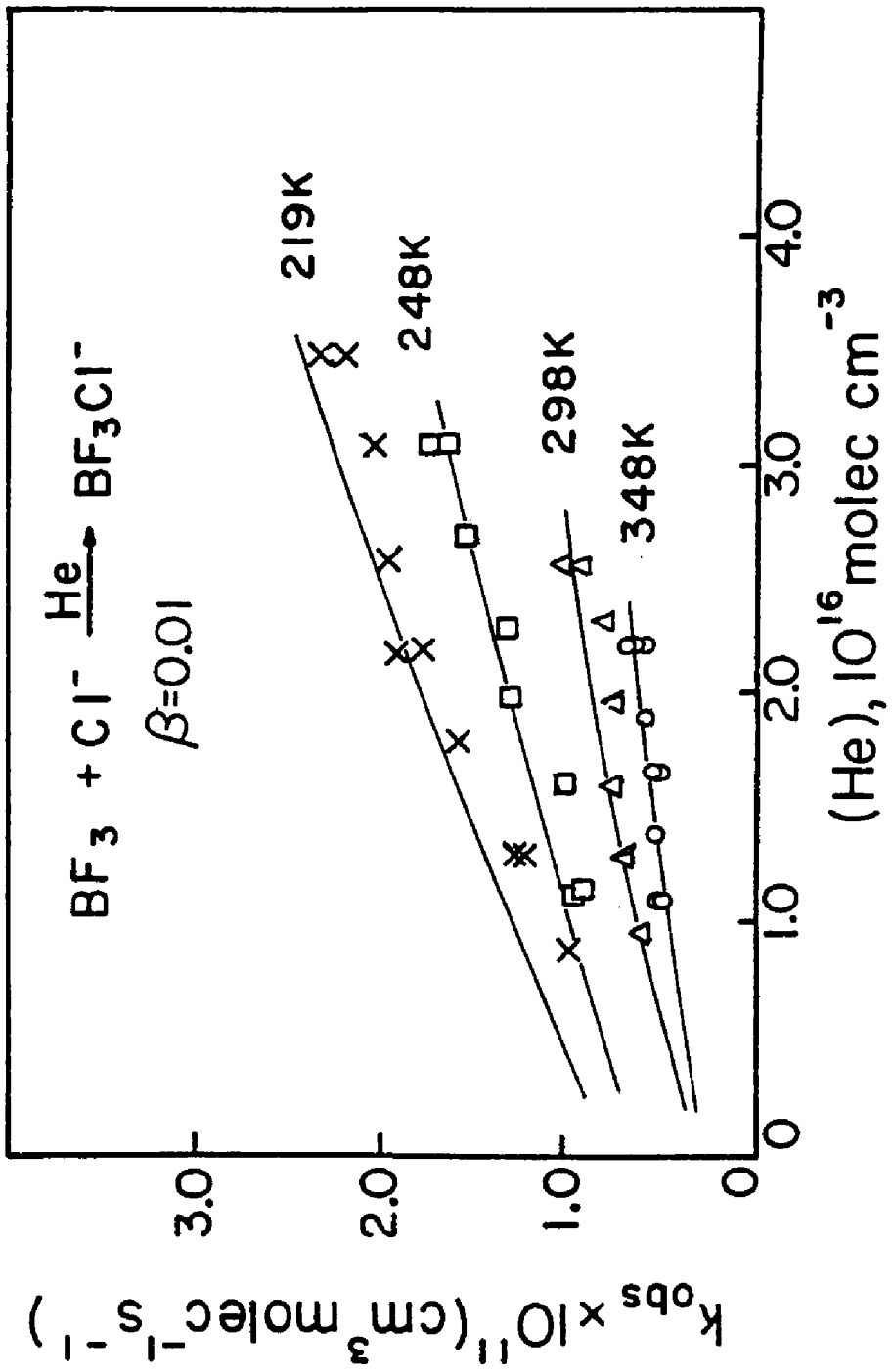

Figure 4.6. Pressure and temperature dependence of k_{obs} for halide ion addition.

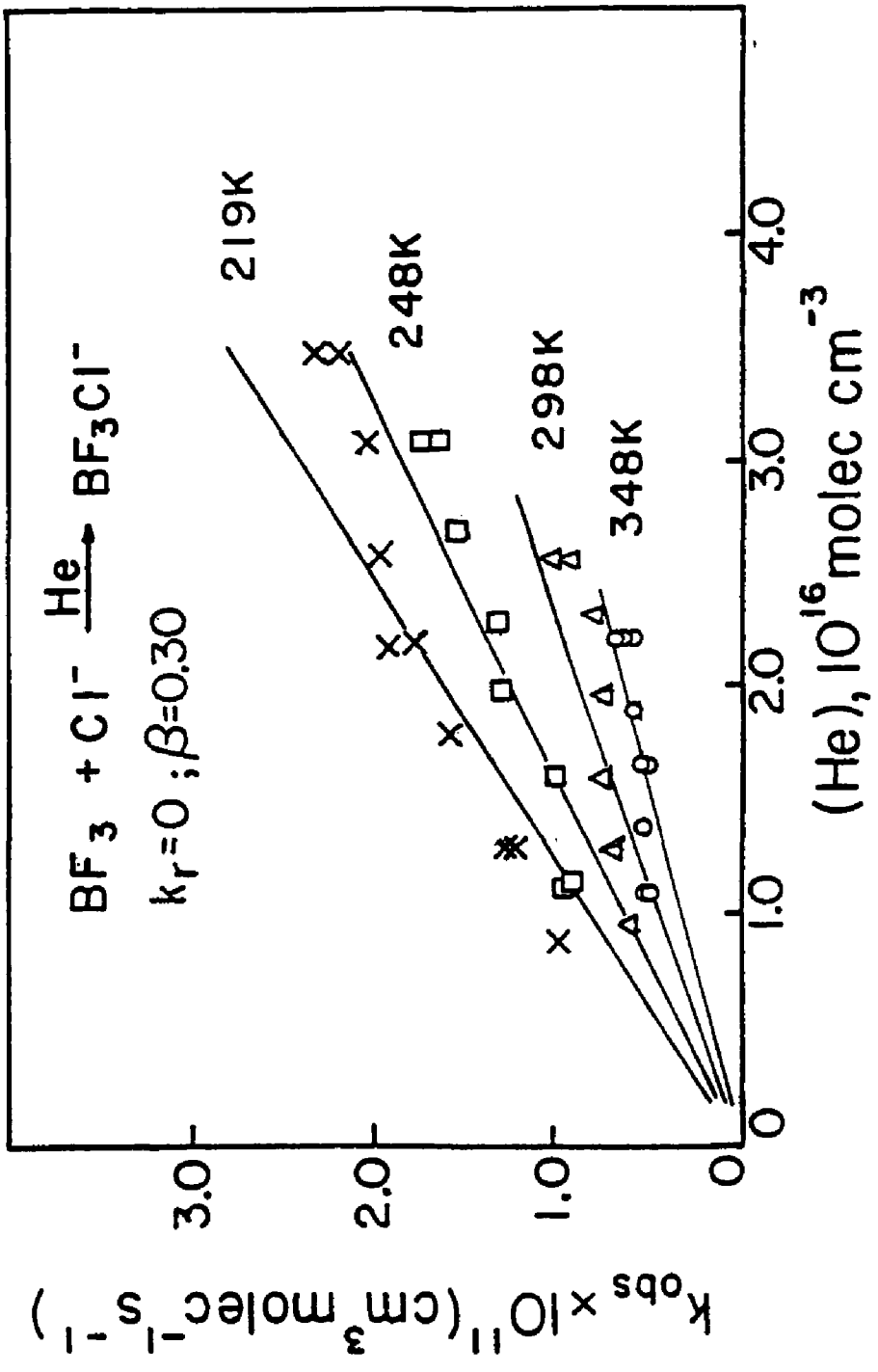

Figure 4.7. Pressure and temperature dependence of k_{obs} for halide ion addition.

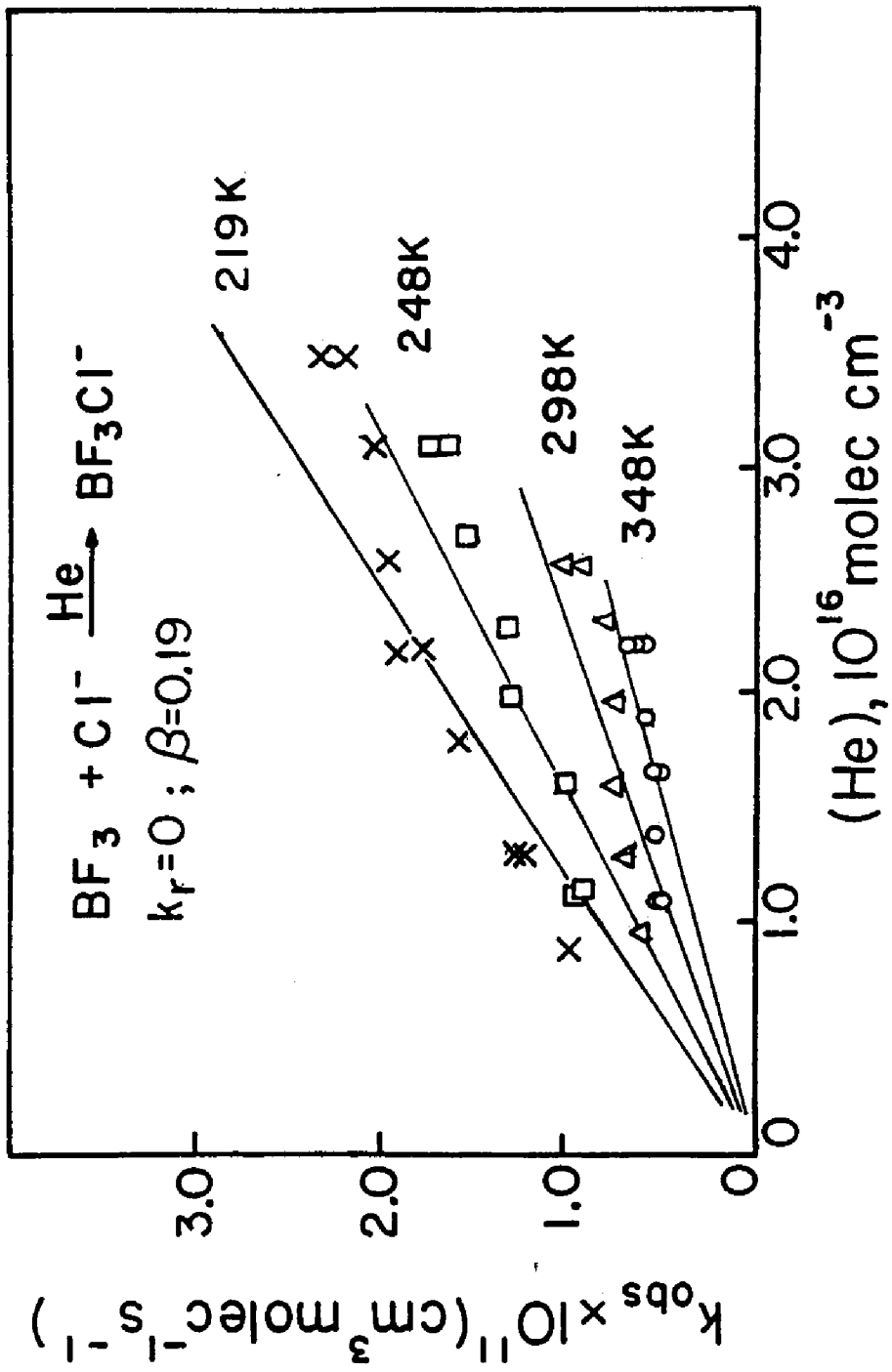

Figure 4.8. Pressure and temperature dependence of k_{obs} for halide ion addition.

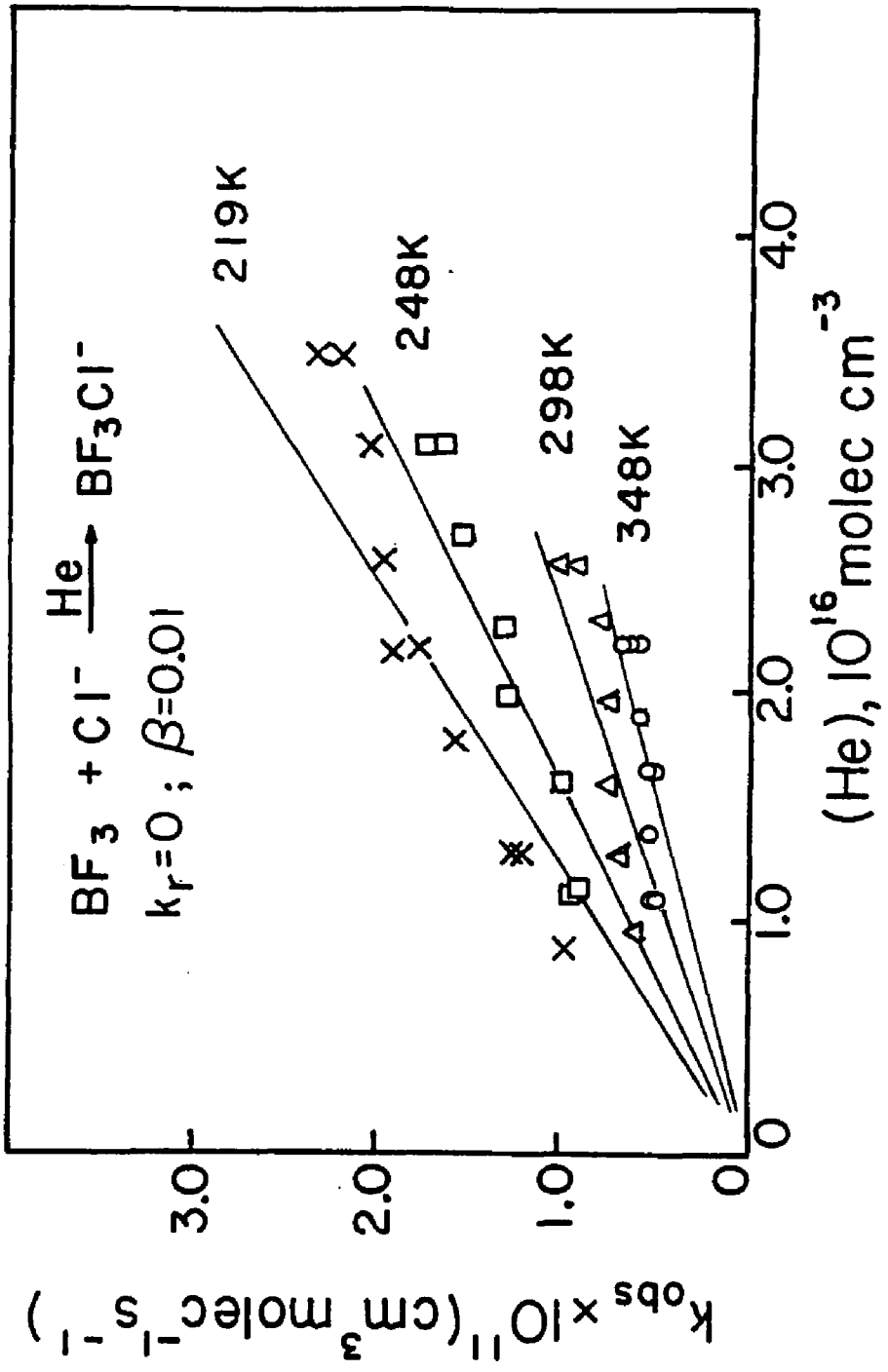

Figure 4.9. Pressure and temperature dependence of k_{obs} for halide ion addition.

value for k_{obs} at (M) = 0 for this system is not available. Certainly, though, one would not expect the value for the intercept to be any larger than listed above which sets an upper limit for the k_r/k_d ratio. Calculation using an intercept of 0.5 X 10^{-11} cm^3 $molec^{-1}$ s^{-1} reveals that $k_r = 0.005k_{d,\ 298}$. Judging from this ratio, if radiative stabilzation is present in this system it does not contribute much. Thus the data analysis was performed with and without a radiative stabilization pathway included to compare the two and determine the extent to which $k_r = 0$ affects the results.

Once $k_r/k_{d,\ 298}$ is known, the next step is to determine k_d/β for each third-body listed above to obtain β_{rel}. Because the data at room temperature in these SIFT experiments was approximately 20% lower than that determined previously in He, [4] separate k_d/β values were calculated for the two sets of data and then the average of the two was taken; the average was used for further data analysis. An average k_d/β was calculated at 298 K for each third-body, M, by use of equation (1.10). This was done by substitution in equation (1.10) of the Langevin rate coefficients k_a and k_s (see Appendix (11) and (12)) for this system, along with k_r where $k_r = 0.005k_{d,298}$. The results are shown in Table (VIII). Next, k_d for the M = He data was determined by multipling k_d/β for He by β_{He}, all at 298 K. Table (IX) lists the values obtained for k_d at various β_{He}.

Table VIII

Experimentally Determined Average Values of k_d/β at 298 K for $BF_3 + Cl^- \longrightarrow BF_3Cl^-$

β_M	k_d/β , s^{-1}	β_{rel}
[a]β_{He}	2.43×10^9	0.15
[b]β_{He}	1.29×10^9	0.27
[c]β_{He}	1.86×10^9	0.19
N_2	4.00×10^8	0.89
CO_2	3.56×10^8	1.00

[a]This work

[b]Reference (4)

[c] Average of the above two

TABLE IX

Radiative and Decomposition Rate Coefficients for $(BF_3Cl^-)^*$ at 298 K Based on Different β_{He} Values

β_{He}	$k_{d,\,298}$, s^{-1}	k_r, s^{-1}
0.30	3.57×10^8	1.78×10^6
0.19	3.53×10^8	1.77×10^6
0.01	1.86×10^7	9.30×10^4

The average upper limit, $\beta_{He} = 0.19$ and the corresponding k_r from Table (IX) were used to calculate k_d at the four different temperatures studied from equation (1.10). Calculations for $\beta = 0.30$ and 0.01 were also included for completeness. The results for k_d at different temperatures are shown in Table (X). Finally, k_{obs} values were generated at each temperature by using values of k_a, k_s, k_r, β , and k_d (as $k_d = AT^n$) in equation (1.10). The lines generated are shown in figures (4.4), (4.5), and (4.6) while the points on these plots are the experimental data. Agreement between the two is good.

The k_r/k_d ratio is small for this system because k_d is rather large so the importance of radiative stabilization for this system is diminished. To demonstrate this, k_r was assumed to be zero and the same procedure as above followed. Table (XI) lists the k_d/β values for the different third-bodies and Table (XII) lists the average k_d values calculated at the various temperatures studied in He. Also for this system, k_{obs} values at various (He) at the four different temperatures studied were calculated as above with $k_r = 0$. In figures (4.7), (4.8), and (4.9), the lines again represent the calculated k_{obs} at various (He) while the points are actual experimental data. Again the agreement of experimental and calculated values is good, though qualitatively not as good as the case where $k_r \neq 0$. Within experimental error, the calculations for $k_r \neq 0$ and $k_r = 0$ are both consistent with experimental data. However, the

TABLE X

Average Values of $k_d(T)$ for Different Values of β_{He} for BF_3Cl^-

Temp., K	$^{a}k_d$, s^{-1}	$^{b}k_d$, s^{-1}	$^{c}k_d$, s^{-1}
348	7.30×10^8	5.65×10^8	3.05×10^7
298	5.22×10^8	4.04×10^8	2.18×10^7
248	3.52×10^8	2.69×10^8	1.45×10^7
219	2.66×10^8	2.02×10^8	1.07×10^7

[a] $\beta_{He} = 0.30$

[b] $\beta_{He} = 0.19$

[c] $\beta_{He} = 0.01$

TABLE XI

Experimentally Determined Average Values of k_d/β at 298 K for $BF_3 + Cl^- \longrightarrow BF_3Cl^-$ With $k_r = 0$

M	k_d/β , s^{-1}	β_{rel}
[a]He	1.06×10^9	0.18
[b]He	1.02×10^9	0.19
[c]He	1.01×10^9	0.19
N_2	2.45×10^8	0.80
CO_2	1.97×10^8	1.00

[a]This work

[b]Reference (4)

[c]Average of the above two

TABLE XII

Average Values of $k_d(T)$ for Different Values of β_{He} for BF_3Cl^- with $k_r = 0$

Temp., K	$^{a}k_d$, s^{-1}	$^{b}k_d$, s^{-1}	$^{c}k_d$, s^{-1}
348	4.44×10^8	2.81×10^8	1.48×10^7
298	3.19×10^8	2.02×10^8	1.06×10^7
248	2.25×10^8	1.43×10^8	7.52×10^6
219	1.72×10^8	1.09×10^8	5.74×10^6

[a] $\beta_{He} = 0.30$

[b] $\beta_{He} = 0.19$

[c] $\beta_{He} = 0.01$

fit is somewhat better for $k_r \neq 0$ and this supports the general phenomenom of radiative stabilization in the boron trihalide systems, although the importance for BF_3Cl^- is extremly small.

(c). Results for the Magnitude of the TD, n.

Experimental values of k_{obs} at various (He) in which (He) = 1.94 X 10^{16} molec cm^{-3} were measured at 348, 298, and 248 K as shown in Table (XIII). A plot of log k_{obs} vs. log T yields a slope of -2.6 as shown in Figure (4.10). If the temperature dependence is represented as $k_{obs} = AT^{-n}$, then one finds n = 2.6 and A = $10^{-4.78}$ as shown in Table (XIV).

A graph of log k_d vs. log T in which the values of k_d are taken from Table (X) and $k_r \neq 0$, yields n = 2.2 as shown in Figure (4.10). For the case where $k_r = 0$, the values of k_d as taken from Table (XII) yield n = 2.0.

The values of n calculated from theory are listed in Table (VII). Theoretical results are also is plotted in figure (4.10).

Tables (XIV), (XV) and (XVI) list the values for the preexponential factor and for n derived from experimental data with and without k_r.

TABLE XIII

Values of k_{obs} at Constant (He) at Different Temperatures for BF_3Cl^-

Temp., K	(He)	k_{obs}
348	1.94	5.5
298	1.94	7.7
248	1.95	13.0

(He) units: 10^{16} molec cm^{-3}

k_{obs} units: 10^{-12} cm^3 $molec^{-1}$ s^{-1}

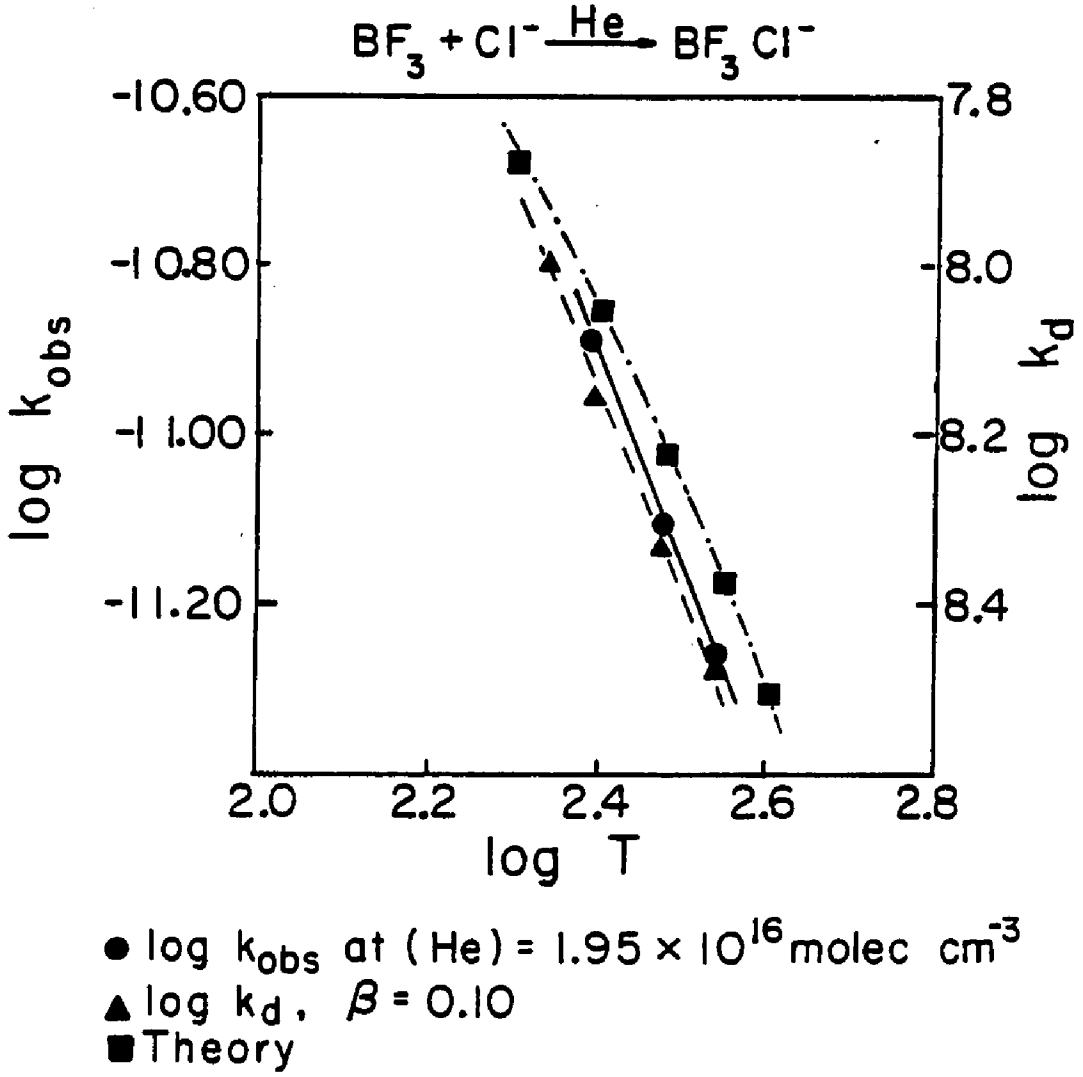

Figure 4.10. Temperature dependence of ion-molecule association reactions.

TABLE XIV

Temperature Dependence of k_{obs} for BF_3Cl^-

A	n
$10^{-4.78}$	2.6

TABLE XV

Temperature Dependence of k_d with $k_r \neq 0$ for BF_3Cl^-

β_{He}	A	n
0.30	$10^{3.34}$	2.2
0.19	$10^{3.11}$	2.2
0.01	$10^{1.76}$	2.2

TABLE XVI

Temperature Dependence of k_d with $k_r = 0$ for BF_3Cl^-

β_{He}	A	n
0.30	$10^{3.49}$	2.0
0.19	$10^{3.31}$	2.0
0.01	$10^{2.02}$	2.0

IV. $BF_3 + Br^-$ Results

(a). General Results

This system was studied over a pressure range of 0.3 to 0.8 torr at only one temperature, 219 K. At higher temperatures the overall rate of association is so small that k_{obs} could be measured only at the highest pressure, 0.8 torr, and here only with difficulty and a high degree of uncertainty. The unimolecular decay rate coefficient, k_d, for this system is most likely large causing k_{obs} to lie at the low end of the working range of a SIFT. Because k_a and k_s do not change appreciably from one boron system to another k_d is the rate coefficient primarily responsible for differences in the magnitude of k_{obs}. The only product observed was BF_3Br^-, but the quadrupole mass spectrometer mass range was too narrow to observe the cluster product $BF_3Br^- \cdot BF_3$, if it was formed. Table (A3) in Appendix (3) lists the data at 219 K and figure (4.11) shows the plot of k_{obs} vs. (He) at 219 K. The single points plotted at the other temperatures are the best values obtained at the highest accessible pressure 0.8 torr. The line is a least squares fit.

Needless to say, without other third-body data and only one temperature studied over a range of pressures, determinations of β , k_r, and the TD of k_d could not be done.

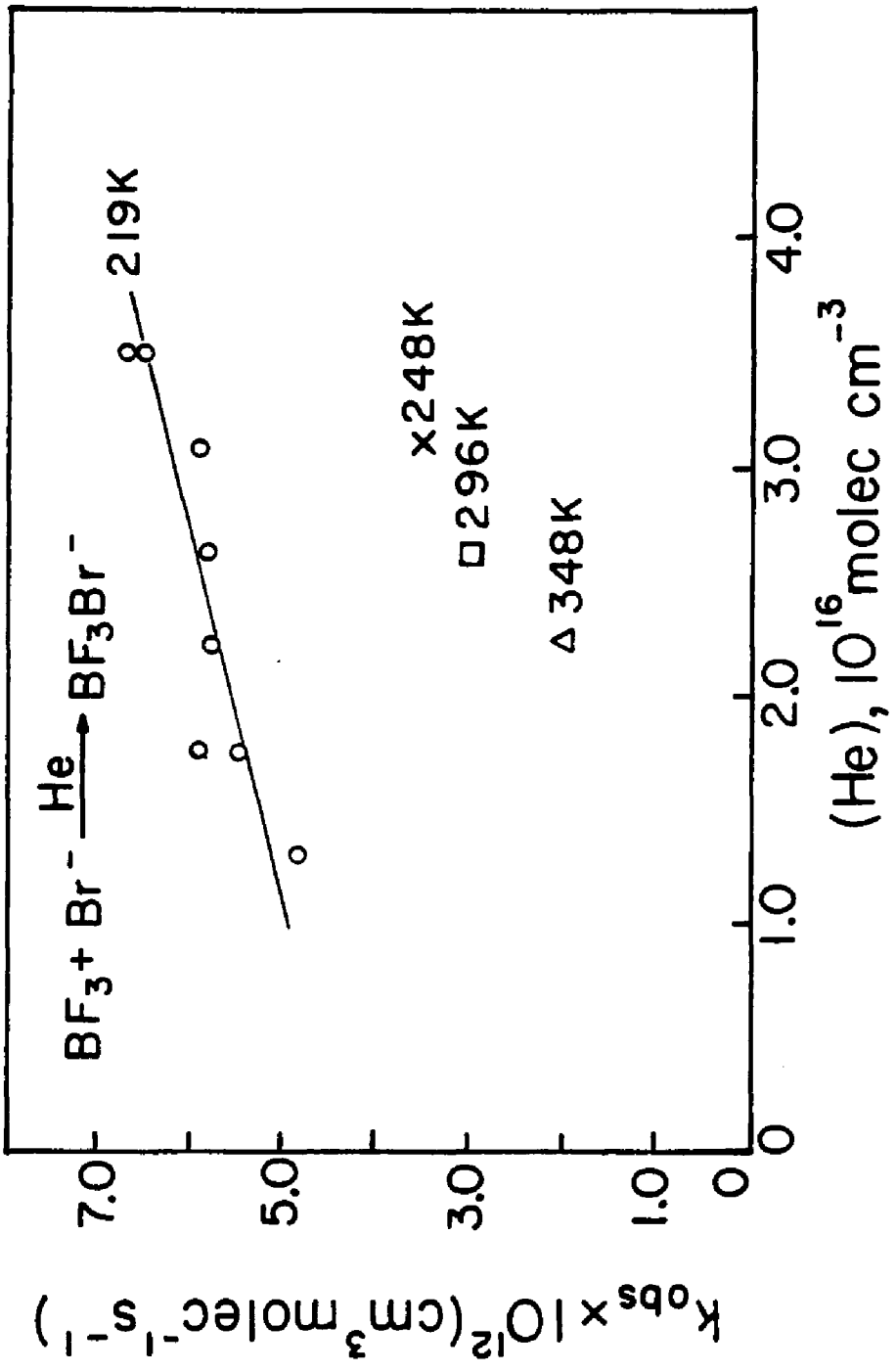

Figure 4.11. Pressure and temperature dependence of k_{obs} for halide ion addition.

V. $BCl_3 + Cl^-$ Results

(a). General Results

This system was studied over a pressure range from 0.2 to 0.8 torr at five different temperatures: 410, 348, 298, 248, and 219 K. The only product observed was BCl_4^-: the cluster product $BCl_4^- \cdot BCl_3$ if present could not be observed because the mass range of the quadrupole mass spectrometer was too narrow. Table (A4) in Appendix (4) lists k_{obs} obtained at various (He) for the five different temperatures studied and in figures (4.12), (4.13) and (4.14) the experimental points are plotted. The lines in the figures are k_{obs} at various (He) as calculated using β , k_d, and k_r values evaluated as below.

(b). Results for Determination of β , k_d, and k_r

This system, $BCl_3 + Cl^-$, has been studied at 298 K with the different third-bodies He, N_2, and CO_2 with a He pressure ranging from 0.3 to 1.0 torr and N_2 and CO_2 pressure ranging from 0.15 to 0.45 torr.[4] As for BF_4^- and BF_3Cl^- formation, plots of k_{obs} at the various (M) show an apparent linear dependence upon (M) with a common average intercept of 3.4×10^{-11} cm^3 $molec^{-1}$ s^{-1}. With the intercept of the data at 298 K for this study included, the average value becomes 3.6×10^{-11} cm^3 $molec^{-1}$ s^{-1}. Low pressure ICR data is not available for this system. Using the above value for the intercept yields $k_r = 0.03k_{d,\,298}$.

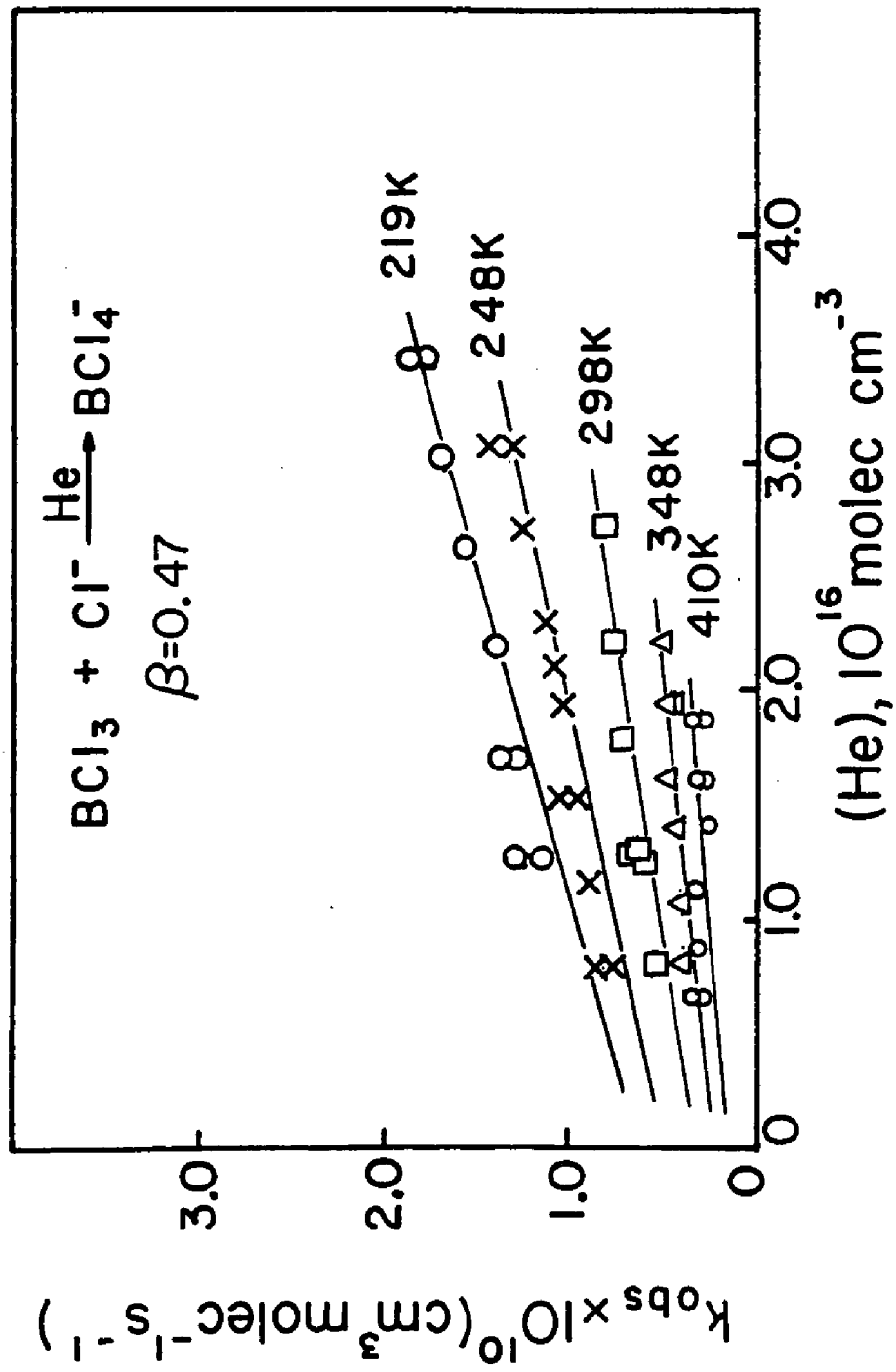

Figure 4.12. Pressure and temperature dependence of k_{obs} for halide ion addition.

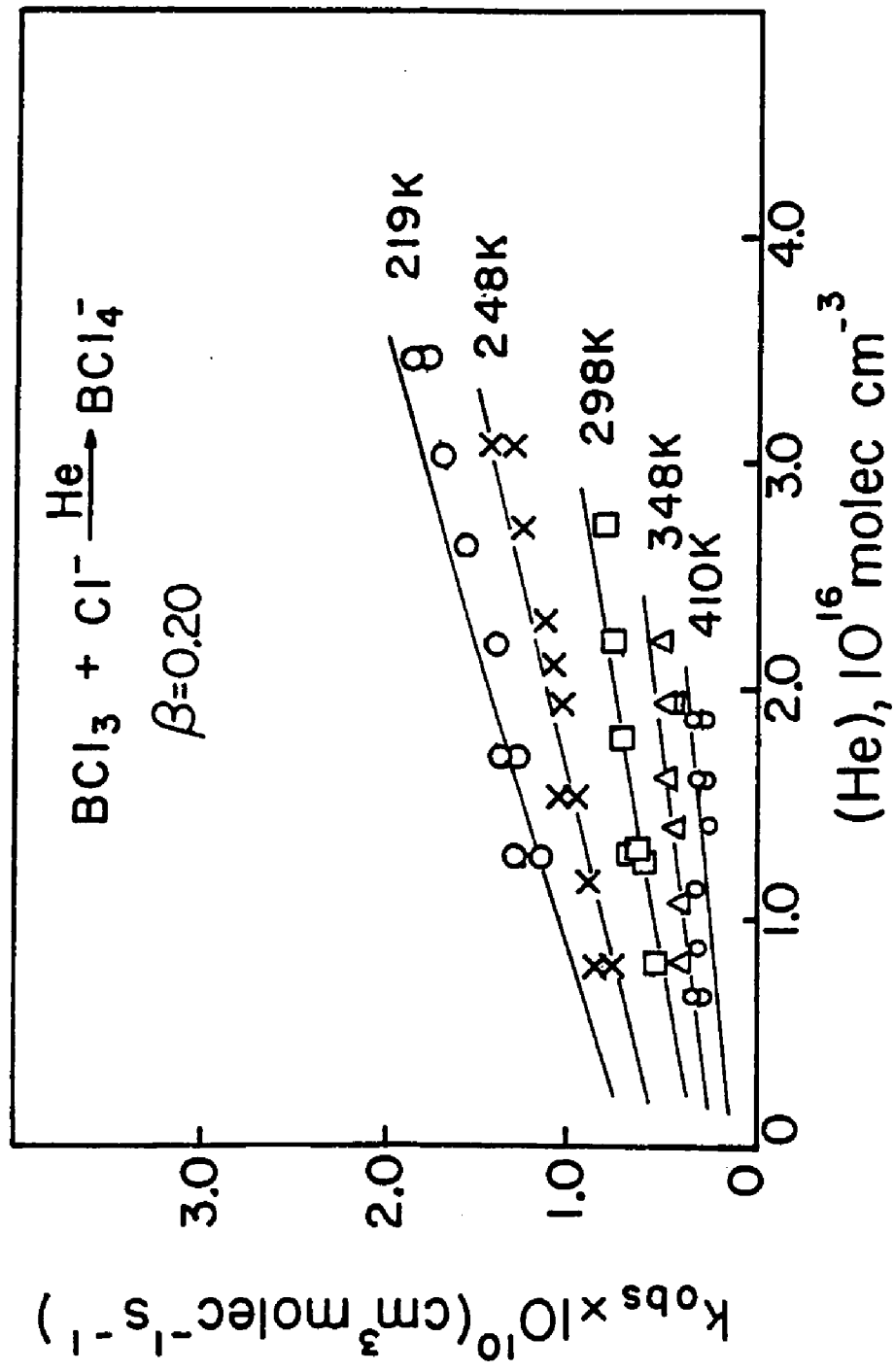

Figure 4.13. Pressure and temperature dependence of k_{obs} for halide ion addition.

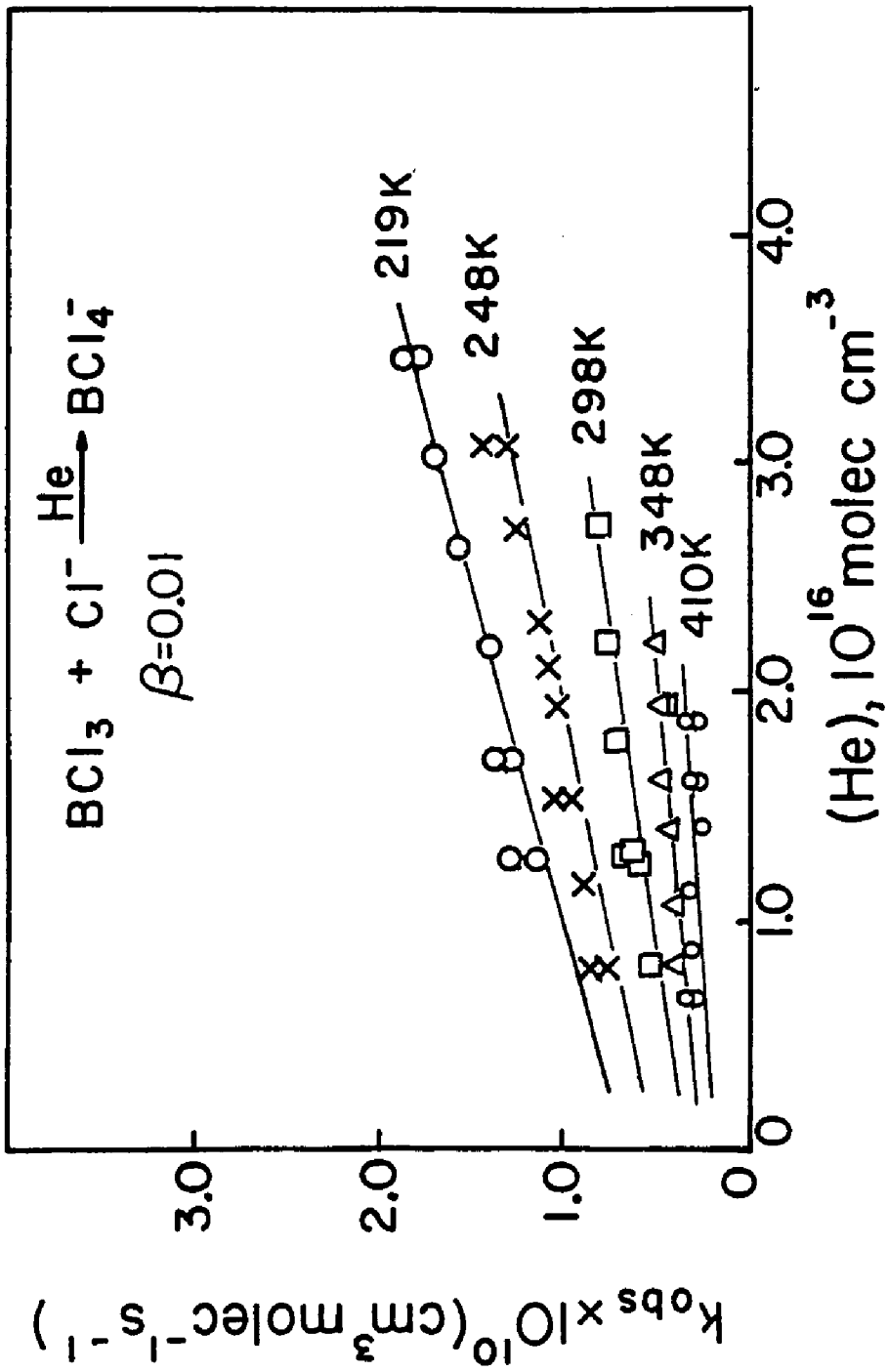

Figure 4.14. Pressure and temperature dependence of k_{obs} for halide ion addition.

(Actually $k_r = 0.026k_{d,\ 298}$ was used for calculations and round off was done at the end of the calculations). Substitution for k_r in equation (1.10) along with k_a for $BCl_3 + Cl^-$ and k_s for the BCl_4^-/He couple (again k_a and k_s are taken as the Langevin rates), yields k_d/β for the different third-bodies at 298 K, as shown in Table (XVII). Using the average k_d/β from this work and reference (4), a value of $\beta = 0.47$ is calculated for the upper limit to He. For $\beta_{He} = 0.47$, 0.20, and 0.01 values of k_r and k_d are calculated; the values for $k_{d,298}$ and k_r for these various β_{He}'s are listed in Table (XVIII). Next, to evaluate k_d at the other four temperatures, the various β_{He}'s and k_r's were substituted into equation (1.10) along with the proper values of k_a and k_s (the Langevin rate coefficients given in Tables (A11) and (A12) in Appendixes (11) and (12)). The results are shown in Table (XIX). Note that the average value of k_d/β from reference (4) and from the data contained herein was used for calculation of $k_{d,\ 298}$ and thus k_r at various β values as given in Table (XVIII). Finally, with β_{He}, k_d, and k_r set, k_{obs} values at various (He) and at all five temperatures were generated for comparison to the experimental values. The lines in figures (4.12), (4.13), and (4.14) are the result: clearly the fit over the range of temperatures and pressures is good.

TABLE XVII

Experimentally Determined Average Values of k_d/β at 298 K for $BCl_3 + Cl^- \longrightarrow BCl_4^-$

M	k_d/β , s^{-1}	β_{rel}
[a]He	3.60×10^8	0.46
[b]He	3.48×10^8	0.48
[c]He	3.54×10^8	0.47
N_2	3.43×10^8	0.49
CO_2	1.67×10^8	1.00

[a]This work

[b]Reference (4)

[c]Average of the above two

TABLE XVIII

[*]Radiative and Decomposition Rate Coefficients for (BCl_4)[*] at 298 K Based on Different β_{He} Values

β_{He}	$k_{d,\,298}$, s^{-1}	k_r, s^{-1}
0.47	1.66×10^8	4.31×10^6
0.20	7.20×10^7	1.87×10^6
0.01	3.60×10^6	9.36×10^4

[*]Average k_d/β from Table (XVII) used for these calculations

TABLE XIX

***Average Values of $k_d(T)$ for Different Values of β_{He} for BCl_4^-**

Temp., K	$^a k_d$, s^{-1}	$^b k_d$, s^{-1}	$^c k_d$, s^{-1}
410	3.28×10^8	1.41×10^8	7.07×10^6
348	2.50×10^8	1.08×10^8	5.38×10^6
298	1.70×10^8	7.27×10^7	3.64×10^6
248	1.08×10^8	4.65×10^7	2.32×10^6
219	8.26×10^7	3.54×10^7	1.77×10^6

[a] $\beta_{He} = 0.47$

[b] $\beta_{He} = 0.20$

[c] $\beta_{He} = 0.01$

*k_d/β from this work was used for calculation of $k_{d,\ 298}$

(c). Results for the Magnitude of the TD, n.

At the concentration (He) = 0.82 molec cm^{-3}, k_{obs} was measured at 348, 298, and 248 K, yielding n = 2.4 from the slope of a plot of log k_{obs} vs. log T (where $k_{obs} = AT^{-n}$). The values for k_{obs} at (He) = 0.82 molec cm^{-3} at the various temperatures are listed in Table (XX) and the log/log plot is shown in figure (4.15).

From a plot of log k_d vs. log T, where k_d was taken from Table (XIX), n is found to be 2.3 for all β_{He} (where $k_d = AT^n$). This is represented graphically in figure (4.15).

Theoretically, n is found to range from 2.33 in the temperature range from 200 to 250 K with only one vibration considered active, to 3.87 in the temperature range from 400 to 450 K with all vibrational modes participating. The values for log "$k^{(3)}$" vs. log T in which all vibrational modes are considered active are plotted in figure (4.15).

Table (XXI) and Table (XXII) list the preexponential factor, A, and n from k_{obs} and k_d data respectively. Table (XXIII) lists the values of n calculated from theory over 50 K intervals with varying vibrational contributions.

TABLE XX

Values of k_{obs} at Constant (He) at Different Temperatures for BCl_4^-

Temp., K	(He)	k_{obs}
348	0.83	3.44
298	0.81	5.11
248	0.82	7.65
248	0.82	8.16

(He) units: 10^{16} molec cm^{-3}

k_{obs} units: 10^{-11} cm^3 $molec^{-1}$ s^{-1}

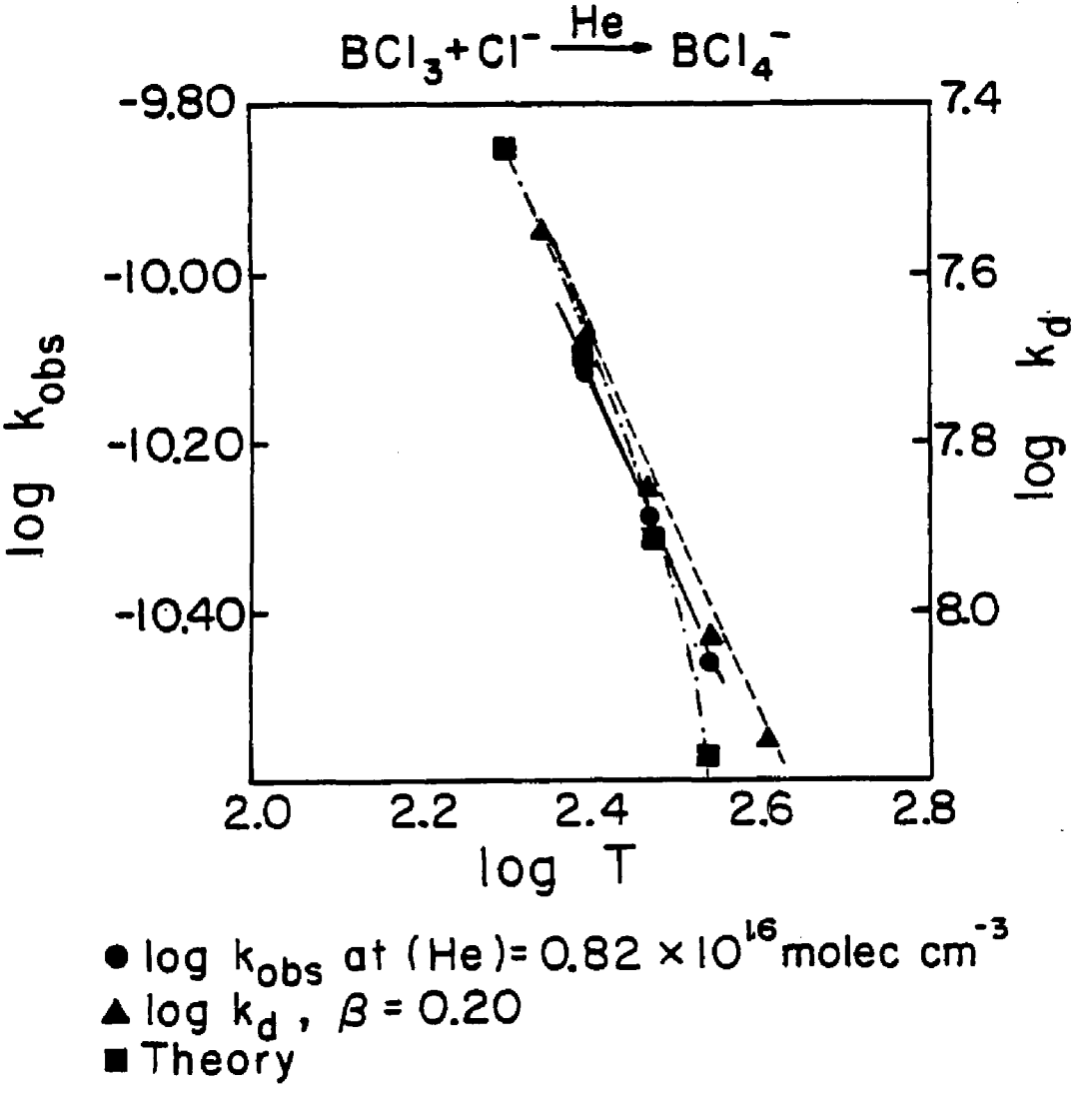

Figure 4.15. Temperature dependence of ion-molecule association reactions.

TABLE XXI

Temperature Dependence of k^{obs} for BCl^{4-}

A	n
$10^{-4.25}$	2.4

TABLE XXII

Temperature Dependence of k^{d} for BCl^{4-}

β_{He}	A	n
0.47	$10^{2.63}$	2.3
0.20	$10^{2.25}$	2.3
0.01	$10^{0.94}$	2.3

TABLE XXIII

A Compilation of Calculated n Values Demonstrating Vibrational Contributions for $BCl_3 + X^-$

Temp. Range, K	a_n	b_n	c_n	d_n
200-250	2.33	2.48	2.64	2.67
250-300	2.49	2.72	2.94	3.01
300-350	2.61	2.91	3.20	3.33
350-400	2.71	3.07	3.42	3.61
400-450	2.79	3.20	3.60	3.87

[a]Frequencies: 243(2) cm^{-1}

[b]Frequencies: 243(2), 462 cm^{-1}

[c]Frequencies: 243(2), 462, 471 cm^{-1}

[d]Frequencies: 243(2), 462, 471, 958(2) cm^{-1}

Vibrational frequencies are from:

JANAF thermochemical Tables, 2nd ed. NSRDS-NBS 37 June 1971, Washington D.C.

VI. $BCl_3 + Br^-$ Results

(a). General Results

This system was studied over the pressure range 0.2 to 0.8 torr and at five different temperatures: 410, 348, 298, and 219 K. The only product observed was BCl_3Br^-; the cluster product if present could not be observed because the mass range of the quadrupole mass spectrometer was too narrow. Table (A5) in Appendix (5) lists k_{obs} at various (He) obtained experimentally at the five different temperatures. The points shown in figures (4.16), (4.17), and (4.18) are the experimental values of k_{obs} at various (He) designated by the indicated symbols. The lines are k_{obs} values determined as a result of the calculations of β, k_d, and k_r as a function of both (M) and T.

(b). Results for the Calculation of β, k_d, and k_r.

For this system, BCl_3Br^-, data for k_{obs} at various (M) with different third-bodies is not available, nor is low pressure ICR data available. However, since this system behaves essentially the same as the other boron trihalide systems, we feel confident in analyzing it in the same manner.

Due to the lack of third-body information β must be estimated. Because the results for this system and for the BCl_4^- system are so similar, the upper limit of $\beta = 0.46$ that was found for BCl_4^- was used for BCl_3Br^-. The average

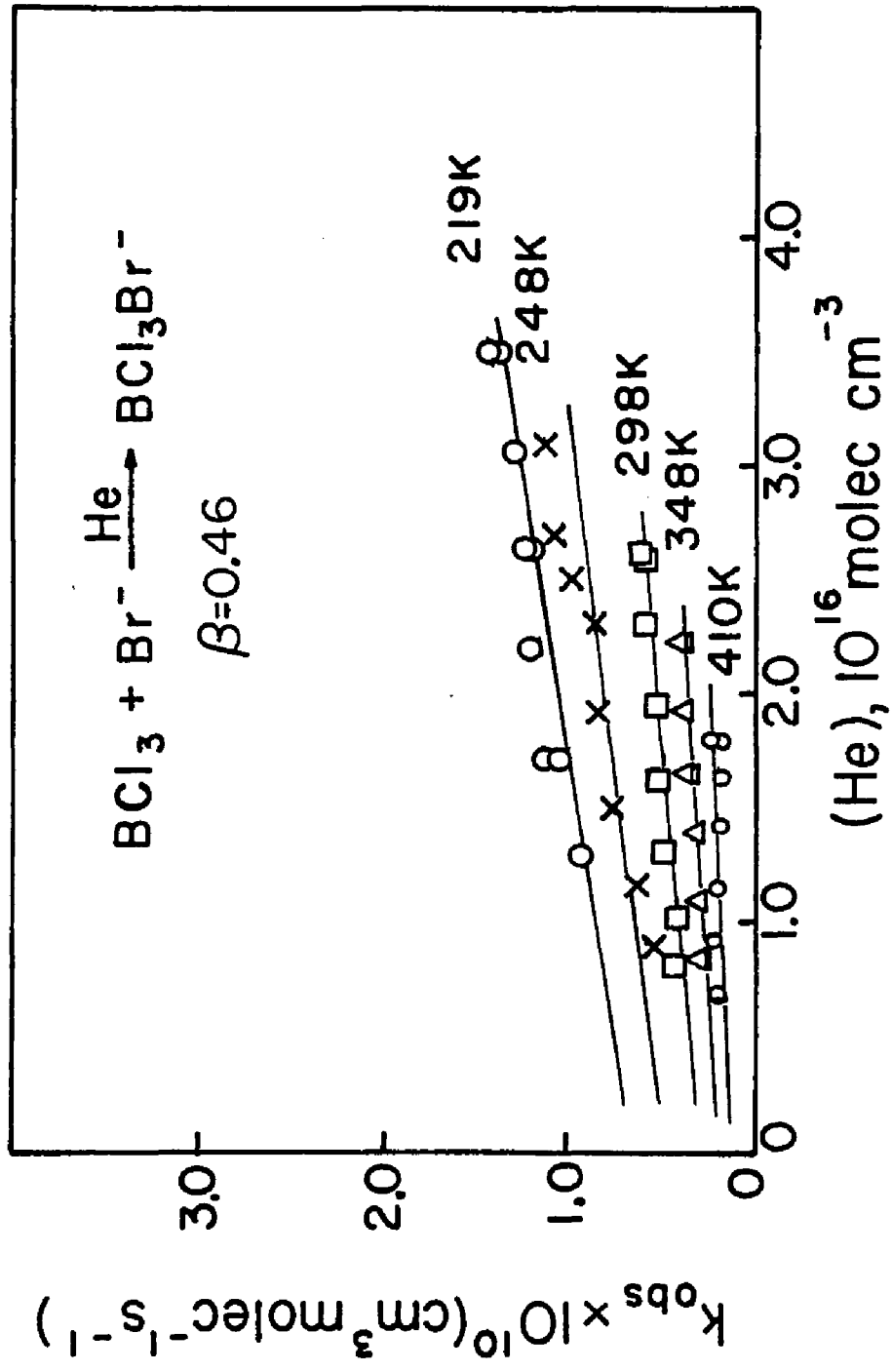

Figure 4.16. Pressure and temperature dependence of k_{obs} for halide ion addition.

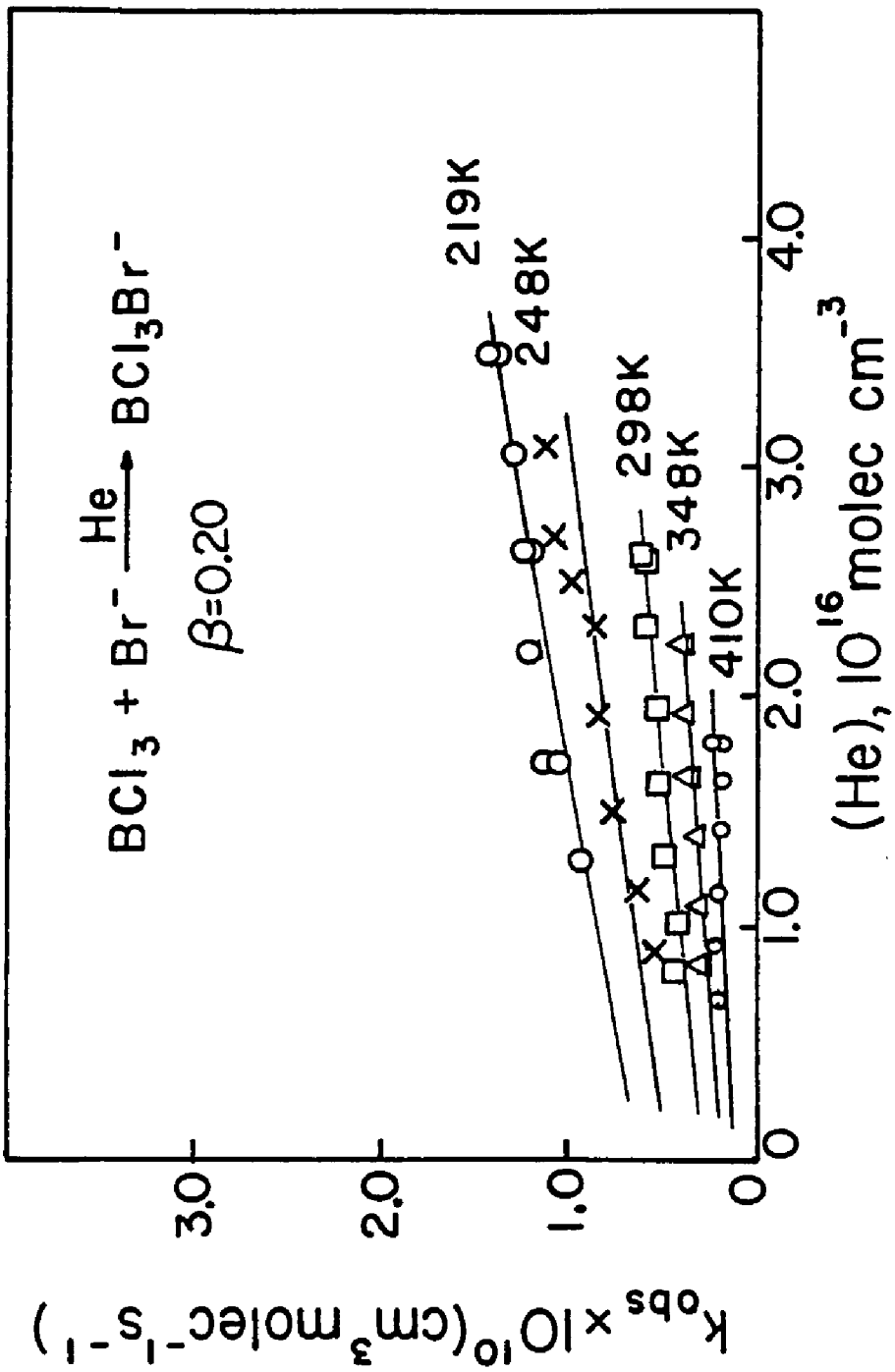

Figure 4.17. Pressure and temperature dependence of k_{obs} for halide ion addition.

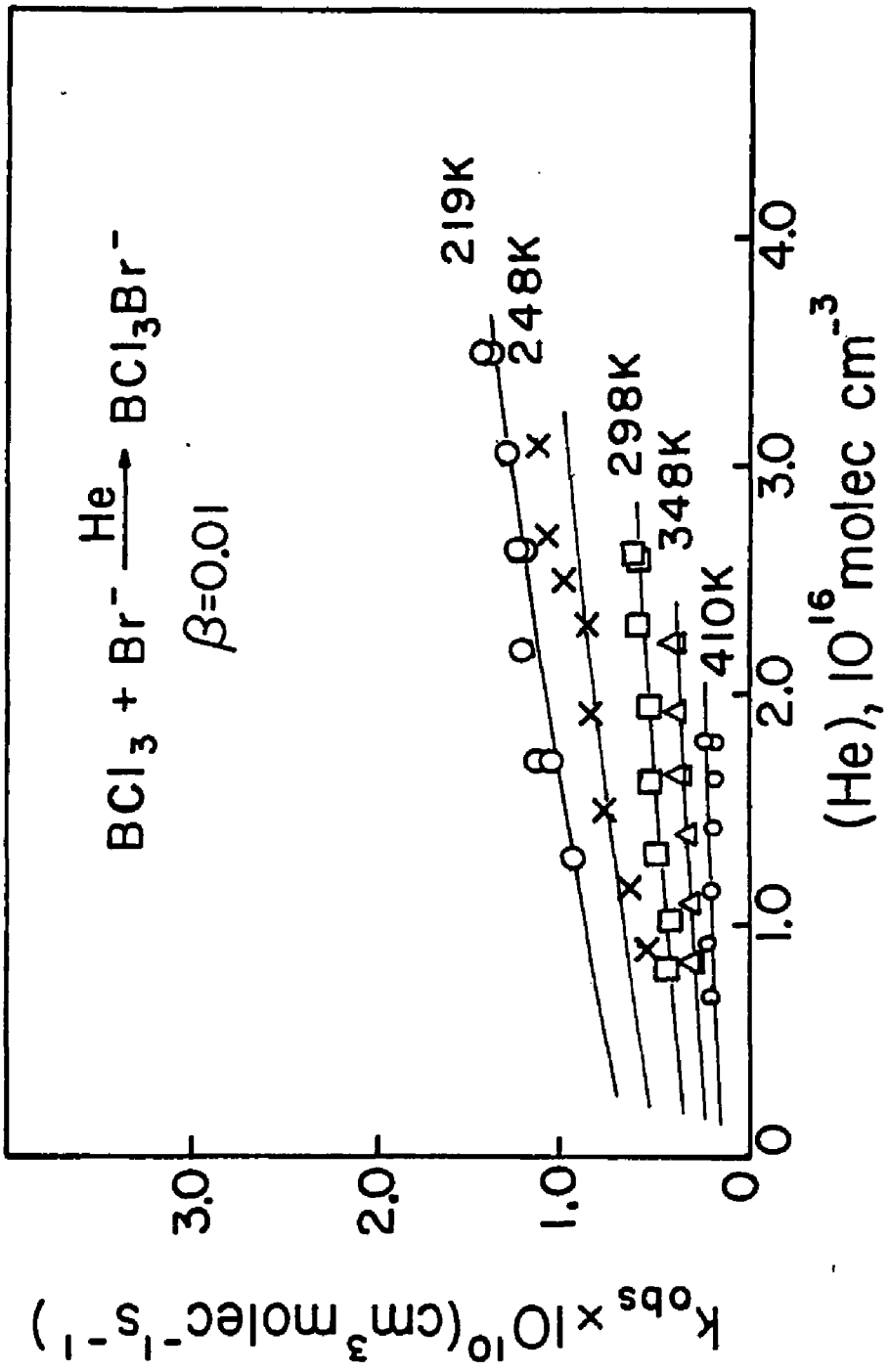

Figure 4.18. Pressure and temperature dependence of k_{obs} for halide ion addition.

k_d/β value for this system and the estimated upper limit to β are shown in Table (XXIV), while Table (XXV) lists various values of chosen along with the corresponding values of $k_{d,\ 298}$ and k_r. Table (XXVI) lists the subsequent average values of k_d obtained at the other four temperatures at various values of β . Again, after evaluation of β , k_d, and k_r, k_{obs} at all five temperatures and various values of β were calculated. The lines in the plots of k_{obs} vs. (He) in figures (4.16), (4.17), and (4.18) are the result of these calculations. Again agreement with experimental data is excellent over the entire pressure and temperature range.

(c). **Results for the Magnitude of the TD, n.**

Experimentally, at (He) = 1.65 X 10^{16} molec cm^{-3}, k_{obs} was determined at 410, 348, and 298 K. The slope of a plot of log k_{obs} vs. log T yields n = -2.5 for $k_{obs} = AT^{-n}$. The values for k_{obs} at (He) = 1.65 molec cm^{-3} at the various temperatures are listed in Table (XXVII).

From a plot of log k_d vs log T, where k_d at various temperatures is taken from Table (XXVI), n is found to be 2.5 for all β_{He}.

Theoretically, n was found to range from 2.33 to 3.87 as discussed earlier and shown in Table (XXIII).

Table (XXVIII) and Table (XXIX) list the preexponential factor and n from experimental values of k_{obs} and from k_d values determined from data. Table (XXIII) lists the

values of n calculated from theory over 50 K intervals with varying vibrational contributions. Figure (4.19) is a plot showing log k_{obs}, log k_d, and log "$k^{(3)}$" vs. log T.

TABLE XXIV

Experimentally Determined Average Values of k_d/β at 298 K for BCl_3Br^-

M	k_d/β	β_{He} (Estimated)
He	4.89×10^8	0.46

TABLE XXV

Radiative and Decomposition Rate Coefficients for $(BCl_3Br^-)^*$ at 298 K Based on β_{He} Values

β_{He}	$k_{d,\,298}$, s^{-1}	k_r, s^{-1}
0.46	2.25×10^8	6.74×10^6
0.20	9.78×10^7	2.93×10^6
0.01	4.89×10^6	1.47×10^5

TABLE XXVI

Average Values of $k_d(T)$ for Different Values of β_{He} for BCl_3Br^-

Temp., K	$^{a}k_d$, s^{-1}	$^{b}k_d$, s^{-1}	$^{c}k_d$, s^{-1}
410	4.73×10^8	2.06×10^8	1.03×10^7
348	3.20×10^8	1.39×10^8	6.98×10^6
298	2.24×10^8	9.73×10^7	4.87×10^6
248	1.31×10^8	5.71×10^7	2.86×10^6
219	9.98×10^7	4.34×10^7	2.17×10^6

[a] $\beta_{He} = 0.46$

[b] $\beta_{He} = 0.20$

[c] $\beta_{He} = 0.01$

TABLE XXVII

Values of k_{obs} at Constant (He) at Different Temperatures for BCl_3Br^-

Temp., K	(He)	k_{obs}
410	1.65	2.17
348	1.66	3.20
348	1.66	3.35
298	1.62	4.76

(He) units: 10^{16} molec cm^{-3}

k_{obs} units: 10^{-11} cm^3 $molec^{-1}$ s^{-1}

TABLE XXVIII

Temperature Dependence of k_{obs} for BCl_3Br^-

A	n
$10^{-4.23}$	2.5

TABLE XXIX

Temperature Dependence of k_d for BCl_3Br^-

β_{He}	A	n
0.46	$10^{2.10}$	2.5
0.20	$10^{1.74}$	2.5
0.01	$10^{0.44}$	2.5

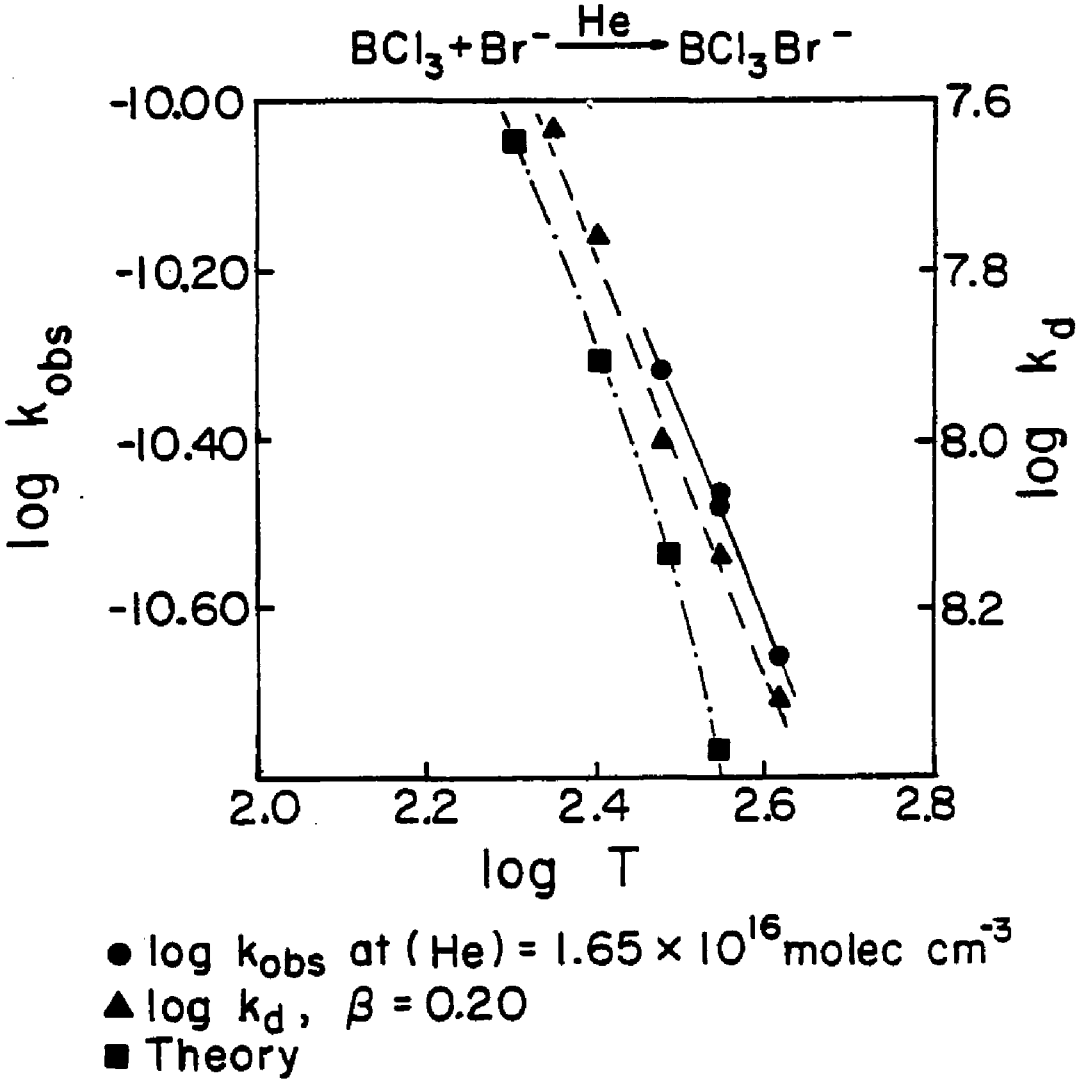

Figure 4.19. Temperature dependence of ion-molecule association reactions.

VII. Discussion

(a). Introduction

The boron trihalide systems offer an excellent opportunity to study both collisional and radiative stabilization, as well as temperature effects upon ion-molecule association reactions. Collisional stabilization is of course evidenced by the direct dependence of k_{obs} upon (He) as seen in plots of k_{obs} vs. (He). Because of this pressure dependence, we have been able to probe the ion-molecule association mechanism and determine important parameters such as the unimolecular decay rate coefficient, k_d, and gain insight into the bond dissociation energies of these systems as well as the lifetimes of the excited complexes. The presence of a bimolecular pathway, which we conclude to be a radiative stabilization channel, is unique and interesting and is clearly evidenced by the common non-zero intercept obtained at (M) = 0 for the different third-bodies,[4] along with low pressure ICR data for the BF_3 + F^- system.[66] Also, these systems allow a systematic study of the temperature dependence of IM association reactions, since the identity of the monatomic ion is the only variable for a given boron trihalide system. Since the temperature dependence is dominated by k_d, this allows us to gain insights into the number of vibrational oscillators participating in the unimolecular decay of the excited complexes. The discussion to follow therefore involves consi-

deration of collisional stabilization in competition with radiative stabilization and unimolecular dissociation, along with the temperature dependence of these halide ion-boron trihalide systems.

(b). General Discussion and Overview of Data

To summarize results for the unimolecular decay process, Table (XXX) is a compilation of $k_{d,\,298}$ at various β_{He} for each boron trihalide system studied. The upper limit for $_{He}$ calculated from k_d/β ratios is certainly consistent with the collisional efficiencies expected for a monatomic ion which have been reported.[14,16] Also the general trend in the order of stabilization efficiencies for M: polyatomics > triatomics > diatomics > monatomics is evidenced by the k_d/β ratios determined for these systems for the different third-bodies. For example, in Table (III) the k_d/β ratio for $BF_3 + F^-$ for the different third-bodies goes in the order $CF_4 < CH_4 < N_2 < He$. Since k_d should be the same for all M, the decrease in k_d/β arises from an increase in β (recall $0 \leq \beta \leq 1$). Clearly k_d/β increases with decreasing molecular complexity as one expects. As shown in the results section, we were able to determine $k_{d,298}$ and k_r for each system and then calculate k_d at each temperature studied. In order to compare values of k_d for each system, a constant β_{He} must be chosen. Because we only know the k_d/β ratio any change in β also changes the absolute value of k_d. The result is that a

TABLE XXX

A Compilation of $k_{d,\ 298}$ and k_r at Various β_{He} for the Halide Ion-Boron Trihalide Systems

$BF_3 + F^-$

β_{He}	$k_{d,\ 298}$, s^{-1}	k_r, s^{-1}
0.30	2.89×10^7	2.60×10^6
0.25	2.41×10^7	2.17×10^6
0.15	3.61×10^6	3.25×10^5
0.01	9.65×10^5	8.69×10^4

$BF_3 + Cl^-$

β_{He}	$k_{d,\ 298}$, s^{-1}	k_r, s^{-1}
0.30	5.58×10^8	2.79×10^6
0.19	3.53×10^8	1.77×10^6
0.01	1.86×10^7	9.30×10^4
0.30	3.19×10^8	0
0.19	2.02×10^8	0
0.01	1.86×10^7	0

$BCl_3 + Cl^-$

β_{He}	$k_{d,\ 298}$, s^{-1}	k_r, s^{-1}
0.47	1.66×10^8	4.31×10^6
0.30	1.06×10^8	2.76×10^6
0.20	7.20×10^7	1.87×10^6
0.01	3.60×10^6	9.36×10^4

TABLE XXX continued,

BCl_3 + Br^-

β He	$k_{d,\ 298}$, s^{-1}	k_r, s^{-1}
0.46	2.25×10^8	6.74×10^6
0.30	1.47×10^8	4.40×10^6
0.20	9.78×10^7	2.93×10^6
0.01	4.89×10^6	1.47×10^5

comparison of k_d's at different values of β would be meaningless and therefore $\beta = 0.30$ with the corresponding k_d and k_r rate coefficients is chosen for purposes of comparison.

The RRK theory[71] as modified[47] for ion-molecule reactions gives the general relationship:

$$k_d \propto (T / D^o)^{s-1} \quad , \qquad (4.6)$$

where k_d is the unimolecular decay rate coefficient as before, T is temperature, D^o is the bond dissociation energy, and s-1 is the number of participating oscillators. As mentioned in the Introduction, s-1 is often less than the actual number of vibrational oscillators (3N-6 or 3N-5). Since we assume the simple form $k_d = AT^n$, then comparison of this with equation (4.6) allows us to set s-1 = n. The above equation then predicts that k_d is directly proportional to temperature: $k_d \propto T^n$, and inversely proportional to the bond dissociation energy: $k_d \propto (1/D^o)^n$. As a rough guide, RRK theory can be used to compare k_d between two different halide ion-boron trihalide systems where the neutral boron trihalide is the same and only the halide ion is different (e.g. BF_3 + F^-, Cl^-, or Br^-). This is so because from the relationship $k_d = AT^n$ it was found that for the BF_3 systems n = 2.0 to 2.2, while for the BCl_3 systems n = 2.3 to 2.5. Since we have said that n = s-1 then it is obvious that n is very nearly the same only for systems in which the neutral is the same as

discussed above. In equation (4.6) above it is seen that both temperature and the bond dissociation energy depend upon k_d with the same value of n. Because n is nearly the same for both the $BF_3 + F^-$ and $BF_3 + Cl^-$ systems for example, any drastic changes in k_d for these systems at a given temperature must be due to changes in D^o. Therefore we are able to use RRK theory as a rough guide for comparison of k_d between the two systems with the same neutral and also compare their bond dissociation energies from the relationship, $k_d \propto (1/D^o)^n$. Because the temperature dependence between the $BF_3 + F^-$ and Cl^-, and $BCl_3 + Cl^-$ and Br^- systems is different, n is different, and so k_d is proportional to temperature and bond strength to a different power of n. So, direct comparisons between these systems with different neutrals: $BF_3 + F^-$, Cl^-, and Br^-, and $BCl_3 + Cl^-$, and Br^-, can only be done by correcting for the temperature dependence as discussed later.

For $BF_3 + F^-$ and Cl^- at $\beta = 0.30$ and 298 K, k_d is 2.89×10^7 s^{-1} and 5.58×10^8 s^{-1} respectively. It is known that the bond energy of (BF_3--F^-) (or fluoride affinity of BF_3) is 3.1 eV [66] and the chloride affinity is 1.1 eV. [65] The bromide affinity for BF_3 is not known, but trends indicate that it is smaller than 1.1 eV. The trend in $k_{d,298}$ in Table (XXX) for $\beta = 0.30$ is consistent with the trend predicted by RRK theory in that as D^o decreases, k_d increases, demonstrating that the data for the boron trifluoride systems is in agreement with the general trend

predicted by this theory. The trend in $k_{d,\ 298}$ is also consistent with the trend in the magnitude of the apparent overall binary rate coefficient, k_{obs}. Considering the expression for k_{obs} and the individual rates making up the expression it can be seen that k_d is the primary rate coefficient controlling changes in the magnitude of k_{obs} from system to system. Because k_a, k_s, k_r and β change very little from system to system, k_d plays the dominant role in changing k_{obs}. Therefore, since k_d oc $(1/D^o)^n$ and since k_{obs} increases as k_d decreases, then k_{obs} must increase as D^o increases at a given temperature for similar systems. From the data of $k_{obs,\ 298}$ vs. (He) it is seen that $k_{obs,\ 298}$ for $BF_3 + F^- \longrightarrow BF_4^-$ is on the order of 10^{-10} cm^3 $molec^{-1}$ s^{-1}; for $BF_3 + Cl^- \longrightarrow BF_3Cl^-$, 10^{-12} to 10^{-11} cm^3 $molec^{-1}$ s^{-1}; and for $BF_3 + Br^- \longrightarrow BF_3Br^-$ < 2.6 X 10^{-12} cm^3 $molec^{-1}$ s^{-1}. Since k_{obs} does indeed decrease as D^o decreases for the two systems where D^o is known, then by the reasoning above k_d must increase. This is confirmed by our determination of k_d as shown in Table (XXX). It should be noted these comparisons are valid only within the same pressure and temperature ranges.

This correlation of k_{obs} with D^o or, more specifically of k_d with $(1/D^o)^n$, allows limits to be placed on the bond dissociation energies of BF_3--Br^-, BCl_3--Cl^-, and BCl_3--Br^- which are unknown. First, $k_{obs,\ 298}$ for $BF_3 + Cl^-$ ranges from 5.6 X 10^{-12} to 1.0 X 10^{-11} cm^3 $molec^{-1}$ s^{-1} over a pressure range from 0.3 to 0.8 torr, while $k_{obs,\ 298}$ for

$BF_3 + Br^-$ is < 2.6×10^{-12} at 0.8 torr. By the argument above, if k_{obs} is small, k_d must be large and even though we could not measure $k_{d,\ 298}$ for $BF_3 + Br^-$, we know $k_{d,\ Br^-} > k_{d,\ Cl^-} > k_{d,F^-}$. Therefore D^o for BF_3--Br^- must be less than D^o for BF_3--Cl^-, and an upper limit of 1.1 eV can be set for D^o of BF_3--Br^-. In addition, the bond dissociation energies of BCl_3--Cl^- and BCl_3--Br^- (or chloride and bromide affinities of BCl_3) can be estimated by considering $k_{d,\ 298}$ for these systems and those for BF_3--F^- and BF_3--Cl^-. As mentioned, comparison between the BF_3 and BCl_3 systems cannot be done unless the temperature dependence for each system is corrected for. An examination of equation (4.6) shows that the ratio of k_d at a given temperature and pressure for two systems is equal to the ratio of the temperature dependencies multiplied by the inverse ratio of the bond dissociation energies:

$$\frac{(k_d)_1}{(k_d)_2} = \frac{(T_1^n)(D_2^o)^n}{(T_2^n)(D_1^o)^n} \quad . \qquad (4.7)$$

From Table (XXX), it is seen that $k_{d,\ 298}$ for the $BF_3 + F^-$ and $BF_3 + Cl^-$ systems is $2.89 \times 10^7\ s^{-1}$ and $5.58 \times 10^8\ s^{-1}$ respectively. The values for $k_{d,\ 298}$ for the $BCl_3 + Cl^-$ and Br^- systems are $1.06 \times 10^8\ s^{-1}$ and $1.47 \times 10^8\ s^{-1}$ respectively. Also, from Table (XXXI), the magnitude of the temperature dependence, n, for the $BF_3 + F^-$ and $BF_3 + Cl^-$ systems is 2.0 and 2.2 respectively, as determined from values of $k_d(T)$ evaluated from experimental data. The val-

ues of n for BCl_3 + Cl^- and Br^- are 2.3 and 2.5 respectively. These too were evaluated from $k_d(T)$ determined from experimental data. From these experimentally determined temperature dependencies, n, and k_d values, one can calculate D^o for an unknown system by comparing it to a system where D^o is known. Since the bond dissociation energy for $F_3B{-}{-}F^-$ is well known[73] and we have measured k_d and n for the other boron systems, we can make rough estimates of D^o for the unknown bonds using equation (4.7). Using $k_{d,\,298}$ values from Table (XXX) and n values from Table (XXXI) as listed above, values of D^o for $F_3B{-}{-}Cl^-$, $Cl_3B{-}{-}Cl^-$ and $Cl_3B{-}{-}Br^-$ have been calculated. The first, BF_3Cl^-, is already known and we calculate it from equation (4.7) for comparison, in order to evaluate the accuracy of this approach. With this method, $D^o(F_3B{-}{-}Cl^-)$ is calculated as 1.2 eV in excellent agreement with the experimental value of 1.1 eV.[65] Values for $D^o(Cl_3B{-}{-}Cl^-)$ and $D^o(Cl_3B{-}{-}Br^-)$, which are unknown, are determined to be 3.2 eV and 4.0 eV respectively. While the agreement with experiment is gratifying for the $F_3B{-}{-}Cl^-$ system, without further corroboration of this method by comparison to other experimental values, we hesitate to attach exact quantitative meaning to the bond dissociation energies calculated for the $Cl_3B{-}{-}Cl^-$ and $Cl_3B{-}{-}Br^-$ systems. They are, however, a good indication that bond strengths for all of the boron systems, with the exception of BF_3Cl^- are comparable. It would be interesting to see how closely this method

predicts the actual bond strengths.

It is interesting to note that a change of ~2 eV in D^o results in going from F^- to Cl^- for the BF_3 systems, while a change of probably less than 1.0 eV in D^o occurs in going from Cl^- to Br^- for the BCl_3 systems (0.8 eV according to our rough calculations). This trend can be rationalized by considering size effects of the halide ions. The univalent radii for the three ions are as follows: F^- = 136 pm, Cl^- = 181 pm, and Br^- = 195 pm.[72] The change in size from F^- to Cl^- is 45 pm while the change from Cl^- to Br^- is only 14 pm. Thus if we consider the bond strength to be inversely related to the size of the halide ion, the change in D^o is greatest in going from F^- to Cl^-, while naturally the change is less in going from Cl^- to Br^-. This trend is evidenced in the known values for D^o for $F_3B{-}{-}F^-$ and $F_3B{-}{-}Cl^-$ as well as the subsequent trend in k_d as determined for all of the boron trihalide systems discussed above.

In summary, the trend in k_d for the boron trihalide systems, BF_3 + F^- and Cl^- and BCl_3 + Cl^- and Br^- as calculated from experimental data is consistent with RRK theory, the magnitude of k_{obs} for each system, and the size of the atomic halide ion. It also allows us to set limits on bond strengths: the bromide affinity of BF_3 was determined to be < 1.1 eV and the chloride and bromide affinities of BCl_3 were determined to be on the order of 3 eV within the approximations of equation (4.7).

(c). Collisional Stabilization and Average Lifetimes

Knowledge of k_d is important because from it the average lifetime of the excited complex can be determined. It is known that $k_d = 1/\tau_d$, where k_d is a thermal average and τ_d is the average lifetime. The lifetime of an excited complex must be shorter than the time between stabilizing collisions in order for it to unimolecularly decay back to reactants and/or stabilize itself by emission of a photon. For example, the frequency of collisions can be calculated by multiplication of the collision rate of the excited complex/third-body couple, k_s, by the concentration of the third-body, (M). For BF_4^-/He, $k_s = 5.42 \times 10^{-10}$ cm^3 molec^{-1} s^{-1} and, assuming an average pressure of 0.55 torr, (He) = 1.78×10^{16} molec cm^{-3} at 298 K. Therefore the collision frequency is: $k_f = 9.66 \times 10^6$ s^{-1}. If we assume $\beta = 0.30$ and that it gives the fraction of collisions that are stabilizing collisions ,then the frequency of stabilizing collisions, $k_{f,sc}$, is given by the product $k_f(\beta)$. For this case $k_{f,\,sc} = 2.09 \times 10^6$ s^{-1}. Inverting $k_{f,\,sc}$ gives the maximum average lifetime of a complex that can either unimolecularly decay and/or stabilize itself by emission of a photon. This average lifetime is 3.45×10^{-7} s. For $BF_3 + F^-$, $k_d = 2.89 \times 10^7$ s^{-1} giving $\tau_d = 3.46 \times 10^{-7}$ s, and $k_r = 2.60 \times 10^6$ s^{-1} giving $\tau_r = 3.84 \times 10^{-7}$ s. So it is apparent that both k_d and k_r for $(BF_4^-)^*$ can compete with collisional stabilization at 0.55 torr at 298 K. Analysis of the other boron trihalide systems displays similar re-

sults. That is, average lifetimes τ_d and τ_r are consistent with the experimental constraints set by the time between stabilizing collisions. The information gained about the lifetimes of the excited complexes for unimolecular decay and especially for the emission of a photon is very important. As indicated, the knowledge of average lifetimes allows us to determine if unimolecular decay and radiative stabilization can compete with collisional stabilization and, in the case of radiative stabilization, knowledge of the lifetime, τ_r, is important in evaluation of the type of radiative transition that is occurring, as discussed below.

(d). Radiative Stabilization

Radiative stabilization in gas phase ion-molecule systems has been proposed for only a few[73-75] systems of the thousands that have been studied.[76] As discussed earlier, magnitudes of radiative rates in the infrared region are for the most part thought to lie in the range from 10 to 10^3 s^{-1}, [33] however, a reexamination of the reaction $CH^{3+} + H_2 \longrightarrow CH_5^+$ by Bates[38] predicts k_r to be on the order of 10^4 s^{-1} for an IR transition. So it is clear that radiative rates for infrared transitions may be larger than originally thought, and further investigation may reveal more about radiative lifetimes. In an investigation of the ion-molecule association reaction of CH_3^+ with HCN, McEwan et al.[40] have proposed a k_r on the order of 10^5 s^{-1}; they have interpreted this to be indicative of an electronic

transition.

An examination of the radiative rate coefficient for all the boron trihalide sytems studied demonstrates that k_r ranges from an upper limit of $\sim 10^6$ s^{-1} at β_{max} to $\sim 10^4$ at $\beta = 0.01$, as shown in Table (XXX). As discussed in the results section, the evidence for radiative stabilization is given by the presence of a bimolecular process occurring at (M) = 0 indicated in plots of k_{obs} vs. (M) for several different buffer gases. Also the same the intercept for $BF_3 + F^-$ was obtained using a low pressure ion-molecule technique, ICR, at a pressure five orders of magnitude lower than that found in a FA. This, combined with the common intercepts from the various buffer gases, the good fit of the lines generated assuming $k_r \neq 0$ and the similarity in all of the boron systems, leads us to conclude that a radiative channel is present in the $BF_3 + F^-$, $BCl_3 + Cl^-$ and Br^- sytems. While the radiative stabilization pathway may be present in $BF_3 + Cl^-$ it is diminished in importance by a large unimolecular decay rate coefficient. If we look at the $BF_3 + F^-$ system, $k_r = 8.69 \times 10^4$ s^{-1} for $\beta = 0.01$ which is the same order of magnitude as the largest vibrational radiative rate as calculated by Bates.[38] For k_r to be in the 10^3 s^{-1} range, $\beta = 10^{-4}$ would be required which seems unreasonable when compared to other known values of β. For larger values of β, k_r is on the order of 10^5 to 10^6 s^{-1}. For $\beta = 0.30$ values for k_r for all the BX_3 systems are approximately 3×10^6 s^{-1}.

This is perhaps indicative of an electronic transition. A possible route for this electronic transition to occur is through an intersystem crossing (ISC) as shown below:

$$BX_3 + X^- \rightleftharpoons (BX_4^-)^*,vib \rightleftharpoons (BX_4^-)^*,elec \rightarrow BX_4^- + h\nu \quad , \quad (4.8)$$

where the vibrationally excited complex transfers into an upper electronic state by intersystem crossing and radiatively relaxes by emission of a photon from this electronic state. This would account for the similarity of k_r for all systems as the intersystem crossing (ISC) controls the rate at which the emitting electronic state is populated. This also accounts for k_r being lower than one would expect for fluorescence or phosphorescence since k_r would be a composite of forward and reverse ISC and radiative steps.

(e). Temperature Dependence

As noted in the Results, the temperature dependence of the boron trihalide systems was studied over a range of approximately 200 K. The data of k_{obs} vs. (He) at the various temperatures shows a negative dependence upon temperature, i.e., $k_{obs} = AT^{-n}$. The majority (and we assume all) of the temperature dependence of k_{obs} is due to that of the unimolecular decay rate coefficient, k_d. The functional form for $k_{obs}(T)$ in the fall-off region is not actually a simple exponential expression because the entire expression for k_{obs} (equation (1.10)) must be considered. Thus, contributions from $k_s(M)$ and k_r are not negliable and

this can affect the determination of n.

The magnitude of the temperature dependence, n, was determined by evaluation of the slope of plots of log k_{obs}, log k_d, and log "$k^{(3)}$" vs. log T, as discussed in the Results section. Table (XXXI) lists the values of n for each method of determination. Clearly the trend in k_{obs} indicates that most of the temperature dependence is indeed in k_d, but since other terms are involved in the expression for k_{obs}, the relationship $k_{obs} = AT^{-n}$ is not strictly true. Recall that k_{obs} is given by:

$$k_{obs} = \frac{k_a(\beta k_s(M) + k_r)}{k_d + \beta k_s(M) + k_r}. \qquad (4.9)$$

In the fall off-region where $k_s(M)$ becomes important and/or in cases where $k_r = 0$, the approximation $k_{obs} \propto T^{-n}$ becomes less accurate. Therefore quantitative discussion of the temperature dependence will deal primarily with the temperature dependence of k_d.

In the $BF_3 + F^-$ and Cl^- systems the values of n obtained for the TD of k_d are 2.0 and 2.2 respectively (2.0 for $BF_3 + Cl^-$ with $k_r = 0$). The thermal theory first proposed by Bates[19,51] and Herbst[27,52,53] predicts "$k^{(3)}$" $\propto T^{-\ell/2}$ where ℓ is the total number of rotational degrees of freedom of the reactants; this predicts n = 1.5 for all of the boron trihalide systems. Inspection of Table (XXXI) shows this is not the case for any of the systems no matter what method is used to calculate n; the temperature depen-

TABLE XXXI

A Compilation of the Magnitude of the Temperature Dependence, n, for the Halide Ion-Boron Trihalide Systems

$BF_3 + F^-$

Data Set	n
k_{obs}	1.6
k_d,exp	2.0
"$k^{(3)}$", Theory	1.79 to 2.77

$BF_3 + Cl^-$

Data Set	n
k_{obs}	2.6
k_d,exp	2.2 ($k_r \neq 0$
k_d,exp	2.0 ($k_r = 0$)
"$k^{(3)}$", Theory	1.79 to 2.77

$BCl_3 + Cl^-$

Data set	n
k_{obs}	2.4
k_d,exp	2.3
"$k^{(3)}$", Theory	2.33 to 3.87

$BCl_3 + Br^-$

Data Set	n
k_{obs}	2.5
k_d,exp	2.5
"$k^{(3)}$", Theory	2.33 to 3.87

dence is always larger indicating that perhaps more than rotational modes alone participate. The modified thermal theory as given by Viggiano[56] includes vibrational contributions where the condition $h\nu >> kT$ is not true, and is better at predicting the temperature dependencies obtained for the boron trihalide systems. For the $BF_3 + F^-$ system, n = 2.0 as evaluated from log k_d vs. log T plots. Table (VII), which is a compilation of n values determined from theory over 50 K intervals with varying vibrational contributions, predicts an average n = 2.0 over the temperature range from 200 to 400 K when only the lowest vibrational mode (a doubly degenerate mode at 480 cm^{-1}) is active. For the $BF_3 + Cl^-$ system, n = 2.2 ($k_r = 0$) as evaluated from a log k_d vs. log T plot. Since k_{obs} for this system is small (on the order of 10^{-12} cm^3 $molec^{-1}$ s^{-1}) it could only be measured in the temperature region from 348 to 219 K. If an average n is calculated over this range from Table (VII), a maximum value of only 2.1 is obtained when <u>all</u> vibrational modes are active. This is unreasonable when the following argument is considered. For the halide ion-boron trihalide systems, only the boron trihalide molecule possesses rotational and vibrational degrees of freedom, and thus should be solely responsible for the temperature dependence of these systems according to theory.[19,27,50-52] So, the theory, as put forth, should predict the same value of n for both of the above BF_3 systems for a given temperature range. Therefore it is

unreasonable that all of the vibrational modes would suddenly become active for the $BF_3 + Cl^-$ system over the same temperature range simply because a different halide ion is present. This argument of course assumes n = 2.0 for $BF_3 + F^-$ to be the correct value. In actuality these two values 2.0 and 2.2 are within experimental error of each other which makes it difficult to ascertain exactly how many vibrational modes are active. At the minimum it is one at 480 cm^{-1} and at the maximum it is three at 480, 691, and 888 cm^{-1}. In both cases, the temperature dependences as calculated are larger than the 1.5 as predicted on the basis of rotational partition functions only, and this points to the conclusion that at least some of the vibrations of BF_3 must be considered in determining the temperature dependence of k_d. It is interesting to note that n = 2.0 is predicted for BF_3Cl^- in the case where k_r = 0. As discussed above, we expect the importance of k_r to be diminished by the relatively large unimolecular decay rate coefficient in this case.

For the $BCl_3 + Cl^-$ system, n = 2.3 and for the $BCl_3 + Br^-$ system, n = 2.5 as shown in Table (XXXI); these are obtained from plots of log k_d vs. log T. Again these two values are close enough within experimental error to be considered the same, but certainly large enough to be considered different from those for the BF_3 systems; this demonstrates a definite trend in n. The polyatomic BCl_3 has more lower lying vibrational modes than BF_3 and so the

temperature dependence for the BCl_3 systems should be larger in magnitude as predicted by theory, and indeed this is so. Table (XXIII) which lists the values of n calculated over 50 K intervals with varying vibrational contributions, predicts n = 2.5 over the temperature range from 400 to 200 K, where one mode at 243 cm^{-1} is active; this mode is doubly degenerate. This value of n = 2.5 is identical to the experimental value for the $BCl_3 + Br^-$ system obtained from $k_d(T)$; it is 0.2 higher than that calculated for $BCl_3 + Cl^-$, but they are the same within experimental error. This indicates that at most only one vibration (the lowest lying) of BCl_3 is active and contributing to the temperature dependence. This also suggests that at most one vibrational oscillator for BF_3 is active and contributing to the temperature dependence of these systems as well. Noting the vibrational frequencies listed in Table (VII) and Table (XXIII) it is seen that the lowest lying vibration for BF_3 is 480 cm^{-1} almost twice that of the lowest lying vibration of BCl_3 at 243 cm^{-1}. Thus it is reasonable that if only one vibration for BCl_3 is active, then at most only one should be active for BF_3.

For evaluation of n, we have used the relation $k_d = AT^n$. Although it might seem that k_d must increase in the boron trihalide systems as n increases, this would not be true if the preexponential factor, A, varied significantly from one system to another or if the bond energy differs from one system to another. Any factor other than T which

changes k_d makes use of the magnitude of n as a guide to the magnitude in k_d difficult. But, in a qualitative sense, as k_d becomes larger from one system to another, especially for similar such as those presented here, one might expect k_d to follow the trend in n. For instance, for the BF_3 + Cl^- system, k_d is large compared to the other sytems and thus, as, shown D^o (F_3B-- Cl^-) is small compared to the other systems. This means that in order to break the F_3B--Cl^- bond of the excited complex in which the energy has been redistributed, an energy equal to or greater than the bond strength must be concentrated in the B--Cl^- bond. In going from a low to a high temperature (for example say 220 to 410 K as done in this study) more energy is imparted to the participating molecules. As a result, there is a higher probability of concentrating enough energy in the particular B--Cl^- bond for dissociation (because more energy is available to the system) and k_d increases. For the BF_3 + F^- system where k_d is small and D^o large as compared to the other systems, the small amount of extra energy imparted to the participating molecules due to the increased temperature has a smaller effect in promoting dissociation of the strong B--F^- bond. Therefore a larger temperature dependence might be expected for systems with comparatively larger k_d's. For the two BF_3 systems this is the case: k_d for BF_3 + Cl^- system is larger than k_d for BF_3 + F^-. But in comparison to the BCl_3 + Cl^- and Br^- systems, BF_3 + Cl^- should have the

largest value of n since k_d is larger for this system. This is not the case of course, and in fact both BCl_3 + Cl^- and Br^- possess larger temperature dependences than the BF_3 + Cl^- system. Apparently the lower lying vibration for BCl_3 at 243 cm^{-1} is enough to offset the smaller k_d and cause its temperature dependence to be larger, although not by much. In conclusion, comparison of the magnitude of the temperature dependence as a guide to the magnitude of k_d is not reliable when comparing different neutrals, but may be a good qualitative guide for reactions of the same neutral.

To summarize, the simple exponential form of $k_{obs} = AT^{-n}$ is actually only an approximation to the more complex form describing the fall-off region, making accurate determination of n in this region difficult. Direct quantitative comparison of values of n obtained by this method cannot be made with those obtained experimentally from $k_d(T)$ and theoretically from "$k^{(3)}$". Low pressure conditions are assumed in this theory ($k_s(M) << k_d$), and if one assumes that all of the temperature dependence of the low pressure rate is in k_d, then $k^{(3)} = BT^{-n}$ (where B includes k_a and k_s terms in addition to A), and n here is the same as in the expression for $k_d(T)$. In comparing values of n determined from $k_d(T)$ and theory it is predicted that at most one vibration of BF_3 and BCl_3 is active over the temperature range from 200 to 400 K studied herein.

(f). Ligand Switching in the BF_3 + Cl^- System

The products resulting from the BF_3 + Cl^- system yielded some interesting results. The products observed were the main association product BF_3Cl^-, the cluster product, $BF_3Cl^-\cdot BF_3$, observed at 248 and 219 K, and another mass at 153 amu which was also observed at 248 and 219 K. It was determined that this product was the cluster $BF_4^-\cdot BF_3$ (155 amu) resulting from a ligand exchange with the cluster $BF_4^-\cdot BF_2Cl$. This cluster is the result of a rearrangement within the cluster $BF_3Cl^-\cdot BF_3$. Several factors lead to this conclusion: (1) this product at 155 amu was observed only at the low temperatures, 248 and 219 K; these two temperatures are the only ones where the cluster $BF_3Cl^-\cdot BF_3$ was observed, (2) BF_4^- is never observed which means that $BF_4^-\cdot BF_3$ is not simply a direct result of the clustering of BF_3 with BF_4^-, and (3) the product plot (which is a plot of percent counts of each product vs. neutral concentration) is consistent with the above interpretation. Figure (4.20) shows the product plot obtained. The proposed mechanism for this ligand exchange process is as follows:

$$BF_3Cl^- + BF_3 \longrightarrow BF_3Cl^-\cdot BF_3 \qquad (4.10)$$

$$BF_3Cl^-\cdot BF_3 \longrightarrow BF_4^- BF_2Cl + BF_3 \longrightarrow BF_4^-\cdot BF_3 + BF_2Cl \quad . \qquad (4.11)$$

Because the formation of the cluster $BF_3Cl^-\cdot BF_3$ is a slow process and in general, ligand exchange processes are

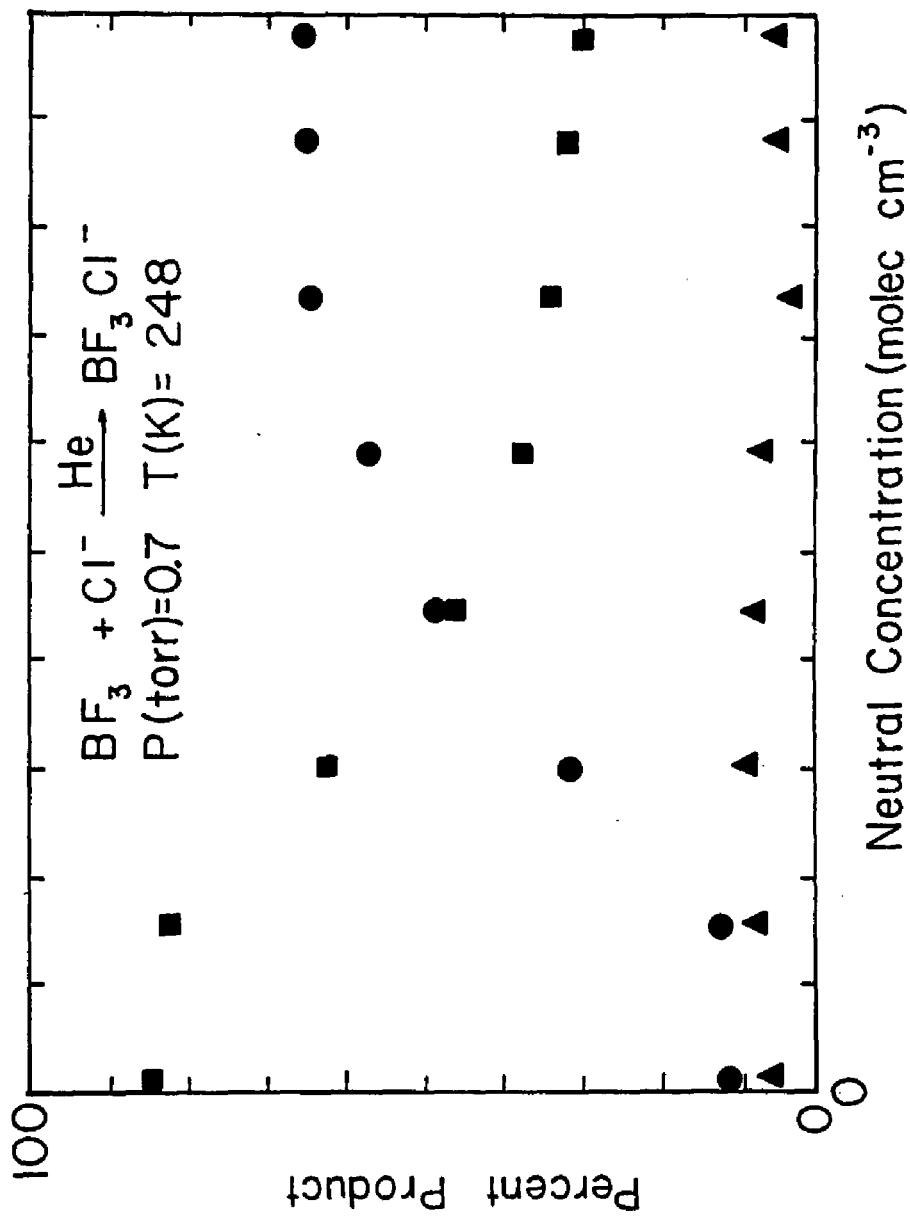

Figure 4.20. Product plot for $BF_3 + Cl^- \longrightarrow BF_3Cl^-$.
■ BF_3Cl^-, ▲ $BF_4^-BF_2Cl$, ● $BF_4^-BF_3$

fast,[44,77] then the steady state assumption can be applied to the cluster $BF_3Cl^- \cdot BF_3$ or $BF_4^- \cdot BF_2Cl$ the rearranged cluster. This rearrangement is reasonable because the fluoride affinity of BF_3 is approximately three times the chloride affinity of BF_3 as pointed out earlier. A kinetic analysis of a system with this mechanism would show the concentration of the main association product, BF_3Cl^- decreasing, the concentration of the cluster at 155 amu, $BF_4^- \cdot BF_3$, increasing, and the concentration of $BF_3Cl^- \cdot BF_3$ remaining small and constant as the reaction proceeds. This behavior is seen in the product plot in figure (4.20). It appears from our experimental evidence that the above mechanism is a likely route to formation of the cluster product $BF_4^- \cdot BF_3$. These results are interesting and further examination of this reaction at low temperatures would be interesting.

CHAPTER 5

ESULTS AND DISCUSSION OF THE HALIDE ION-SILICON TETRAFLUORIDE SYSTEMS

I. Silicon tetrafluoride

Silicon tetrafluoride is a tetrahedral molecule with sp^3 bonding. Some of the ion chemistry of SiF_4 has been examined in a study of its Lewis acid properties[66] as well an examination of some bimolecular reactions of SiF_4 with OH^-, OCH_3, and OH^- H_2O.[78] Silicon tetrafluoride has the ability to expand its octet and employ 3d orbitals in bonding.[72] Addition of a halide ion to SiF_4 results in the formation of a trigonal bipyramidal anion as shown below:

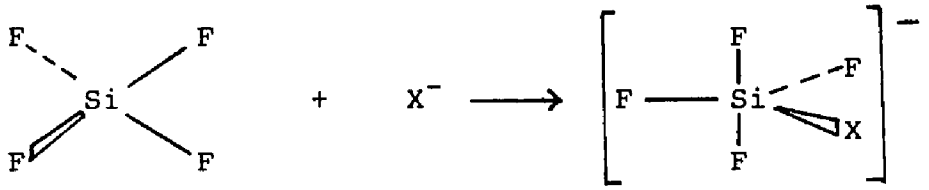

II. $SiF_4 + F^-$ Results

(a). General Results

This system was studied over the pressure range 0.3 to 0.8 torr and at five different temperatures: 408, 348, 298, 248, and 219 K. Figure (5.1) is a plot of k_{obs} vs. (He) at all temperatures studied. Because k_{obs} for this system was essentially the collision rate and displayed no appreciable pressure dependence, an average k_{obs} for each temperature was calculated. Table (A6) in Appendix (6), lists the values of k_{obs} obtained at each pressure for a given temperature and Table (XXXII) lists the average values of k_{obs} determined at each temperature. The lines in figure (5.1) are average values of k_{obs} at each temperature. The only products observed were SiF_5^- at 123 amu along with a very small amount of an addition product of an ether impurity, $((SiF_3)_2OF)^-$, at 205 amu. An impurity in the neutral reactant would increase k_{obs} since the actual neutral concentration of the species of interest would be smaller than the flow indicated. From the manufacturer's listed purity (99.99%) and the small amount of impurity actually seen, we judge the increase in k_{obs} to be no more than 1% (this assumes only 99% purity). Within our experimental error of $\pm$ 20% this is insignificant. The apparent overall rate coefficient, k_{obs}, displayed no detectable pressure dependence and ranged in value from 0.9×10^{-9} cm^3 $molec^{-1}$ s^{-1} at 408 K to 1.5×10^{-9} cm^3 $molec^{-1}$ s^{-1} at 219 K. These

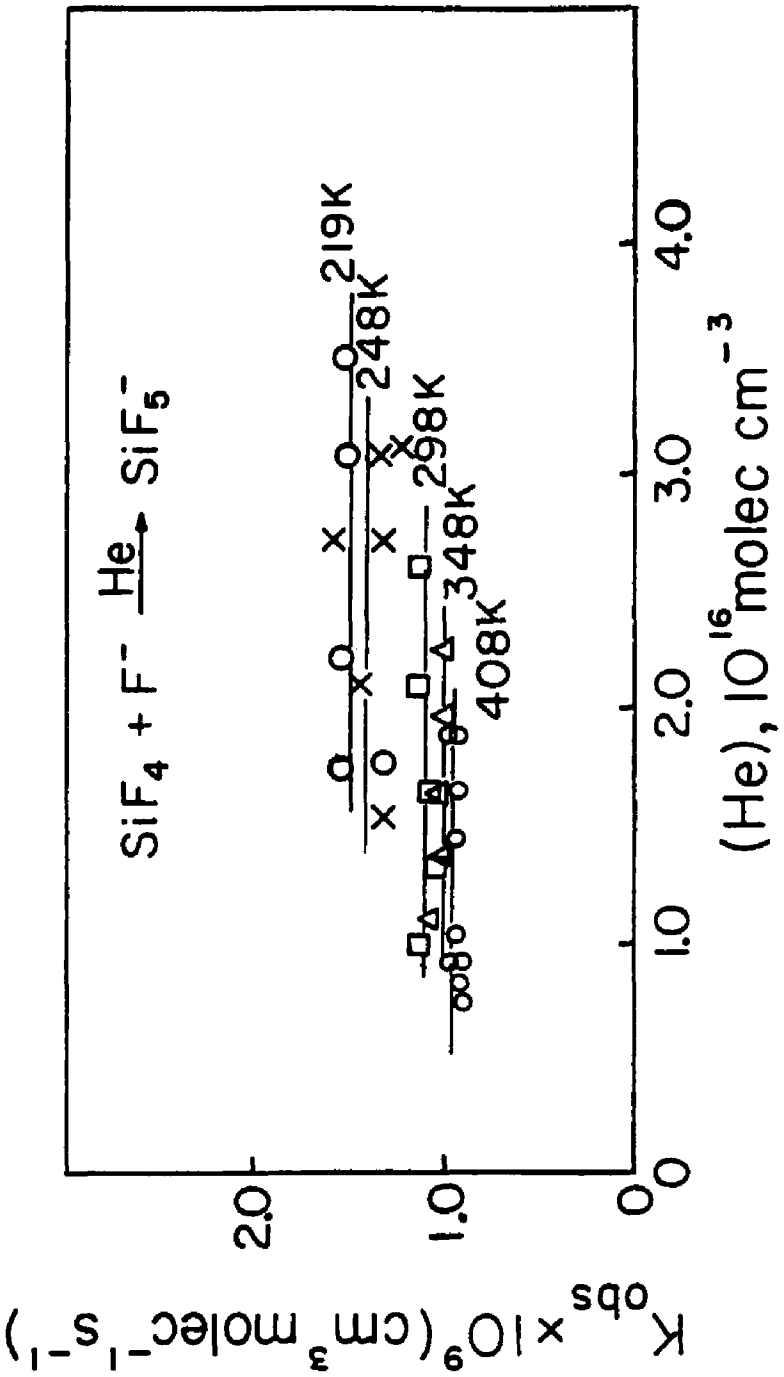

Figure 5.1. Pressure and temperature dependence of k_{obs} for halide ion addition.

TABLE XXXII

Averages of k_{obs} at the Different Temperatures Studied for $SiF_4 + F^- \longrightarrow SiF_5^-$

T, K	k_{obs}
408	0.9
348	1.0
298	1.1
248	1.4
219	1.5

k_{obs} units: 10^{-9} cm^3 $molec^{-1}$ s^{-1}

values are averages of k_{obs} at various (He) since no appreciable pressure dependence was observed as noted, although a slight temperature dependence in k_{obs} was detected: a factor of 1.7 increase in going from 408 to 219 K. The collision rate for this system as calculated using Langevin theory gives $k_L = 1.4 \times 10^{-9}$ cm^3 molec^{-1} s^{-1}. The Langevin rate is independent of temperature, and it is expected that systems going at or near this rate should be temperature independent. Obviously $SiF_4 + F^-$ is such a system in the sense that $k_{obs} < k_L$; however, it seems to possess a temperature dependence in contrast to what one would expect. Two explanations are possible: (1) a systematic error in the SIFT yields a false temperature dependence, or (2) the trend in k_{obs} is real and k_{obs} is going at a rate far enough removed from the collision rate to demonstrate a slight temperature dependence. We feel the latter explanation is the correct one in that the lowest value of k_{obs} of 0.9×10^{-9} cm^3 molec^{-1} s^{-1} at 408 K is 35% below k_L. This is well outside of our expected error range and therefore we feel k_{obs} at 408 K is a precise value. Using the average k_{obs} at 408, 348, and 298 K and taking the least squares values for a plot of log k_{obs} vs log T we obtain a temperature dependence of $T^{-0.5}$. The average values of k_{obs} at 248 and 219 K were not used for the calculation of n because $k_{obs} = k_L$ at these temperatures and is independent of temperature as one expects. Since we are very near or in the high pressure region, the calcu-

lated temperature dependence is simply an empirical one; the measured temperature dependence of k_d is diminished by the relatively large contribution of $k_s(M)$ and, unlike the other systems, the temperature dependence is not expected to equal that of k_d itself.

As a result, calculations for β , k_d, and k_r were not attempted here since k_{obs} is so near the collision rate. When a reaction proceeds at the collision rate and exhibits little or no dependence upon temperature and/or pressure, little information can be extracted about the details of the reaction.

III. SiF_4 + Cl^- Results

(a). General Results

This system was studied over the pressure range 0.2 to 0.8 torr and at five different temperatures: 408, 348, 298, 248, and 219 K. The values for k_{obs} range from 1.5 X 10^{-11} cm^3 $molec^{-1}$ s^{-1} at 0.375 torr and 408 K, to 2.4 X 10^{-10} cm^3 $molec^{-1}$ s^{-1} at 0.8 torr and 219 K. Table (A8) lists the values of k_{obs} vs. (He) obtained at the five different temperatures. This data is shown in figures (5.2), (5.3), and (5.4) as represented by the symbols, while the lines represent values of k_{obs} at various (He) and temperatures calculated from the data analysis. Note the positive dependence of k_{obs} upon pressure and the negative dependence upon temperature. With the exception of a very,very small amount of cluster product of the ether impurity mentioned previously $(SiF_3)_2O$ Cl^-, the only product observed was SiF_4Cl^-.

The pressure dependence of this system at room temperature was also studied using our flowing afterglow (FA) at LSU in which the upper limit of the pressure range was increased from 0.8 to 1.4 torr.[79] The data at 298 K for this system is an average of AFGL-SIFT data and the LSU-FA data. Combination of these two sets of data yields an intercept in a plot of k_{obs} vs. (He) which is very near zero within instrumental limits: 1.2X10^{-12} cm^3 $molec^{-1}$ s^{-1}. Subsequent evaluation of the k_r/k_d ratio yields a value

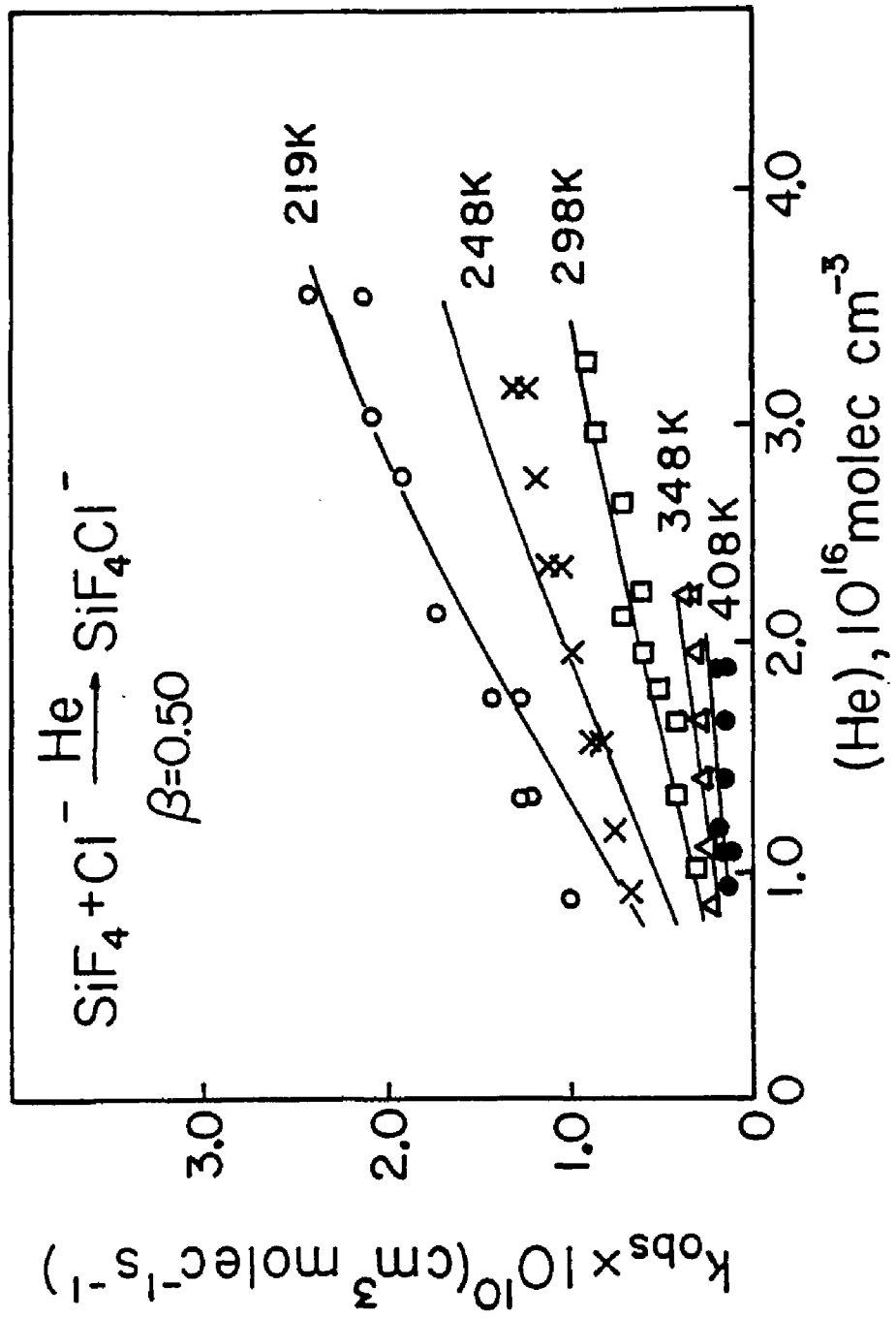

Figure 5.2. Pressure and temperature dependence of k_{obs} for halide ion addition.

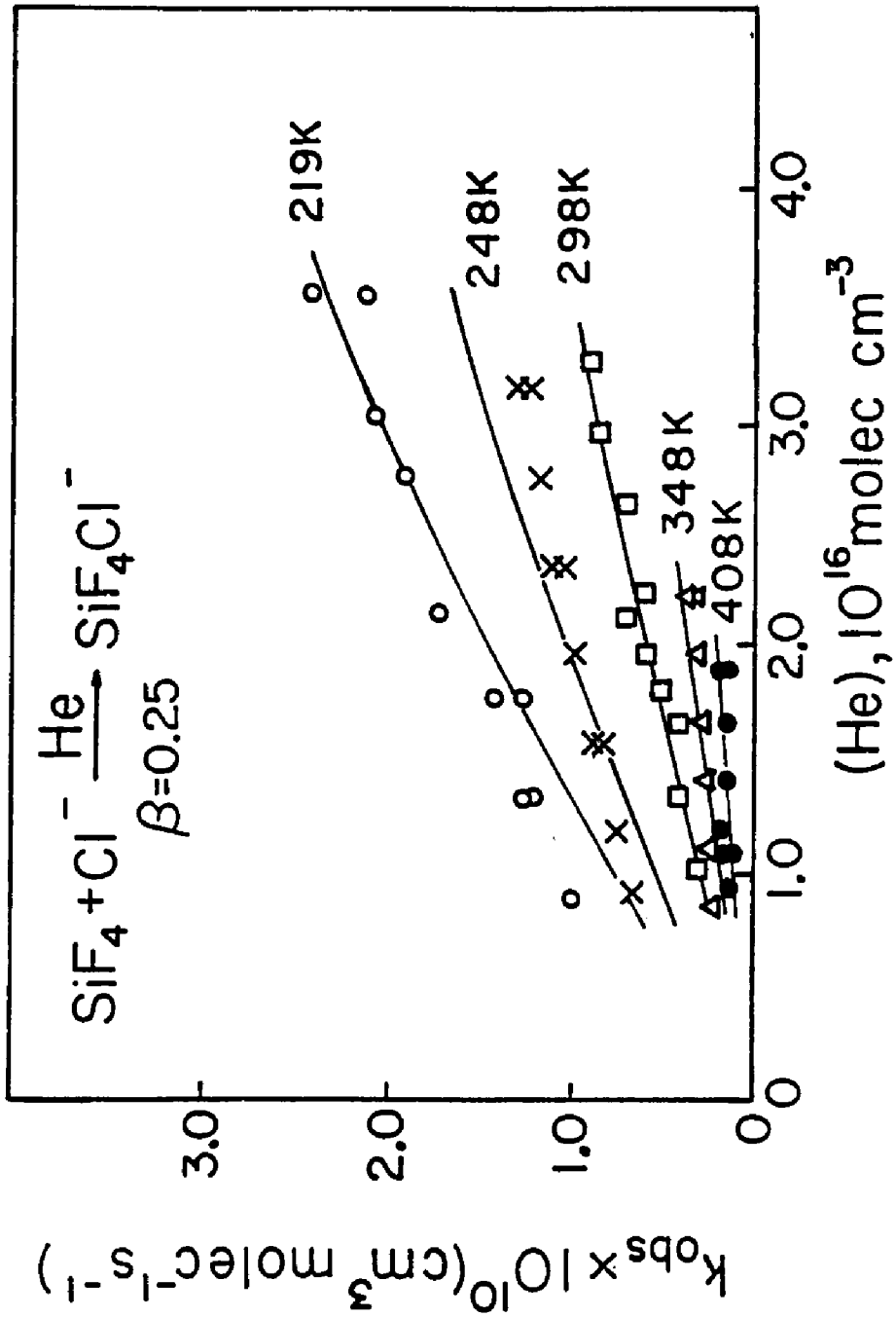

Figure 5.3. Pressure and temperature dependence of k_{obs} for halide ion addition.

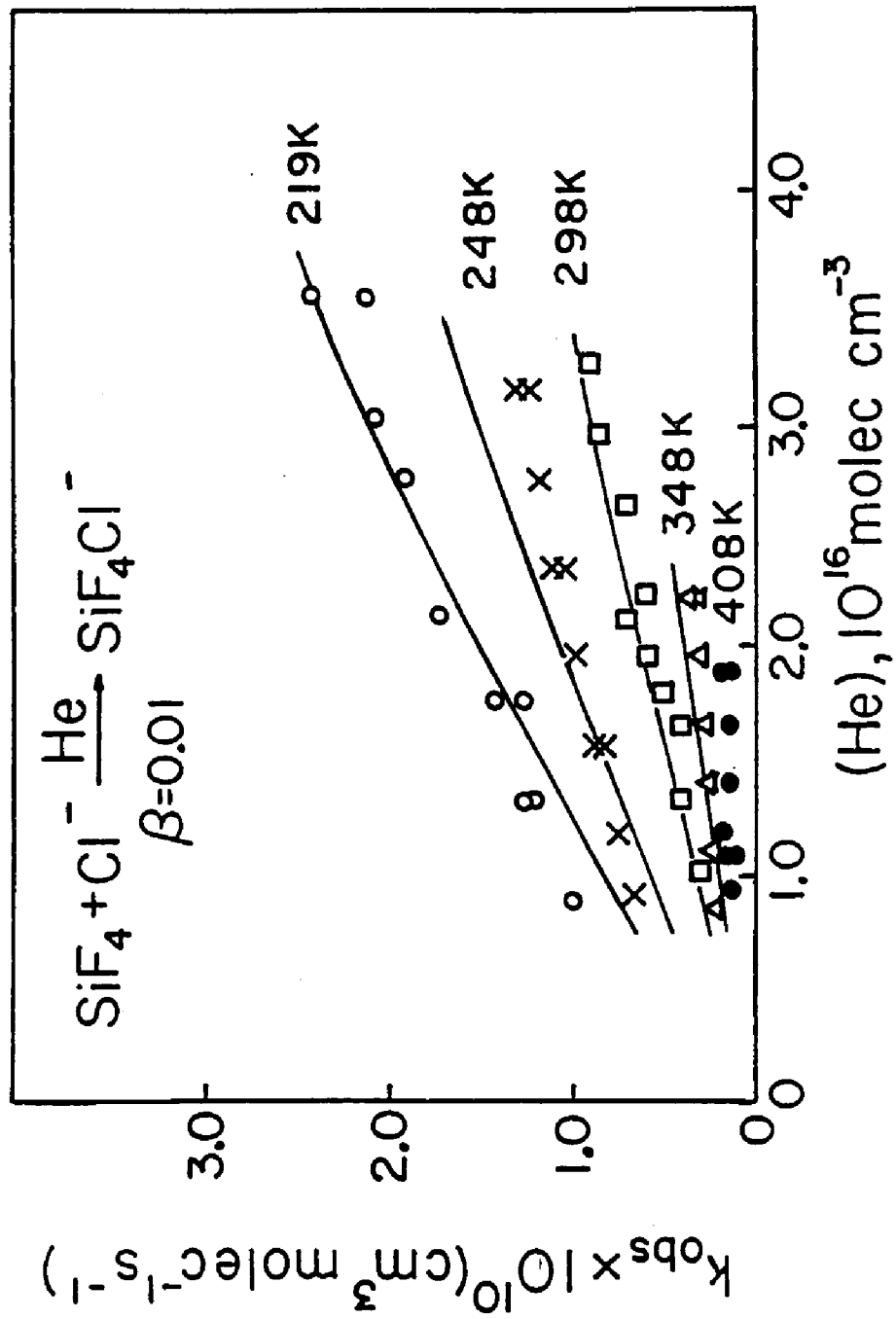

Figure 5.4. Pressure and temperature dependence of k_{obs} for halide ion addition.

of 1 X 10^{-3}. This value is smaller than the ratio for BF_3 + Cl^- in which the presence of radiative stabilization is unlikely. Also, this system was studied with N_2 in the LSU FA as the third-body and here the intercept was also very near zero.[79] Thus the evidence strongly suggests that k_r = 0 for this system, and the subsequent data analysis was performed accordingly. Plots of k_{obs} vs. (He) at the various temperatures, especially at 248 and 219 K, appear very similar to those for the boron trihalide systems and extrapolation outside of the pressure range studied yields a non-zero intercept. Although the systems appear qualitaively similar, we feel confident that the boron trihalide systems do indeed have a bimolecular (radiative) stabilization channel because of the supporting data in which a non-zero intercept was obtained from a FA third-body study[4] and the ICR low pressure study[65] as discussed. In contrast, we feel that extrapolation to a non-zero intercept for the silicon system is solely the result of being in the fall-off region as indicated by the FA data taken at room temperature with He and N_2 as the third-bodies. Examination of the plots of k_{obs} vs. (He) shows that the lines generated from the data analysis fit very well with the exception of the points at the two lowest temperatures, 248 and 219 K, for the two lowest pressures 0.2 and 0.3 torr. This is most likely due to scatter in these points resulting simply from experimental error. In conclusion then, this system does not exhibit a radiative stabilization channel

as evidenced by the zero intercept obtained from extrapolation at 298 K of two sets of k_{obs} for M = He and N_2. The data analysis for determination of k_d and its temperature dependence was done assuming $k_r = 0$ as discussed below.

(b). Results for Calculation of β and k_d

This system, $SiF_4 + Cl^-$, has been studied with both He and N_2 as the inert third-body. The data in N_2 are used here only qualitatively to confirm the absence of a radiative stabilization channel, and will not be discussed further. As done before where adequate third-body data was lacking, β_{max} was estimated using known values for β_{He} and β for other gases as a guide. The data analysis was carried out as previously described. The collision rate, k_a, for $SiF_4 + Cl^-$ is 1.06×10^{-9} cm^3 $molec^{-1}$ s^{-1} and the collision rate for the excited complex/He couple, k_s, is 5.37×10^{-10} cm^3 $molec^{-1}$ s^{-1}. A value of $\beta = 0.50$ was estimated for β_{max}. Values of k_d were determined at each temperature for evaluation of the temperature dependence of $k_d(T)$. Table (XXXIII) lists the values of $k_d(T)$ for each temperature for different values of β. Using the values given for k_a, k_s, β, and the temperature dependence of k_d, k_{obs} values at various (He) were generated. The lines in figures (5.2), (5.3), and (5.4) are the result. Again the points are experimental data. In general the agreement with experimental data is good.

TABLE XXXIII

Average Values of $k_d(T)$ for Different Values of β_{He} for SiF_4Cl^-

T, K	$^{a}k_d$, s^{-1}	$^{b}k_d$, s^{-1}	$^{c}k_d$, s^{-1}
408	2.53×10^8	1.27×10^8	5.07×10^6
348	1.38×10^8	6.91×10^7	2.76×10^6
298	9.83×10^7	4.93×10^7	1.96×10^6
248	5.22×10^7	2.61×10^7	1.04×10^6
219	3.11×10^7	1.55×10^7	6.21×10^5

[a] $\beta_{He} = 0.50$

[b] $\beta_{He} = 0.25$

[c] $\beta_{He} = 0.01$

(c). Results for the Magnitude of the TD, n

At (He) = 2.22 molec cm^{-3}, experimental values of k_{obs} were determined at 348, 298, and 219 K. From the slope of a plot of log k_{obs} vs. log T one finds that n = 3.5. The above data is listed in Table (XXXIV).

From a plot of log k_d vs. log T where k_d was taken from Table (XXXIII), n, the exponential dependence upon temperature, is found to be 3.3 for all values of β.

Theoretically n is found to range from 2.25 at 200-250 K with only one vibration considered active, to 4.69 in the temperature interval from 400 to 450 K with all vibrational modes considered active. Table (XXXV) and Table (XXXVI) list the preexponential factors and values of n determined experimentally from the temperature dependence of k_{obs} and from the temperature dependence of k_d respectively. Table (XXXVII) lists the values of n calculated from theory over 50 K intervals with varying vibrational contributions. Figure (5.5) is a plot of log k_{obs}, log k_d, and log "$k^{(3)}$" vs. log T. Note the agreement among all three values of n determined as above is excellent.

TABLE XXXIV

Values of k_{obs} at Constant (He) at Different Temperaures for SiF_4Cl^-

T, K	(He)	k_{obs}
348	2.22	3.4
298	2.27	6.1
219	2.21	17.1

(He) units: 10^{16} molec cm^{-3}

k_{obs} units: 10^{-11} cm^3 $molec^{-1}$ s^{-1}

TABLE XXXV

Temperature Dependence of k_{obs} for SiF_4Cl^-

A	n
$10^{-1.65}$	3.5

TABLE XXXVI

Temperature Dependence of k_d for SiF_4Cl^-

β_{He}	A	n
0.50	$10^{0.79}$	3.3
0.25	$10^{0.37}$	3.3
0.01	$10^{0.015}$	3.3

TABLE XXXVII

A Compilation of Calculated n Values Demonstrating Vibrational Contributions for $SiF_4 + X^-$

Temp. Range	a_n	b_n	c_n	d_n
200-250	2.25	2.91	2.95	2.97
250-300	2.41	3.32	3.38	3.46
300-350	2.54	3.66	3.76	3.91
350-400	2.64	3.93	4.08	4.31
400-450	2.72	4.17	4.36	4.69

[a]Frequencies: 268(2) cm^{-1}

[b]Frequencies: 268(2), 391(3) cm^{-1}

[c]Frequencies: 268(2), 391(3), 800 cm^{-1}

[d]Frequencies: 268(2), 391(3), 800, 1031(3) cm^{-1}

Vibrational frequencies taken from:

JANAF Thermochemical Tables, 2nd ed., NSRDS-NBS 37, June 1971, Washington, D.C.

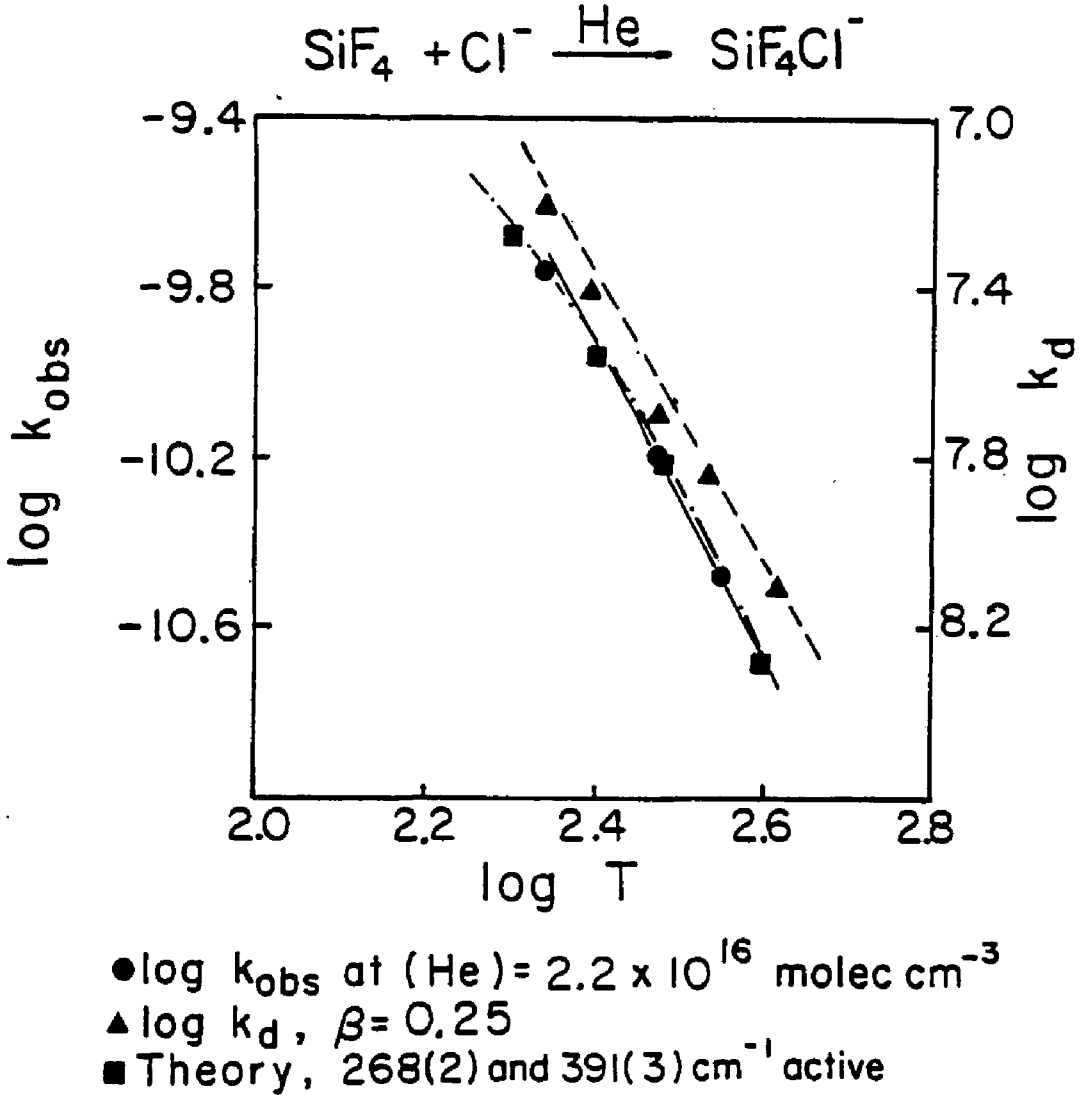

Figure 5.5. Temperature dependence of ion-molecule association reactions.

IV. $SiF_4 + Br^-$ Results

(a). General Results

This system was studied over the pressure range 0.3 to 0.8 torr and over the temperature range 408 to 219 K. Only at 248 and 219 K could reliable data be obtained for the above pressure range. The apparent overall binary rate coefficient is very small for this system, ranging from < 2 x 10^{-12} cm^3 $molec^{-1}$ s^{-1} at 0.8 torr and 348 K, to 1.79 X 10^{-11} cm^3 $molec^{-1}$ s^{-1} at 0.8 torr and 219 K. The values of k_{obs} determined at 348 and 298 K at 0.8 torr represent upper limits at those temperatures and pressures, and were found to be < 2 X 10^{-12} and < 5 X 10^{-12} cm^3 $molec^{-1}$ s^{-1} respectively. The k_{obs} vs. (He) data at 248 and 219 K is listed in Table (A8) while figures (5.6) and (5.7) are plots of the above data in which the symbols represent the actual data in Table (A8) and the lines are best fits as calculated using the previously described data analysis. Only two values of β were chosen for plotting: 0.5 and 0.01. Note the good general agreement of the experimental data with the calculated values of k_{obs}. The only product observed was SiF_4Br^-. The quadrupole mass spectrometer mass range was not large enough to detect any clustered ether impurity analogous to that seen in the other SiF_4 systems. Because k_{obs} is so small for this system and because systems behaves similar to $SiF_4 + Cl^-$, we conclude that radiative stabilization is unimportant,

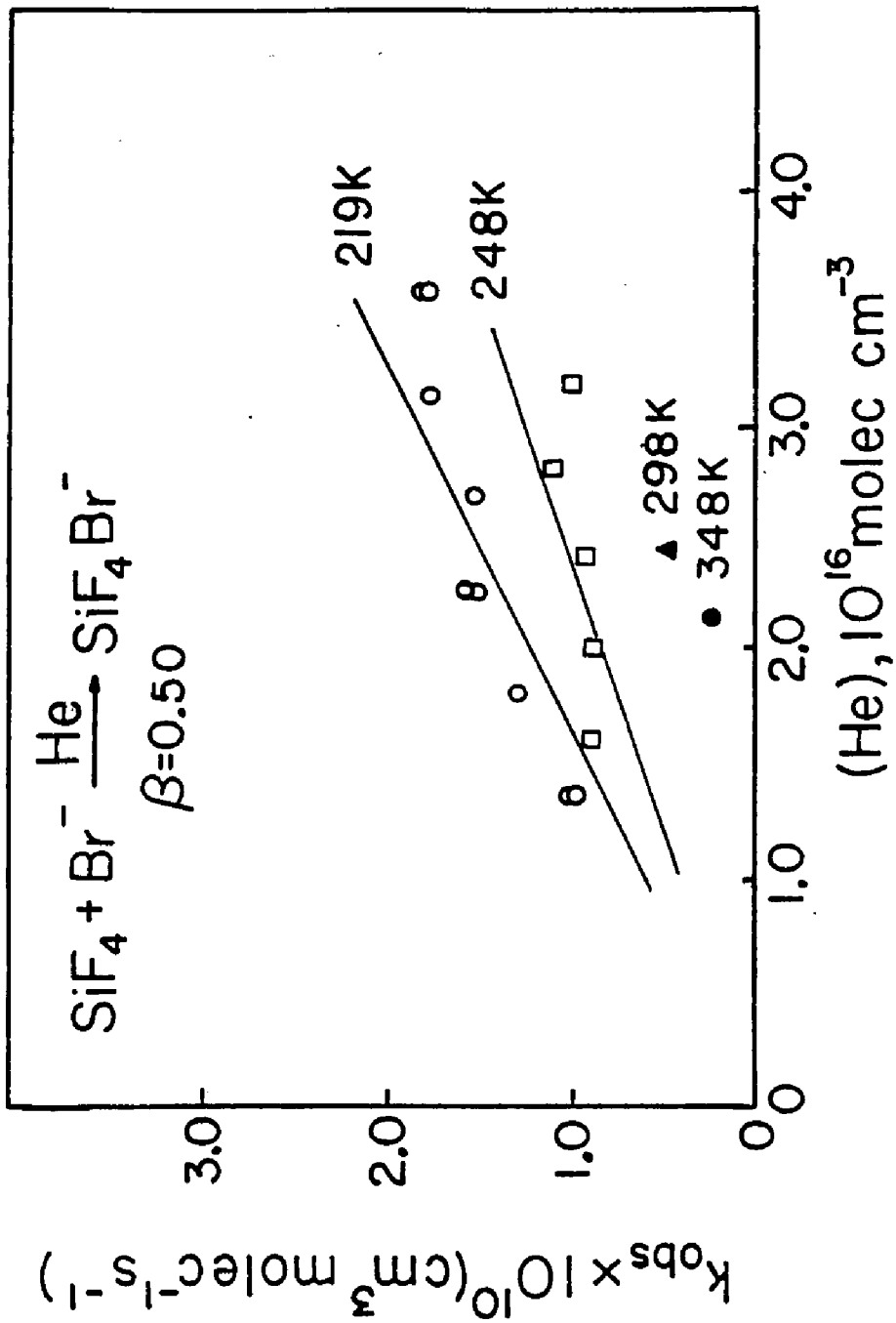

Figure 5.6. Pressure and temperature dependence of k_{obs} for halide ion addition.

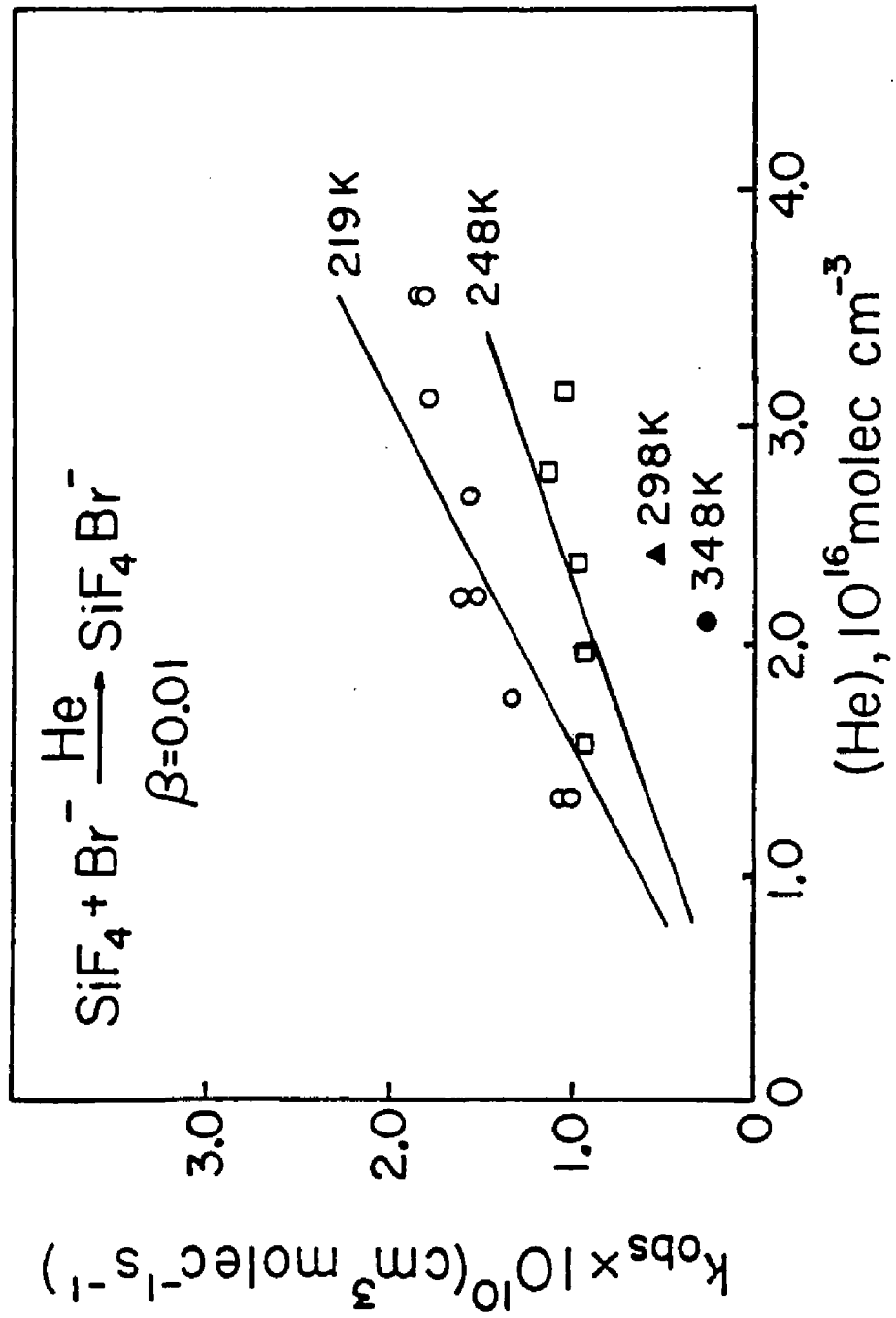

Figure 5.7. Pressure and temperature dependence of k_{obs} for halide ion addition.

and the data analysis was performed accordingly as discussed in the next section.

(b). Results for Calculation of β and k_d.

For this system, SiF_4 + Br^-, there is no radiative stabilization channel and no third-body data for evaluation of relative k_d/β ratios. As a result calculation of an average k_d at 248 and 219 K was carried out, and β_{max} was simply estimated. The results show that k_d ranges from 5.05×10^8 s^{-1} at 248 K and $\beta = 0.50$ to 6.79×10^6 s^{-1} at 219 K and $\beta = 0.01$. Table (XXXVIII) lists the average values of k_d for these temperatures at the other β values used. The temperature dependence of k_d was then evaluated for each β and was found to be 3.2 for all. It should be noted that average values of k_d were available for only two temperatures which certainly gives a higher probability for error in the determination of the value of n, the magnitude of the temperature dependence. This, in turn, results in more uncertainty in the calculated k_{obs} values at various (He) used for curve fitting. But it should be noted that the value of $n = 3.2$ is certainly reasonable and compares well with that of 3.3 obtained for the SiF_4 + Cl^- system. In addition, the fit of the generated lines with the experimental data is good. So the data anlysis appears reasonable and yields viable results which can be used with confidence at least for purposes of comparison. Once β and the temperature dependence of k_d were determined, using k_a =

8.13×10^{-10} cm^3 $molec^{-1}$ s^{-1} and $k_s = 5.36 \times 10^{-10}$ cm^3 $molec^{-1}$ s^{-1} (the Langevin values for this system), values of k_{obs} at various (He) were generated and the results are the lines in figures (5.6) and (5.7).

(c). Results for the Magnitude of the TD, n.

At (He) = 3.12 molec cm^{-3}, k_{obs} was measured at 248 and 219 K. From the slope of a plot of $\log k_{obs}$ vs. log T one finds that n = 4.7. As in all other cases, we have assumed the simple functional form for $k_{obs}(T)$ given in equation (3.1). The data is listed in Table (XXXIX).

From a plot of lof k_d vs. log T, where k_d was taken from Table (XXXVIII), n = 3.2 was determined for all values of β .

The values of n determined from the simple theory are listed in Table (XXXVII). Tables (XL) and (XLI) list the values of the preexponential factor and n calculated from experimental k_{obs} and $k_d(T)$ data respectively. Figure (5.8) is a plot of log k_{obs}, log k_d, and log "$k^{(3)}$" vs. log T. Note that even for only two temperatures from which to determine the temperature dependence, n, of k_{obs} and k_d, agreement with theory is excellent.

TABLE XXXVIII

Average Values of $k_d(T)$ at Different Values of β_{He} for SiF_4Br^-

T, K	$^{a}k_d$, s^{-1}	$^{b}k_d$, s^{-1}	$^{c}k_d$, s^{-1}	$^{d}k_d$, s^{-1}
248	5.05×10^8	3.30×10^8	2.52×10^8	1.01×10^7
219	3.40×10^8	2.04×10^8	1.70×10^8	6.79×10^6

[a] $\beta_{He} = 0.50$

[b] $\beta_{He} = 0.30$

[c] $\beta_{He} = 0.25$

[d] $\beta_{He} = 0.01$

TABLE XXXIX

Values of k_{obs} at Constant (He) at Different Temperatures for SiF_4Br^-

T, K	(He)	k_{obs}
248	3.12	1.0
219	3.09	1.8

(He) units: 10^{16} molec cm^{-3}

k_{obs} units: 10^{-11} cm^3 $molec^{-1}$ s^{-1}

Table XL

Temperature Dependence of k_{obs} for SiF_4Br^-

A	n
$10^{2.08}$	4.7

Table XLI

Temperature Dependence of k_d for SiF_4Br^-

β_{He}	A	n
0.50	$10^{12.3}$	3.2
0.30	$10^{7.24}$	3.2
0.25	$10^{6.61}$	3.2
0.01	$10^{0.23}$	3.2

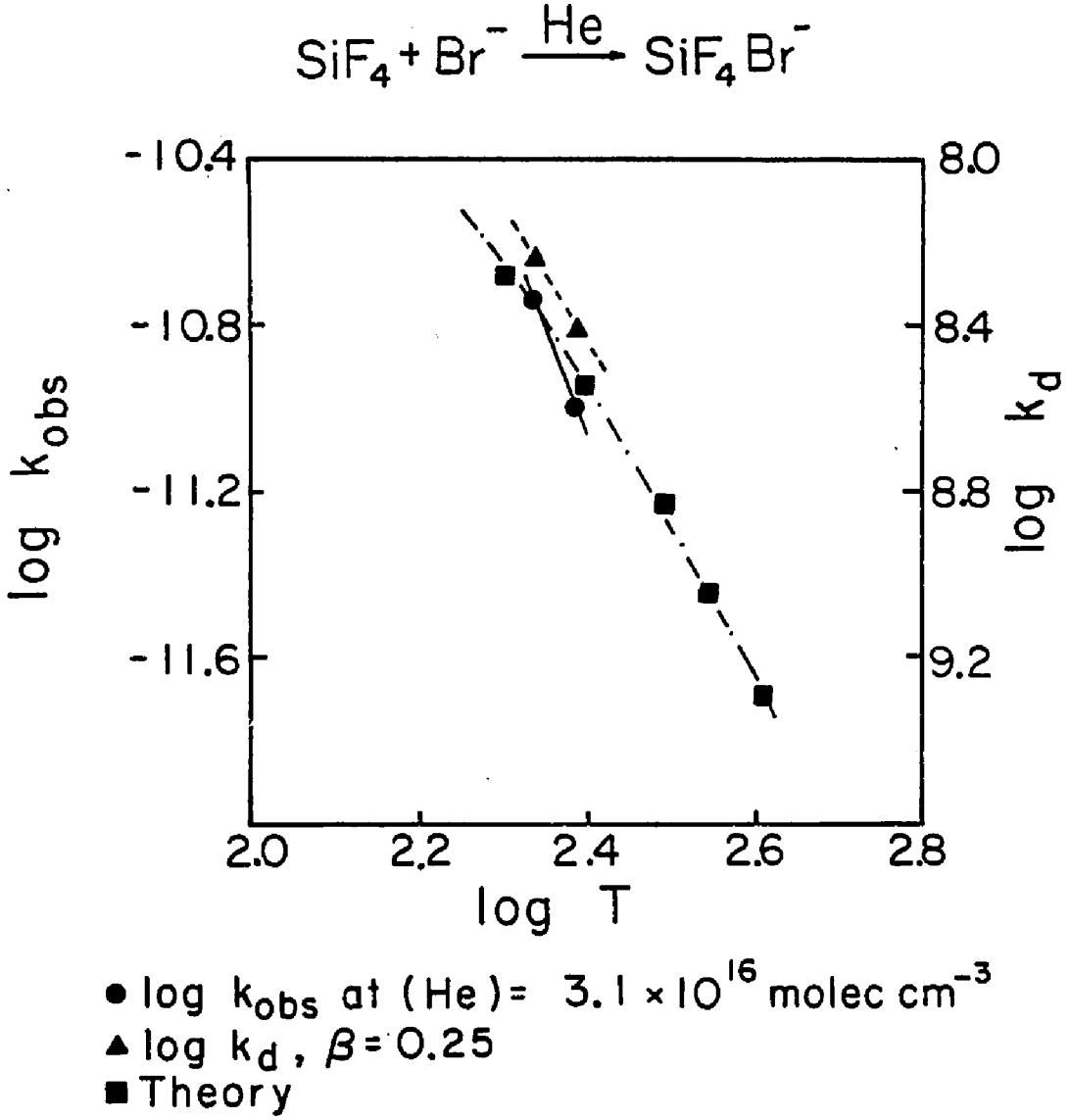

Figure 5.8. Temperature dependence of ion-molecule association reactions.

V. Discussion

(a). Introduction

The halide ion-silicon tetrafluoride systems are different from the halide ion-boron trihalide systems in that radiative stabilization at the pressures and temperatures accessible for these systems is unimportant. However, both systems possess the same general characteristics; i.e., they both have a positive dependence upon pressure (with the exception of $SiF_4 + F^-$ which shows no appreciable dependence upon pressure but occurs at almost the collision rate) and an inverse dependence upon temperature. As before, this pressure dependence allows us to evaluate the unimolecular decay rate coefficient, k_d, and thus to determine the average lifetime of the excited complex $(SiF_4X^-)^*$ Also, by application of RRK theory, it permits us to confirm the trend seen for k_d and to set an upper limit for the bond dissociation energy of SiF_4Br^-, $D^o(F_4Si--Br^-)$. Again, as before, these reactions allow a systematic study of the temperature dependence with the only change from one system to another being the identity of the monatomic halide ion. From this, evaluation of the number of vibrational oscillatiors of SiF_4 that participate in the unimolecular decay of the nascent excited complex is possible. This discussion therefore follows the same general format as that for the halide ion-boron trihalide systems in that it involves consideration of the unimolecular decay rate

coefficient and its trend from system to system, along with the temperature dependence of these halide ion-silicon tetrafluoride systems.

(b). General Discussion and Overview of Data

Table (XLII) is a compilation of $k_{d,248}$ at various values of β_{He} for SiF_4 + Cl^- and Br^-. Absent from Table (XLII) are values of k_d for the SiF_4 + F^- system. The overall rate coefficient, k_{obs}, for this system was essentially the Langevin or collision rate, and displayed no detectable pressure dependence. This means we are in the high pressure or saturated region for this system where $k_{obs} = k_a$ and no information about k_d could be extracted. Also note that only values of k_d at 248K are listed. This is because the overall rate coefficient, k_{obs}, for the SiF_4 + Br^- system was so small at room temperature and 0.8 torr, $< 5 \times 10^{-12}$ cm^3 $molec^{-1}$ s^{-1} that the system could not be studied effectively over the usual pressure range, 0.3 to 0.8 torr. A value of k_{obs} on the order of 10^{-12} cm^3 $molec^{-1}$ s^{-1} is the lower limit of the analytical range of most flowing afterglow and selected-ion flow tubes. Therefore in order to compare trends in Br^- addition to SiF_4 to trends in the F^- and Cl^- additions to the same neutral results at 248 K are used; the analysis could as well be done at 219 K.

Recalling the expression for k_d from RRK theory:

$$k_d \propto (T/D^o)^n \qquad (5.1)$$

TABLE XLII

A Compilation of $k_{d,\ 248}$ at Various β_{He} for the Halide Ion-Silicon Tetrafluoride Systems

$SiF_4 + Cl^-$

β_{He}	$k_{d,\ 248}$, s^{-1}
0.50	5.22×10^7
0.25	2.61×10^7
0.01	1.04×10^6

$SiF_4 + Br^-$

β_{He}	$k_{d,\ 248}$, s^{-1}
0.50	5.05×10^8
0.25	2.52×10^8
0.01	1.01×10^7

where k_d is the unimolecular decay rate coefficient, T is the temperature, D^o is the bond dissociation energy, and n is the number of participating oscillators (the s-1 of equation (4.6)). This expression predicts k_d to be directly proportional to temperature raised to some power n and inversely proportional to D^o also to the power n. Since the neutral (and thus the number of oscillators since the ion is monatomic) is the same for all systems, a comparison of k_d for a given temperature should yield at least qualitative information about D^o values. Also, a rough value for $D^o(F_4Si{-}{-}Br^-)$ which is unknown can be determined from equation (4.7) as done earlier for the boron trihalide systems. The bond dissociation energies of $F_4Si{-}{-}F^-$ and $F_4Si{-}{-}Cl^-$ are known, they are $D^o(F_4Si{-}{-}F^-)$ = 2.7 eV [66] and $D^o(F_4Si{-}{-}Cl^-)$ = 1.0 eV. [65] Because we were able to determine $k_d(T)$ and the temperature dependence for $SiF_4 + Br^-$, we were able to calculate $D^o(F_4Si{-}{-}Br^-)$ and thus make comparisons on the basis of bond dissociation energies and k_d. For the $SiF_4 + F^-$ system, neither $k_d(T)$ nor its temperature dependence could be determined, but since its fluoride affinity is known, comparisons with the other two silicon systems are possible. Also, an upper limit of k_d could be set from assumptions made in the saturated region. For the $SiF_4 + F^-$ system we must consider the overall rate coefficient k_{obs}. As discussed earlier, k_d should be the predominant term leading to differences in k_{obs} since k_a and k_s do not change appreciably when X^- is changed.

Since we know k_d and the bond dissociation energy for SiF_4Cl^- most reliably, comparison of the other systems is done relative to this . At 248 K, k_{obs} for $SiF_4 + Cl^-$ ranges from 6.6 X 10^{-11} cm^3 $molec^{-1}$ s^{-1} at 0.225 torr to 12.8 X 10^{-11} cm^3 $molec^{-1}$ s^{-1} at 0.800 torr. For the $SiF_4 + F^-$ system k_{obs} at 248K has an average value of 1.4 X 10^{-9} cm^3 $molec^{-1}$ s^{-1}. Recall that k_{obs} for this system is pressure independent. Because k_d is the predominant term controlling the magnitude of k_{obs} we can set an upper limit of k_d in two different ways. First for $\beta = 0.25$, the value of $k_{d,\,248}$ for $SiF_4 + Cl^-$ from Table (XLII) is 2.61 X 10^7 s^{-1}. Because k_{obs} for this system is smaller by an order of magnitude as compared to k_{obs} for $SiF_4 + F^-$ at 248 K, then $k_{d,\,248}$ for $SiF_4 + Cl^-$ is an upper limit for $k_{d,\,248}$ of $SiF_4 + F^-$. Second, the upper limit can also be set by considering the assumption commonly made in the high pressure region, i.e. $k_s(M) >> k_d$. If we assume $\beta = 0.25$ and that we are at a pressure of 0.5 torr at 248K, then (He) = 1.95 X 10^{16} molec cm^{-3}. The Langevin rate for the SiF_5^-/He couple, k_s, is 5.38 X 10^{-10} cm^3 $molec^{-1}$ s^{-1}. A quick calculation gives $\beta k_s(M)$ = 2.62 X 10^6 s^{-1}. Since $\beta k_s(M)$ must be much greater than k_d a good assumption would be that k_d is at least an order of magnitude smaller than $\beta k_s(M)$. This sets an upper limit to k_d for the $SiF_4 + F^-$ system of 2.62 X 10^5 s^{-1}. This makes $k_{d,248}$ for $SiF_4 + F^-$ two orders of magnitude smaller than $k_{d,248}$ for $SiF_4 + Cl^-$, which is 2.61 X 10^7 s^{-1}. This smaller k_d is consis-

tent with the larger bond dissociation energy seen for SF_5^- (recall k_d oc $(1/D^o)^n$).

For the $SiF_4 + Br^-$ system, k_{obs} at 248K is 0.9 X 10^{-11} cm^3 $molec^{-1}$ s^{-1} as compared to k_{obs} at 298K for the SiF_4 + Cl^- system which ranges from 6.6 X 10^{-11} cm^3 $molec^{-1}$ s^{-1} to 12.8 X 10^{-11} cm^3 $molec^{-1}$ s^{-1} at 0.800 torr. Examination of Table (XLII) shows that at $\beta = 0.25$ $k_{d,\ 248} = 2.52$ X 10^8 s^{-1} for SiF_4 + Br^-, and $k_{d,\ 248} = 2.61$ X 10^7 s^{-1} for SiF_4 + Cl^-. This of course follows the trend that k_{obs} is inversely related to k_d. Because the bond dissociation energy of $F_4Si{-}{-}Br^-$ is unknown, the trend in k_d with bond dissociation energy cannot be examined. It seems reasonable to assume that $D^o(F_4Si{-}{-}Br^-)$ is less than $D^o(F_4Si{-}Cl^-)$ based on the relationship from RRK theory that k_d oc $(1/D^o)^n$ as has been shown to hold true for the boron trihalide systems. A method available to estimate $D^o(F_4Si{-}{-}Br^-)$ was described in the boron discussion section. If we take the ratio of k_d for SiF_4Cl^- to k_d for SiF_4Br^- then D^o for $F_4Si{-}{-}Br^-$ can be determined. If k_d and the magnitude of the temperature dependence for both systems is known along with $D^o(F_4Si{-}{-}Cl^-)$, then from equation (4.7), $D^o(F_4Si{-}{-}Br^-)$ can be calculated. Substituting the appropriate data from Tables (XLII) and (XLIII), we obtain a value of 0.4 eV for $D^o(F_4Si{-}{-}Br^-)$. This certainly is consistent with the trend seen for these two systems; that is k_d is larger for SiF_4Br^- as compared to SiF_4Cl^-. In summary, only an upper limit of 2.62 X 10^5 s^{-1} for k_d of SiF_5^- can be estimated.

This is consistent with its larger bond dissociation energy. Also a rough calculation of $D^{o}(F_4Si\text{--}Br^{-})$ reveals that $D^{o} \simeq 0.4$ eV. As before the trend in the bond dissociation energy is consistent with the trend in k_{obs} in that k_{obs} increases as the bond dissociation energy increases.

(c). Temperature Dependence

These systems were studied over the temperature range 219 to 408 K, with the $SiF_4 + Br^{-}$ system possessing a measurable k_{obs} at only two temperatures: 248 and 219K. As for the boron trihalide systems, k_{obs} displayed an inverse dependence upon temperature, i.e. $k_{obs} \propto T^{-n}$. However, as mentioned, because we are in the fall off region, the actual form of the temperature dependence of k_{obs} is more complex than this simple exponential and interpretation of the temperature dependence of k_{obs} in this region cannot be done unambiguously. The best values of the magnitude of the temperature dependence, n, to compare are those obtained from log/log plots of experimental k_d values and "$k^{(3)}$" values vs. temperature, where "$k^{(3)}$" is calculated from theory as described previously. Table (XLIII) lists the values of n as determined from each of the above listed methods.

Note in Table (XLIII) that n was evaluated for the $SiF_4 + F^{-}$ system using the relation $k_{obs}=AT^{-n}$. A value of n = 0.5 was obtained. Because this system is in the saturated region or nearly saturated region, k_d is not

TABLE XLIII

A Compilation of the Magnitude of the Temperature Dependence, n, for the Halide Ion-Silicon Tetrafluoride Systems

$SiF_4 + F^-$

Data Set	n
k_{obs}	0.5

$SiF_4 + Cl^-$

Data Set	n
k_{obs}	3.5
k_d,exp	3.3
"$k^{(3)}$", Theory	2.25 to 4.69

$SiF_4 + Br^-$

Data Set	n
k_{obs}	4.7
k_d,exp	3.2
"$k^{(3)}$", Theory	2.25 to 4.69

playing a dominant role in the expression for k_{obs} as evidenced by the lack of noticeable pressure dependence at all temperatures studied; in the saturated region $k_{obs}=k_a$. Because SiF_4 lacks a permanent dipole, Langevin theory, in which the rate coefficient is independent of temperature, was used to calculate k_a. Because k_{obs} at 408K is 35% below the Langevin rate of 1.4×10^{-9} cm^3 $molec^{-1}$ s^{-1}, we feel justified in determining a temperature dependence of k_{obs} at the higher temperatures. Certainly, a value of n = 0.5 is the lowest of any of the systems studied and it is most likely that β $k_s(M)$ is so much larger than k_d that the TD of k_d is diminished by this term.

For the SiF_4 + Cl^- system the values of n determined from all three methods are in general agreement. The value of n = 3.3 as calculated from $k_d(T)$ data, in comparison with n determined from theory where the average is 3.5 over the temperature range 200 to 400K, suggests that two vibrational modes (268 and 391 cm^{-1}) are active. The oscillator at 268 cm^{-1} is doubly degenerate and the one at 391 cm^{-1} is triply degenerate. Table (XXXVII) lists the values of n determined over the indicated temperature intervals with varying vibrational contributions. This is consistent with the number and magnitude of the oscillators predicted to be active for the halide ion-BF_3, BCl_3 systems. In those cases only one oscillator at most was predicted to be active. In the case of SiF_4 the oscillators at 268(2) cm^{-1} and 391 (3) cm^{-1} are predicted to be active, where 391 is

89 cm^{-1} below 480 cm^{-1} which is the lowest energy oscillator for the BF_3 systems.

For the $SiF_4 + Br^-$ system only two temperatures were available for determination of n from the relations $k_{obs} = AT^{-n}$ and $k_d = AT^n$. Again, the propensity for error using only two temperatures is greater. This is clear when one considers that k_{obs} varies as $T^{-4.7}$ which is much higher than one would expect based on theory or on comparison with the other systems we have studied. The value of n determined from $k_d(T)$ data on the other hand is consistent with that obtained for the $SiF_4 + Cl^-$ system. Theory predicts the temperature dependence of all the $SiF_4 + X^-$ systems to be the same since only the vibrational partition functions of the reactants are considered and the halide ion, which is monatomic, possesses no vibrational or rotational degrees of freedom. Again, theory predicts the oscillators at 268 (2) and 391 (3) cm^{-1} to be active.

In summary, the temperature dependence of the $SiF_4 + F^-$ system was estimated only from k_{obs} data since k_{obs} is at or near collision rate. The magnitude of the temperature dependence, n, for the $SiF_4 + Cl^-$ and Br^- as calculated from $k_d(T)$ data are consistent with one another and comparison with theory suggests that at most two vibrational modes at 268 (2) and 391 (3) cm^{-1} are active.

CHAPTER 6

RESULTS AND DISCUSSION OF THE HALIDE ION-SULFUR TETRAFLUORIDE SYSTEMS

I. Sulfur Tetrafluoride

Sulfur tetrafluoride has a trigonal bipyramidal structure with a lone pair of electrons occupying an equatorial position. This structure is shown below:

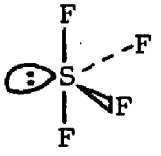

Sulfur tetrafluoride is of interest from the point of view of bonding because it can violate the Lewis octet rule by expanding its octet. This molecule is used as a fluorinating agent for organic, inorganic, and organometallic compounds.[80] It can act as a weak Lewis base because of the lone pair of electrons, or as a weak Lewis acid by bonding with its unoccupied d-orbitals.[81] The addition reaction of SF_4 with a halogen ion results in the formation of a distorted tetragonal pyramid[82] as shown below:

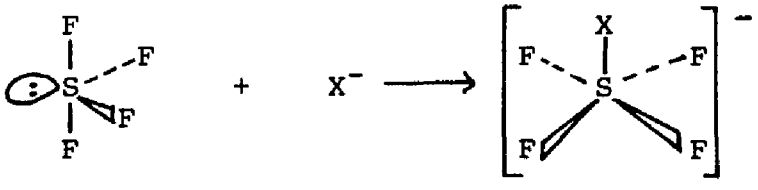

where the lone pair of electrons occupies an axial position with the sulfur atom lying slightly out of the equatorial

plane. The axial bonding is considered to be a three-center four-electron bond which is stabilized in proportion to the amount of charge separation, i.e. more electronegative ligands should be better at stabilizing the SF_4X^- molecule in its expanded octet state.

II. $SF_4 + F^-$ Results

(a). General Results and Discussion

This sytem was studied over the pressure range 0.3 to 0.8 torr and at five temperatures: 408, 348, 298, 248 and 219 K. The only product observed was the association product SF_5^-. The values of k_{obs} ranged from 5.0×10^{-10} cm^3 $molec^{-1}$ s^{-1} at 0.325 torr and 408 K, to 1.5×10^{-9} cm^3 $molec^{-1}$ s^{-1} at all pressures studied and 219 K. The data obtained for k_{obs} at the various (He) employed in this study are listed in Table (A10). The lecture bottle of SF_4 obtained from Matheson is listed as being only 90 to 94% pure. The main impurity, SOF_2, thionyl fluoride, could not be removed by cooling the lecture bottle since SF_4 and SOF_2 have similar boiling points; -40.0 and -43.8 ^oC respectively. On the assumption that the SF_4 was only 90% pure, the values of k_{obs} were multiplied by (100/90) to adjust for the 10% impurity present. Figures (6.1), (6.2), and (6.3) are plots of the above data; the symbols represent actual data points while the lines are values of k_{obs} at various (He) as calculated from the data analysis. The line at 219 K is simply the average of k_{obs} (1.5×10^{-9} cm^3 $molec^{-1}$ s^{-1}) over all pressures since it showed no pressure dependence and was approximately the collision rate (k_{ADO} = 1.60×10^{-9} cm^3 $molec^{-1}$ s^{-1} at 220 K). The fit of the lines to the experimental data is in general good for the data at 408, 348, and 220 K. At 298 K the fit is less

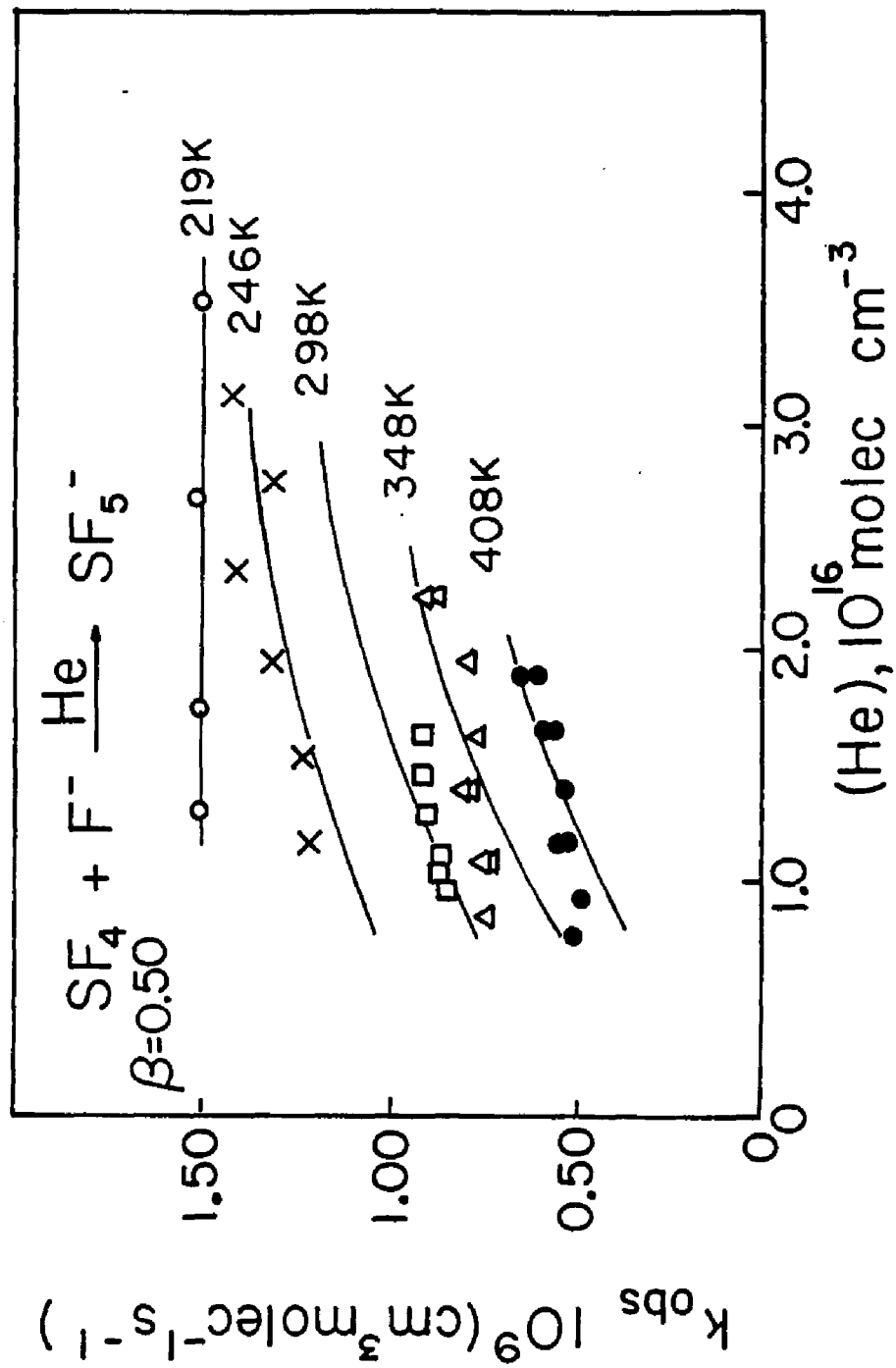

Figure 6.1. Pressure and temperature dependence of k_{obs} for halide ion addition.

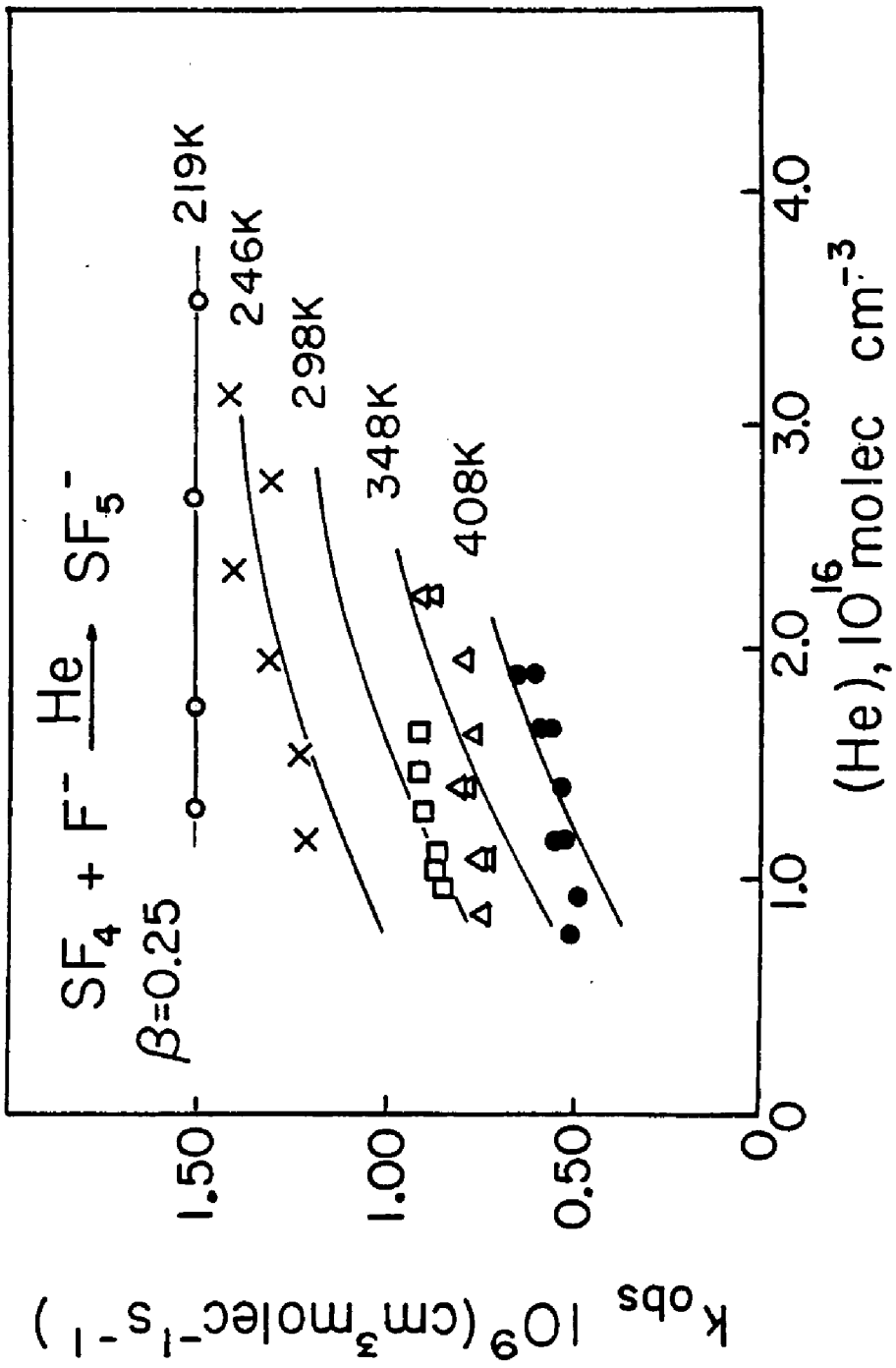

Figure 6.2. Pressure and temperature dependence of k_{obs} for halide ion addition.

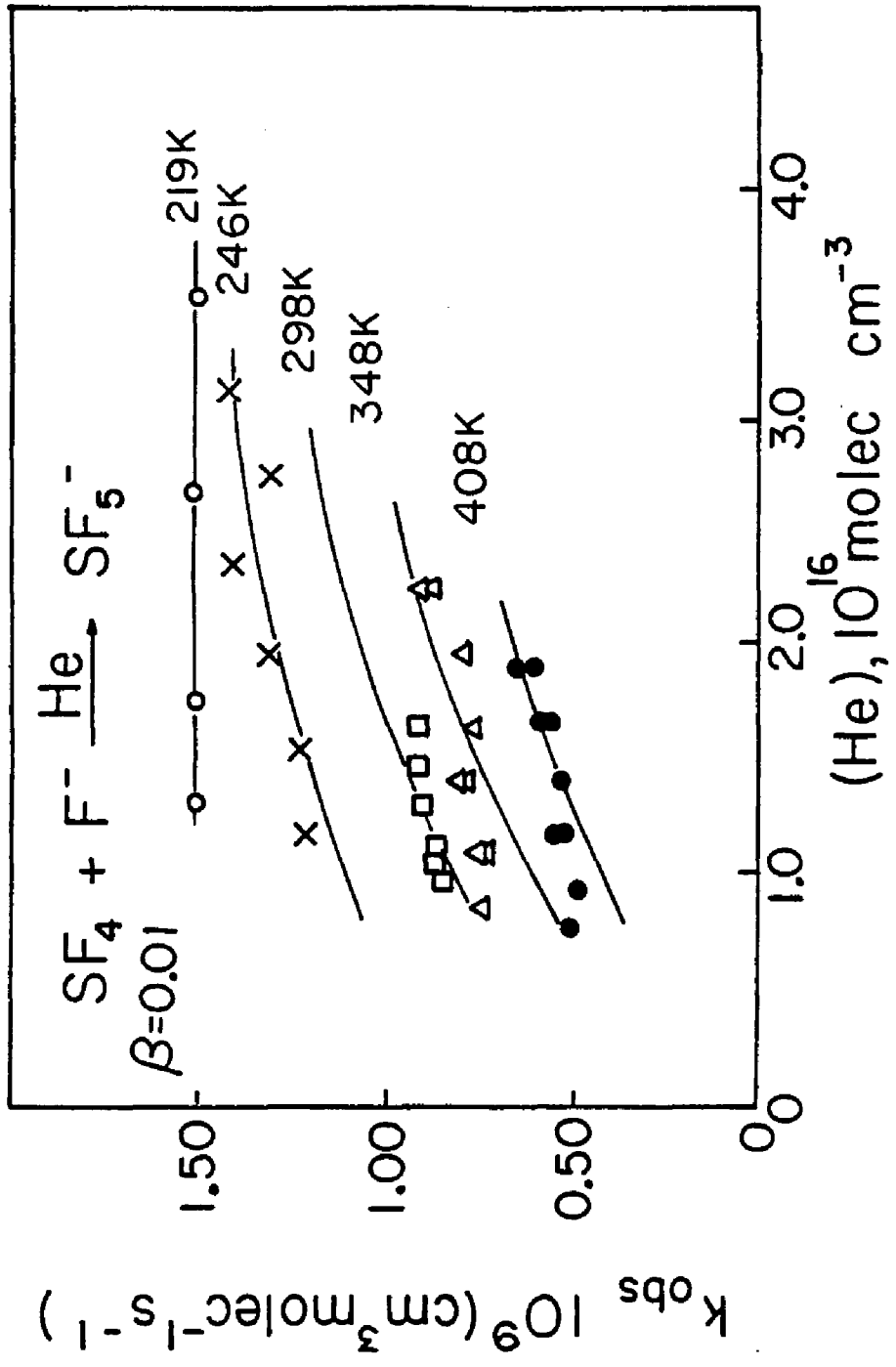

Figure 6.3. Pressure and temperature dependence of k_{obs} for halide ion addition.

gratifying. This is most likely due to the difficulty in obtaining precise data for this reaction at each pressure studied. The values of k_{obs} at a given pressure varied by as much as 15% at times, which is outside the precision usually obtained. In an effort to reduce the scatter in the data, averages of k_{obs} at constant (He) were obtained at each pressure and these averages are plotted in figures (6.1), (6.2) and (6.3). For clarity of presentation data above 0.6 torr at 298 K have been omitted from the figures.

(b). Results for Calculation of β and k_d

Without third-body data or ICR data to the contrary for this system, $SF_4 + F^-$ in He, it was assumed a radiative stabilization pathway was unimportant, and the data analysis was performed accordingly. The average values of $k_d(T)$ were calculated at four temperatures: 408, 348, 298, and 248, for different β's: 0.50, 0.25, and 0.01. These results are tabulated in Table (XLIV). The appropriate values of k_{ADO} and k_s were employed. Table (XLV) lists the values for k_{ADO} at each temperature; $k_s = 5.38 \times 10^{-10}$ cm^3 molec^{-1} s^{-1} as calculated from Langevin theory.

(c). Results for the Calculation of the TD, n.

Because SF_4 possesses a permanent dipole as mentioned, the Average Dipole Orientation (ADO) theory[8] as described in the Introduction was used for calculation of the association rate coefficient, k_a. Since this theory predicts k_a to be

TABLE XLIV

Average Values of $k_d(T)$ for Different Values of β_{He} SF_5^-

T, K	$^a k_d$, s^{-1}	$^b k_d$, s^{-1}	$^c k_d$, s^{-1}
408	6.39×10^6	3.19×10^6	1.28×10^5
348	3.71×10^6	1.86×10^6	7.42×10^4
298	3.22×10^6	1.61×10^6	6.45×10^4
248	1.06×10^6	5.32×10^5	2.13×10^4

[a] $\beta_{He} = 0.50$

[b] $\beta_{He} = 0.25$

[c] $\beta_{He} = 0.01$

inversely dependent upon temperature, another temperature dependent term is included in the expression for k_{obs} which is given by:

$$k_{obs} = \frac{k_a(T)\ \beta\ k_s(M)}{k_d(T) + \beta k_s(M)} \quad . \qquad (6.1)$$

Note that now k_a is a function of temperature. In order to be able to evaluate the temperature dependence for k_{obs} and ultimately $k_d(T)$, the temperature dependence of k_a must be determined. Su and Bowers[10] have parameterized the locking constant (which is a measure of how well the ion "locks in" the dipole) over the temperature range from 150 to 500 K at 50 K intervals. The values of c used for these calculations were obtained from reference 10. Values of k_{ADO} calculated at each temperature along with the appropriate values of the locking constant are listed in Table (XLV). If we assume the form of the temperature dependence of k_{ADO} to be $k_{ADO} = AT^{-n}$, then the magnitude of the temperature dependence, n, for k_{ADO} can be determined from the slope of a plot of log k_{ADO} vs. log T. From the values of k_{ADO} at their respective temperatures listed in Table (XLV), it is found that n = 0.093 also listed in Table (XLVI). Obviously the association rate coefficient, k_a, as determined by k_{ADO}, does not contribute appreciably to the temperature dependence of k_{obs} and the assumption that all of the temperature dependence of k_{obs} lies in k_d remains valid for this system.

TABLE XLV

Values of k_{ADO} at Various Temperatures for $SF_4 + F^-$

T, K	$^a c$	$^b k_{ADO}$
410	0.070	1.51
350	0.079	1.53
298	0.087	1.55
248	0.097	1.58
220	0.099	1.60

$^a c$ = locking constant (see reference 8)

$^b k_{ADO}$ units: 10^{-9} cm^3 $molec^{-1}$ s^{-1}

TABLE XLVI

Temperature Dependence of k_{ADO} for $SF_4 + F^-$

A	n
$10^{-8.58}$	0.093

From experimental data, the temperature dependence of k_{obs} was found to be $T^{-1.5}$. At (He) = 1.94 molec cm^{-3}, k_{obs} was measured at 348 and 248 K, and at (He) = 1.89 molec cm^{-3}, k_{obs} was measured at 408 K. The values of k_{obs} at these three temperatures for this constant (He) are listed in Table (XLVII), and the value of n and the preexponential factor calculated from the above data are listed in Table (XLVIII). Data at 298 K was unreliable and the data at 219 K yielded the collision rate where the influence of k_d is negliable, so these two temperatures were omitted from the calculation of $k_{obs}(T)$. If only the two points at (He) = 1.94 molec cm^{-3} were used for evaluation of n (i.e. the point at 408 K was omitted) it was found that n = 1.3. The value of n was determined from the slope of a plot of log k_{obs} vs. log T as in all other cases.

The determination of n for $k_d(T)$ was also done by evaluating the slope of a plot of log k_d vs. log T. Values of $k_d(T)$ were taken from Table (XLIV) and n was determined for each β used. It was found that n = 3.4 for all β. These values along with the preexponetial factors are listed in Table (XLIX).

From theoretical calculations, the values of n ranged from 2.05 in the temperature range 200-250 K (only one vibrational oscillator considered active) to 4.93 in the temperature range 400-450 K (all vibrational oscillators active). The molecule SF_4 has nine vibrational degrees of freedom and none of the modes are degenerate, so there are

nine different vibrational frequencies. Table (L) lists the values of n calculated over the temperature range 200-450 K at 50 K intervals; n is evaluated with one oscillator considered active, then with two oscillators considered active, and so on until all nine have been taken into account. Figure (6.4) shows log k_{obs}, log $k_d(T)$, and log "$k^{(3)}$" vs. log T, demonstrating the temperature dependence of each.

TABLE XLVII

Values of k_{obs} at Constant (He) at Different Temperatures for SF_5^-

T, K	(He)	k_{obs}
408	1.89	5.4
348	1.94	7.4
248	1.95	11.7

(He) units: 10^{16} molec cm^{-3}

k_{obs} units: 10^{-10} cm^3 $molec^{-1}$ s^{-1}

TABLE XLVIII

Temperature Dependence of k_{obs} for SF_5^-

A	n	
$10^{-5.40}$	1.5	(all points)
$10^{-5.74}$	1.3	(348 K, 248 K)

TABLE XLIX

Temperature Dependence of k_d for SF_5^-

β_{He}	A	n
0.50	$10^{-2.02}$	3.4
0.25	$10^{-2.30}$	3.4
0.01	$10^{-3.70}$	3.4

TABLE L

A Compilation of Calculated n Values Demonstrating Vibrational Contributions for $SF_4 + F^-$

Temp. Range	a_n	b_n	c_n	d_n	e_n
200-250	2.05	2.49	2.75	2.87	2.97
250-300	2.12	2.64	2.98	3.16	3.33
300-350	2.17	2.75	3.16	3.40	3.63
350-400	2.21	2.83	3.30	3.61	3.89
400-450	2.24	2.90	3.42	3.77	4.11

Temp. Range	f_n	g_n	h_n	i_n
200-250	3.04	3.08	3.10	3.12
250-300	3.45	3.53	3.58	3.63
300-350	3.81	3.94	4.02	4.10
350-400	4.12	4.30	4.42	4.54
400-450	4.39	4.62	4.78	4.93

[a]Frequencies: 171 cm^{-1}
[b]Frequencies: 171, 226 cm^{-1}
[c]Frequencies: 171, 226, 353 cm^{-1}
[d]Frequencies: 171, 226, 353, 532 cm^{-1}
[e]Frequencies: 171, 226, 353, 532, 558 cm^{-1}
[f]Frequencies: 171, 226, 353, 532, 558, 645 cm^{-1}
[g]Frequencies: 171, 226, 353, 532, 558, 645, 728 cm^{-1}
[h]Frequencies: 171, 226, 353, 532, 558, 645, 728, 867 cm^{-1}
[i]Frequencies: 171, 226, 353, 532, 558, 645, 728, 867, 891

Vibrational frequencies are taken from:
JANAF Thermochemical Tables, 2nd ed., NSRDS-NBS 37, June 1971, Washington D.C.

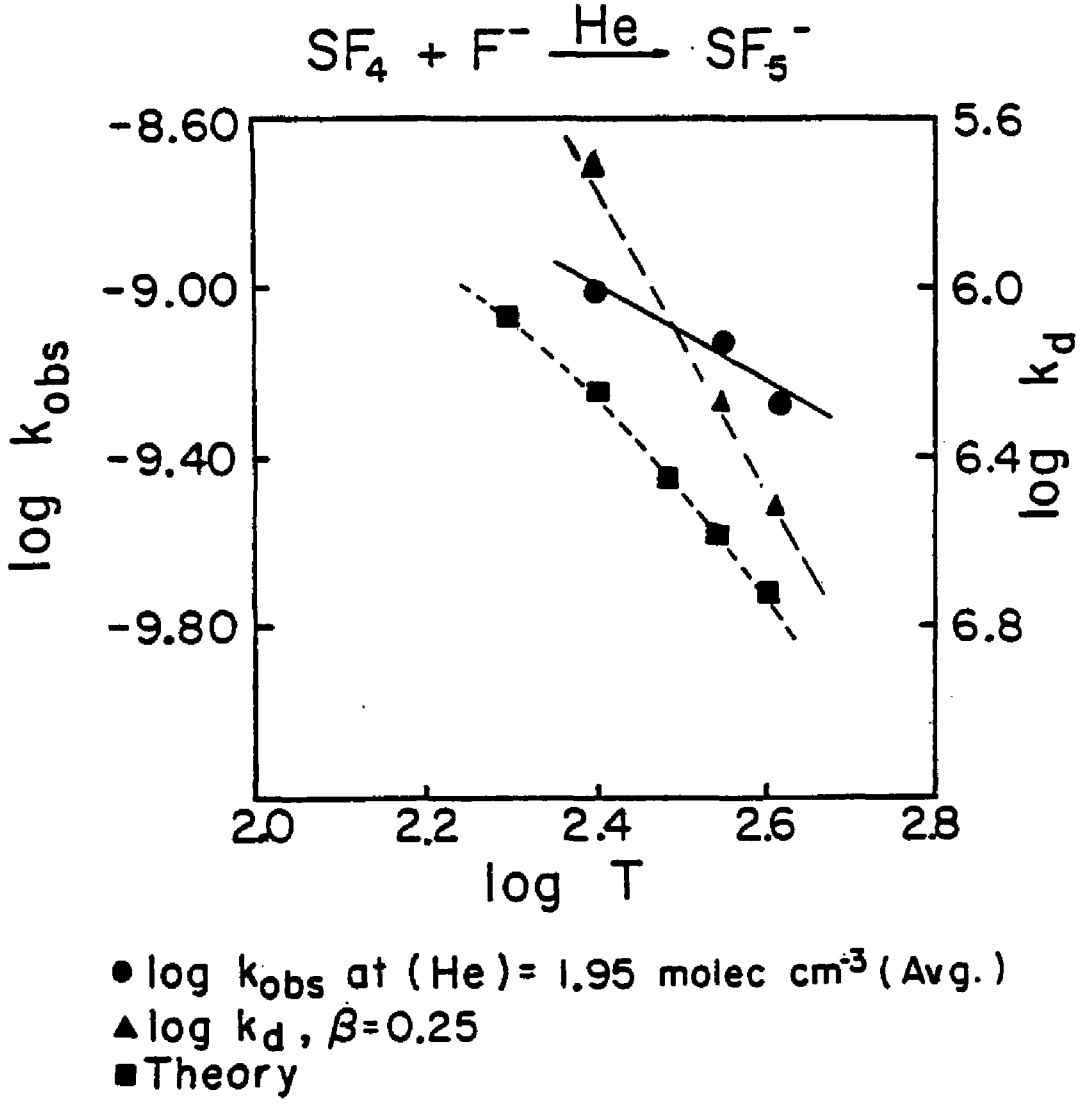

Figure 6.4. Temperature dependence of ion-molecule association reactions.

III. $SF_4 + Cl^-$ Results and Discussion

This system was studied over the pressure range 0.3 to 0.8 torr and at three temperatures: 296, 248, and 220 K. Four products were produced at 220 and 248 K, and three were produced at 296 K. These results were unexpected since $SF_4 + F^-$ gave only one product SF_5^- at all temperatures and pressures studied. The values for k_{obs} ranged from 1.9×10^{-11} cm^3 $molec^{-1}$ s^{-1} at 0.3 torr and 296 K, to 1.1×10^{-10} cm^3 $molec^{-1}$ s^{-1} at 0.8 torr and 220 K. The overall rate coefficient, k_{obs}, displayed a positive dependence upon pressure and an inverse dependence upon temperature. Because these rates are an order of magnitude lower than those for $SF_4 + F^-$, the possibility exists that other reactions can effectively compete, resulting in products not seen for $SF_4 + F^-$. The resolution of the quadrupole mass spectrometer was such that isotopes were unresolved and product masses appeared as broad peaks. This made product identification difficult at times, especially for this system where several products were observed. This system has been studied previously on two seperate occasions with two different instruments at room temperature using the FA technique,[79,83] and this has confirmed the product masses identified below. The resolution of the quadrupole in our FA is sufficient to separate and clearly see the two isotopes of chlorine (35 and 37 amu) as well as the isotopes of boron (10 and 11 amu). The following compilation tabulates the products and their relative abun-

dances at each temperature studied. For the cases in which a mass or series of masses could not be unambiguously determined, the mass range is given.

Temperature: 296 K

MASS (amu)	SPECIE	ABUNDANCE
55, 57	$FHCl^-$	~175
143	SF_4Cl^-	~135
159-176	Unassigned	~65

Temperature: 250 K

MASS (amu)	SPECIE	ABUNDANCE
55, 57	$FHCl^-$	~175
75,77	$(FH)_2Cl^-$	~90
143	SF_4Cl^-	~170
154-178	Unassigned	~120

Temperature: 220 K

MASS (amu)	SPECIE	ABUNDANCE
55,57	$FHCl^-$	~30
119-139	Unassigned	~16
143	SF_4Cl^-	~200
152-173	Unassigned	~50

In order to obtain k_{obs} for these ion-molecule association reactions the loss of the primary ion as a function of added neutral is monitored. The general scheme is as follows:

$$A + X^- \xrightarrow{k_{obs}} AX^- \quad , \qquad (6.2)$$

dances at each temperature studied. For the cases in which a mass or series of masses could not be unambiguously determined, the mass range is given.

Temperature: 296 K

MASS (amu)	SPECIE	ABUNDANCE
55, 57	$FHCl^-$	~175
143	SF_4Cl^-	~135
159-176	Unassigned	~65

Temperature: 250 K

MASS (amu)	SPECIE	ABUNDANCE
55, 57	$FHCl^-$	~175
75,77	$(FH)_2Cl^-$	~90
143	SF_4Cl^-	~170
154-178	Unassigned	~120

Temperature: 220 K

MASS (amu)	SPECIE	ABUNDANCE
55,57	$FHCl^-$	~30
119-139	Unassigned	~16
143	SF_4Cl^-	~200
152-173	Unassigned	~50

In order to obtain k_{obs} for these ion-molecule association reactions the loss of the primary ion as a function of added neutral is monitored. The general scheme is as follows:

$$A + X^- \xrightarrow{k_{obs}} AX^- \quad , \qquad (6.2)$$

where A is the neutral and X^- is the ion. For this scheme the rate of loss of the primary ion is given by the expression:

$$-\frac{d(X^-)}{dt} = k_{obs}(A)(X^-) \quad . \qquad (6.3)$$

If only the one product, AX^-, is formed, the ion-molecule association mechanism given in the introduction applies and expression (1.8) for k_{obs} holds. Even if the primary product, AX^-, goes on to react or associate with another neutral specie, the above conditions are still true since we are only monitoring in the loss of the primary ion, X^- and k_{obs} is unaffected by subsequent reactions. However, if the ion undergoes several parallel reactions as shown below:

$$X^- + A \xrightarrow{k_{obs1}} AX^- \qquad (7.4)$$

$$X^- + B \xrightarrow{k_{obs2}} BX^- \qquad (7.5)$$

$$X^- + C \xrightarrow{k_{obs3}} CX^- \quad , \qquad (7.6)$$

then the equation modeling the loss of X^- becomes more complex as shown below in expression (7.7):

$$-\frac{d(X^-)}{dt} = k_{obs1}(A)(X^-) + k_{obs2}(B)(X^-) + k_{obs3}(C)(X^-). \quad (7.7)$$

Thus the overall rate coefficient $k_{overall}$, contains terms for each of the individual rate coefficients, and the expression for $k_{overall}$ becomes complex. If one is interested in knowing k_{obs1} for example, then k_{obs2} and k_{obs3} would have to be determined independently, all at the same temperature and pressure in order to quantify its temperature and pressure dependence from a measurement of $k_{overall}$. So, for an ion-molecule association reaction in which several parallel reactions are ocurring the overall rate coefficient , k_{obs}, is a composite of all steps, and information about a particular pathway cannot be obtained unless the individual rates of the other pathways are known.

Since the SF_4 systems have multiple products, before meanigful interpretation of data is possible one must first identify the products as primary or secondary. One method of determining if an ion-molecule association reaction with multiple products is proceeding via a set of sequential reactions or via a set of parallel reactions is to monitor the various product ions' signals to obtain a product plot. To construct the product plot, the amount of each product at each neutral flow is divided by the total sum of all the products. The points are then plotted on a graph of percent products vs. neutral flow. If there are two products and the second product is formed from a subsequent reaction of the first (or primary) product, then as the reaction proceeds the primary product ion decreases and

the secondary product ion increases. This is seen in figure (6.5). In this case the value of k_{obs} is not affected by subsequent reactions as discussed above. If two or more parallel reactions are occurring, the percent of each product remains constant throughout the entire reaction and parallel lines are produced in the graph of percent vs. neutral flow. The total percent of the products should of course add up to 100%. This behavior is seen in figure (6.6). So from an analysis of product plots it is possible under ideal conditions to determine whether products are the result of a secondary reaction of a primary product or the result of a series of parallel reactions. For the system $SF_4 + Cl^-$ such product plots were taken. Unfortunately because so many products were present and some unknown masses were detected, it was impossible to determine whether products other than SF_4Cl^- were secondary or primary products. Therefore, any quantitative analysis of this data to determine k_d and its temperature dependence is meaningless. It is important to note however, that the trends in temperature and pressure dependence observed are consistent with the previous association reactions discussed, and that ion-molecule association(s) is the major contributors to k_{obs}.

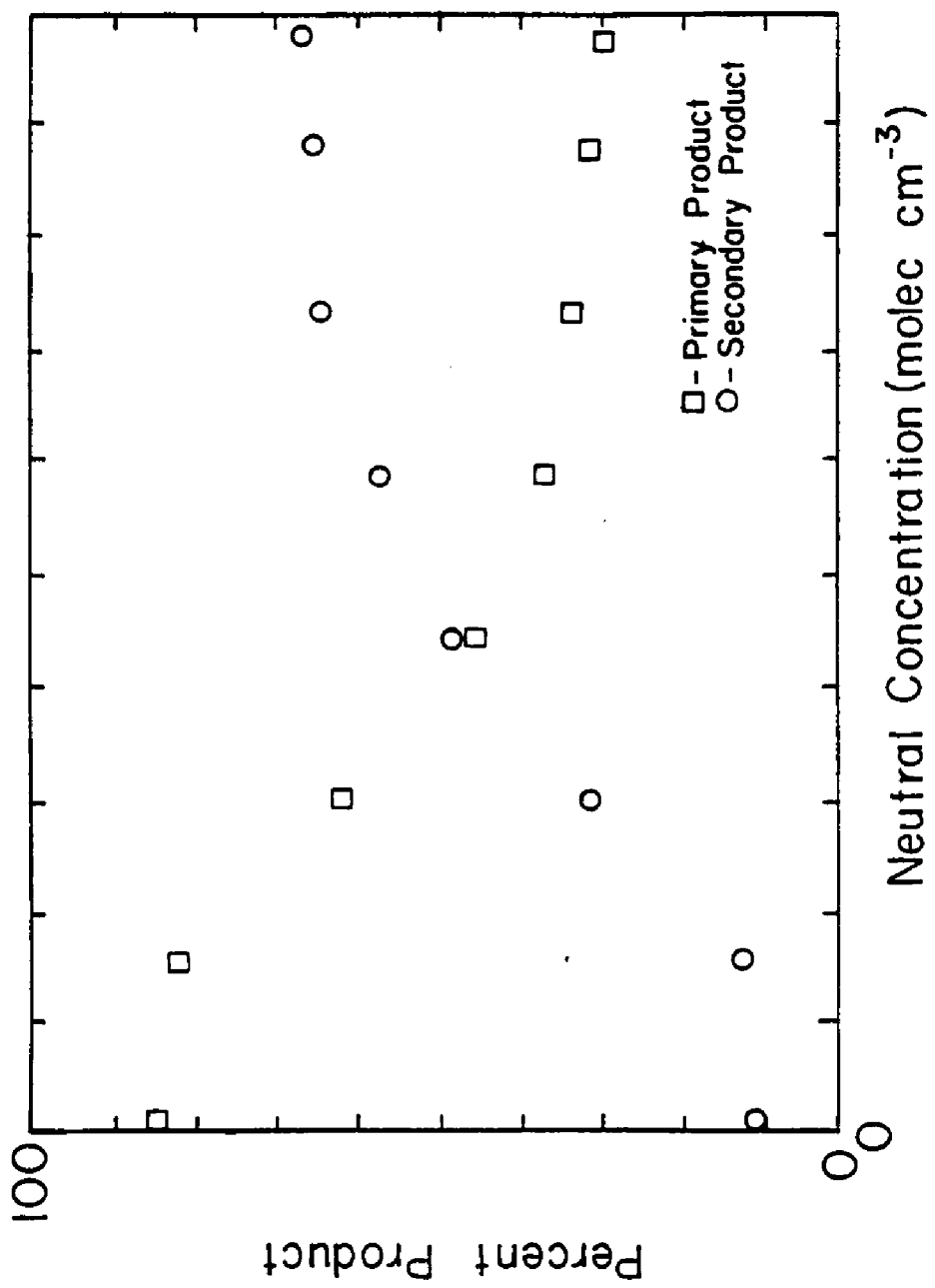

Figure 6.5. Product plot for sequential product formation.

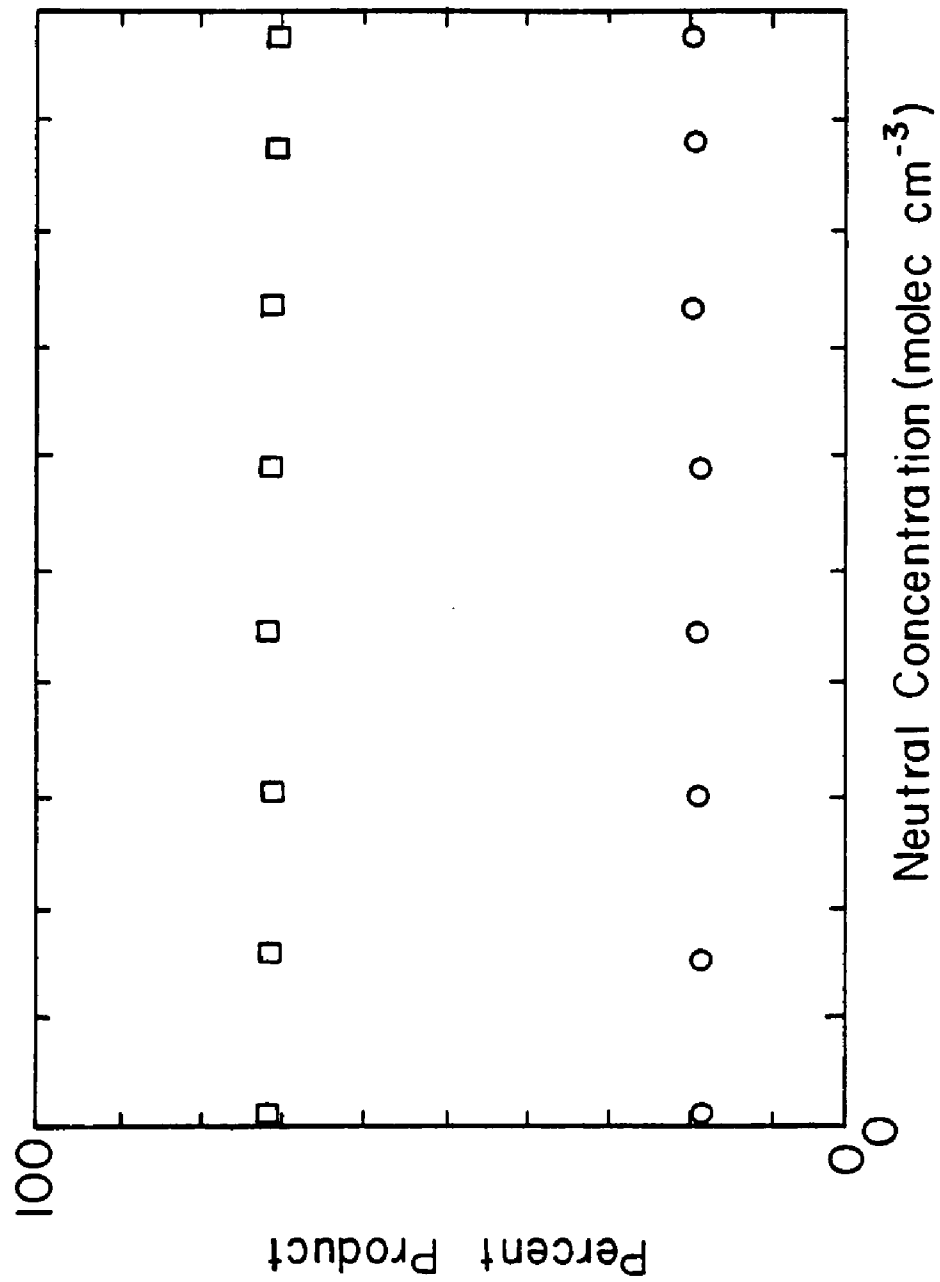

Figure 6.6. Product plot for parallel product formation.

IV. $SF_4 + Br^-$ Results and Discussion

This system was studied over the pressure range 0.3 to 0.8 torr and at three temperatures: 296, 248 and 220 K. Two products were observed at 296 K, four at 248 K, and five at 220 K. The values for k_{obs} ranged from a pressure independent rate of $\sim 8.0 \times 10^{-12}$ cm^3 at 296 K $molec^{-1}$ s^{-1}, to 3.2×10^{-11} cm^3 $molec^{-1}$ s^{-1} at 0.8 torr and 220 K. Note that on the whole, rate coefficients for this system are approximately an order of magnitude less than those for $SF_4 + Cl^-$. The overall rate coefficient displayed a pressure dependence at 248 and 220 K, and also displayed an inverse dependence upon temperature. The same problems encountered with the the $SF_4 + Cl^-$ system were encountered in this system in that several unidentifiable products were detected. Because product plots were ambiguous, again quantitative analysis of this data to determine k_d and its temperature dependence could not be done.

A tabulation of the products observed at each temperature is given below. As before, this system has been qualitatively studied at room temperature on a FA with a quadrupole having enough resolution to separate the chlorine and boron isotopes.[79] This of course aided in assigning masses to the observed products. For those products which could not be assigned a mass range is given. The relative abundance of each product is also given.

Temperature: 296 K

MASS (amu)	SPECIE	ABUNDANCE
188	SF_4Br^-	~40
208-219	Unassigned	~35

Temperature: 248 K

MASS (amu)	SPECIE	ABUNDANCE
99, 101	BrF^-	~140
127	SF_5^-	~45
188	SF_4Br^-	~110
195-223	Unassigned	~180

Temperature: 220 K

MASS (amu)	SPECIE	ABUNDANCE
99, 101	BrF^-	~135
127	SF_5^-	~265
131-152	Unassigned	~45
188	SF_4Br^-	~100
195-226	Unassigned	~115

CHAPTER 7

Conclusions and Future Work

I. Conclusions

In the study of halide ion addition to the selected group of Lewis acids chosen for study in this dissertation, we set out to accomplish three goals: (1) to study the temperature dependence of these systems since this area is one of much experimental and theoretical investigation, (2) to learn what properties of an ion-Lewis acid system must be present for radiative stabilization to occur, and (3) to learn more about the individual processes comprising the ion-molecule association mechanism to determine if a radiative stabilization pathway is present, and to allow us to determine such parameters as the unimolecular decay rate coefficient, k_d, and the radiative rate coefficient, k_r.

In order to achieve these goals a method of data analysis was developed. This method is valid within the given pressure and temperature ranges studied and is able to predict a value of k_{obs} at any value of pressure and temperature within that given range. The method is applicable both for cases where $k_r = 0$ and also where $k_r \neq 0$. Using this method, we can generate curves of k_{obs} as a function of pressure in the range 0.2 to 0.8 torr and of temperature in the range 200 - 400 K. From these curves values of $k_{obs}(P,T)$ not actually measured can be interpolated with confidence.

It was determined that the presence of a radiative stabilization pathway can be inferred from plots of k_{obs} vs. (M) which yield common non-zero intercepts for different third-bodies. This behavior was seen for the halide ion-boron trihalide systems in a previous study,[4] and the value of k_r and calculated values of k_{obs} at various (He) were determined from the method of data analysis implementing the temperature dependent data. For the halide ion-silicon tetrafluoride systems, more specifically $SiF_4 + Cl^-$ system, third-body studies using nitrogen and helium gave an intercept of zero for plots of k_{obs} vs. (M). This indicates that radiative stabilization is absent in this system. Calculation of k_{obs} at various (He) using the temperature dependent data for these systems with $k_r=0$ gave values consistent with the experimental data.

In summary, by use of third-body studies and application of the data analysis method to our temperature dependent data, we have set forth a method to determine whether or not radiative stabilization is present and ultimately predict the value of its rate coefficient.

The results of the data lead us to the conclusion that radiative stabilization is important in the boron trihalide systems and not present in the silicon tetrafluoride systems, while the sulfur tetrafluoride systems proved difficult to study and therefore any conlusions about k_r for these are tenuous.

The radiative stabilization in the boron trihalide

systems is unique in that radiative stabilization can compete with collisional stabilization even at the "high" pressures found in FA and SIFT experiments. The radiative transition may be an IR transition, but is more likely an electronic transition. We have suggested that perhaps intersystem crossing in which V-E transfer occurs is important in permitting radiative stabilization.

In addressing the first goal, the study of the temperature dependence, it was found that for the halide ion-boron trihalide systems, the magnitude of the temperature dependence of $k_d(T)$ ranged from 2.0 to 2.2 for the BF_3 systems, to 2.3 to 2.5 for the BCl_3 systems. For the halide ion-silicon tetrafluoride systems, n was found to be 3.2 while that for the SF_5^- system was 3.4. Note that the value of n increases in going from BF_3 to BCl_3 to SiF_4 and SF_4. All of the above values of n are above the value of 1.5 that would be predicted for all of these systems if only rotational contributions to the temperature dependence were considered. Using the thermal theory modified by Viggiano[56] to include vibrational modes, we found excellent agreement in the values of n determined from calculated $k_d(T)$ data and the values of n detemined from the theory. Not only was good agreement between $k_d(T)$ and theory found for each individual system but the trend in the increasing value of n from system to system is in agreement with theory also. For example, in going from BF_3 to BCl_3, n goes from an average value of 2.1 to an average value of

2.4. The lowest lying mode of BF_3 is a doubly degenerate one at 480 cm^{-1} and for BCl_3 the corresponding mode is at 243 cm^{-1}. It was shown earlier that probably not more than one vibrational mode for both of these systems participates. Because the frequency for BCl_3 is lower than that for BF_3, it contributes more to the vibrational partition function and hence to the overall temperature dependence expected. For SiF_4, n was shown to have an average value of 3.2. The lower lying frequencies of SiF_4 are 268 cm^{-1} (doubly degenerate) and 391 cm^{-1} (triply degenerate). It was found earlier that these two modes had to be active for theory to be consistent with the temperature dependence determined from $k_d(T)$. Note that here up to five contributions to the vibrational partition functions are possible and thus n should be larger than that for either BF_3 or BCl_3, as indeed it is. For the $SF_4 + F^-$ system there are four frequencies: 171, 226, 353, and 532 cm^{-1} which, if considered active, give a value of n consistent with the 3.4 obtained from $k_d(T)$. As compared to the BF_3 and BCl_3 systems, $SF_4 + F^-$ should have a larger temperature dependence because of the larger number of lower lying vibrations present. In comparison to SiF_4, the temperature dependence of SF_4 should be about the same since the SF_4 vibrations are in general lower in energy than those of SiF_4 but fewer vibrational modes are active.

In conclusion, the thermal theory which takes vibrational contributions into account accurately predicts the

experimentally determined temperature dependence for the halide ion-Lewis acid systems. Thus in general, it appears that vibrational contributions to the temperature dependence of ion-molecule systems are important for systems where the conditions $h\nu \simeq kT$ is true.

In addressing the second goal which was to learn what properties of an ion-Lewis acid system must be present for radiative stabilization to occur, definite conclusions cannot be made on the basis of this work. However, from the relatively small number of systems studied herein, it appears that systems with large well-depths and/or with limited molecular complexity are good possibilities. Recall that it was shown that D^{o} (i.e. the well-depth) for the $BF_3 + F^-$, $BCl_3 + Cl^-$, $BCl_3 + Br^-$ systems was on the order of 3 eV. On the other hand, D^{o}'s for the other systems that do not radiate are $\leq$ 1 eV. Also the placement of an upper electronic state for the boron trihalide systems may be important if V-E energy transfer is occurring, making these systems unique. In any event, further study of more systems is warranted.

The last goal, to learn more about the individual steps comprising the ion-molecule association mechanism, was successfully reached. The data analysis method allowed us to calculate k_d and k_r. The data analysis method also allowed us to isolate k_d and calculate $k_d(T)$ at the different temperatures and thus to determine its temperature dependence over our temperature range of 200 to 400 K.

In summary, success was achieved for all three goals which gave us: (1) insights into the temperature dependence of ion-molecule association reactions, (2) insights into the process and requirements for radiative stabilization in the boron trihalide systems and, in general, ion-molecule association reactions, and (3) valuable information about k_d and k_r and their respective lifetimes; and, for k_r, information about the type of radiative transition which might be occurring.

II. Future Work

Subsequent studies which would be interesting to perform with halide ion-Lewis acid systems include a number of different possibilities. First, using a variable temperature FA, third-body studies at different temperatures could be performed. This would confirm the radiative process through the occurrence of a common non-zero intercept at different temperatures for a variety of third-bodies, and also shed some light on the temperature dependence of the stabilization step. Other FA or SIFT studies which could be done are spectroscopic experiments designed to detect the photon resulting from radiative stavilization. Finally, theoretical calculations of k_d and k_r for comparison with experiment would be interesting.

References

(1) T. D. Märk and A. W. Castelman Jr. in "Advances in Atomic and Molecular Physics", D. Bates and B. Bederson, Ed., Academic Press: New York (1985).

(2) E. E. Ferguson, F. C. Fehsenfeld, and A. L. Schmeltekopf, in "Advances in Atomic and Molecular Physics", Academic Press: New York, (1969).

(3) N. G. Adams and D. Smith, Int. J. Mass Spectrom. Ion Phys., 21, 349 (1976).

(4) L. M. Babcock and G. E. Streit, J. Phys. Chem., 88, 5025 (1984).

(5) D. Bates in "Fundamental Processes in Atomic Collision Physics", H. Kleinpoppen, Ed., Plenum Press: New York, (1986).

(6) P. Langevin, Ann. Chim. Phys., 5, 245 (1905).

(7) G. Gioumousis and D. P. Stevenson, J. Chem. Phys., 29, 214 (1958).

(8) T. Su and M. T. Bowers in "Gas Phase Ion Chemistry", Vol. 1, M. T. Bowers, Ed., Academic Press, New York (1979).

(9) T. Su and M. T. Bowers, Int. J. Mass Spectrom. Ion Phys., 12, 347 (1973).

(10) T. Su and M. T. Bowers, Int. J. Mass Spectrom. Ion Phys., 17, 211 (1975).

(11) E. Rabinovitch, Trans. Faraday Soc., 33, 283 (1937).

(12) P. S. Gill, Y. Inel, and G. G. Meisels, J. Chem. Phys.,54, 2811 (1971).

(13) V. G. Anicich and M. T. Bowers, J. Am. Chem. Soc., 96, 1279 (1974).

(14) P. G. Miasek and A. G. Harrison, J. Am. Chem. Soc., 97, 714 (1975).

(15) E. Herbst, Chem. Phys., 68, 323 (1982).

(16) R. D. Cates and M. T. Bowers, J. Am. Chem. Soc., 102, 3994 (1979).

(17) L. M. Bass, P. R. Kemper, V. G. Anicich, and M. T. Bowers, J. Am. Chem. Soc., 103, 5283 (1981).

(18) J. M. Jasinski and J. I. Brauman, J. Chem. Phys., 73, 6191 (1980).

(19) D. R. Bates, J. Phys. B: Atom. Molec. Phys., 12, 4135 (1979).

(20) F. C. Fehsenfeld and E. E. Ferguson, J. Chem. Phys., 70, 1579 (1979).

(21) N. G. Adams and D. Smith, Chem Phys. Lett., 79, 563 (1981).

(22) N. G. Adams, D. Smith, D. G. Lister, A. B. Rakshit, and N. D. Twiddy, Chem Phys. Lett., 61, 608 (1979).

(23) P. J. Robinson and K. A. Holbrook, "Unimolecular Reactions", Wiley Interscience: New York (1972).

(24) W. M. Olmstead, M. Lev-On, D. M. Golden, J. I. Brauman, J. Am. Chem. Soc., 99, 992 (1977).

(25) L. Bass, W. J. Chesnavich, and M. T. Bowers, J. Am. Chem. Soc., 101, 5493 (1979).

(26) J. S. Chang and D. M. Golden, J. Am. Chem. Soc., 103, 496 (1981).

(27) E. Herbst, J. Chem. Phys., 75, 4413 (1981).

(28) P. A. M. van Koppen, M. F. Jarrold, M. T. Bowers, L. M. Bass, and K. R. Jennings, J. Chem. Phys., 81, 288 (1984).

(29) E. Herbst and W. Klemperer, Phys. Tod., June, 32 (1976).

(30) A. Dalgarno, Adv. At. Mol. Phys., 15, 37 (1979).

(31) D. R. Bates, Astrophys. J., 1121, 267 (1983).

(32) D. Smith and N. G. Adams, Int. Rev. Phys. Chem., 1, 271 (1981).

(33) E. Herbst, Astrophys. J., 205, 94 (1976) and references therein.

(34) R. L. Woodin and J. L. Beauchamp, Chem Phys., 41, 1 (1979).

(35) R. C. Dunbar, Spectrochim. Acta, 31A, 797 (1975).

(36) E. Herbst, Astrophys. J., 237, 462 (1982).

(37) E. Herbst, Astrophys. J., 291, 226 (1985).

(38) D. R. Bates, J. Chem Phys., 85, 2624 (1986).

(39) S. E. Barlow, G. H. Dunn, and M. Schauer, Phys. Rev. Lett., 52, 902 (1984).

(40) M. J. McEwan, V. G. Anicich, W. T. Huntress, P. R. Kemper, and M. T. Bowers, Chem Phys. Lett., 75, 278 (1980).

(41) D. K. Bohme, D. B. Dunkin, F. C. Fehsenfeld, and E. E. Ferguson, J. Chem. Phys., 49, 5201 (1968).

(42) P. V. Neilson, M. T. Bowers, M. Chau, W. R. Davidson, and D. H. Aue, J. Am. Chem. Soc., 100, 3649 (1978).

(43) H. Bohringer and F. Arnold, J. Chem. Phys., 77 5534 (1982).

(44) E. E Ferguson, F. C. Fesenfeld, and D. L. Albritton in "Gas Phase Ion Chemistry", Vol. 1, M. T Bowers, Ed., Academic Press: New York (1979).

(45) F. E. Niles and W. W. Robertson, J. Chem. Phys., 49, 3227 (1965).

(46) D. B. Dunkin, F. C. Fehsenfeld, A. L. Schmeltekopf, and E. E. Ferguson, J. Chem. Phys., 49, 1365 (1968).

(47) M. Meot-Ner in "Gas Phase Ion Chemistry", Vol. 1, M. T. Bowers, Ed., Academic Press: New York (1979).

(48) N. G. Adams and D. Smith in "Reactions Of Small Transient Species", A. Fontijn and M. A. A. Clyne, Ed., Academic Press: London (1983).

(49) K. R. Jennings, J. V. Headly, and R. S. Mason, Int. J. Mass Spectrom. Ion Phys., 45, 315 (1982).

(50) D. R. Bates, J. Chem Phys., 73, 1000 (1980).

(51) E. Herbst, J. Chem. Phys., 70, 2001 (1979).

(52) E. Herbst, J. Chem. Phys., 72, 5284 (1980).

(53) E. Herbst, J. Chem. Phys., 75, 4413 (1981).

(54) D. R. Bates, J. Chem. Phys., 81, 298 (1984).

(55) N. G. Adams and D. Smith, Chem. Phys. Lett., 79, 563 (1981).

(56) A. A. Viggiano, J. Chem. Phys., 84, 244 (1986).

(57) S. Lin, M. F. Jarrold, and M. T. Bowers, J. Phys. Chem., 89, 3127 (1985).

(58) E. Herbst, N. G. Adams, and D. Smith, Astrophys. J., 269, 329 (1983).

(59) R. Patrick and D. M. Golden, J. Chem. Phys., 82, 75 (1985).

(60) V. M. Bierbaum, C. H. DePuy, R. H. Shapiro, and J. H. Stewart, J. Am. Chem. Soc., 98, 4229 (1976).

(61) D. Smith and N. G. Adams in "Gas Phase Ion Chemistry", Vol. 1, M. T. Bowers, Ed., Academic Press: New York (1979).

(62) N. G. Adams and D. Smith, Int. J. Mass Spectrom. Ion Phys., 21, 349 (1976).

(63) T. M. Miller, R. E. Wetterskog, and J. F. Paulson, J. Chem Phys., 80, 4922 (1984).

(64) Tylan, Mass Flowmeter Instruction Manual, July 17, (1981).

(65) T. B. McMahon, private communication.

(66) J. C. Haartz, and D. H. McDaniel, J. Am. Chem. Soc., 95, 8562 (1973).

(67) J. H. Stockdale, D. R. Nelson, F. J. Davis, and R. N. Compton, J. Chem. Phys., 56, 3336 (1972).

(68) K. A. G. MacNeil, and J. C. J. Thynne, J. Phys. Chem. , 74, 2257 (1970).

(69) H. C. Brown, and R. R. Holmes, J. Am. Chem. Soc., 78, 2173 (1956).

(70) F. A. Cotton and J. R. Leto, J. Chem. Phys., 56, 3336 (1972).

(71) J. W. Moore and R. G. Pearson, "Kinetics and Mechanism", John Wiley and Sons: New York, (1981); pp. 127, 220, 222.

(72) J. E. Huheay, "Inorganic Chemistry", Second Edition, Harper and Row Publisher: New York (1978);p. 70.

(73) R. L. Woodin and J. L. Beauchamp, Chem. Phys., 41, 1 (1979).

(74) R. L. Woodin, M. S. Foster, and J. L. Beauchamp, J. Chem. Phys. 72, 4223 (1980)

(75) S. E. Barlow, G. H. Dunn, and M. Schauer, Phys. Rev. Lett., 52, 902 (1984).

(76) D. L. Albritton, "At. Nucl. Data Tables", 22, (1978).

(77) D. Smith, N. G. Adams, and E. Alge, Chem. Phys. Lett., 105, 317 (1984).

(78) L.M Babcock and P. S. Ruhr, unpublished results.

(79) L. M. Babcock, C. R. Herd, and W. S. Taylor, unpublished results.

(80) W. Braker and A. L. Morrison, " Matheson Gas Data Book", 6th ed., Matheson Gas Products (1980).

(81) W. C. Smith, Angew. Chem. Int. Ed., 1, 467 (1962).

(82) L. F. Drullinger and J. E. Griffiths, Spectrochim. Acta A, 27, 1973 (1971).

(83) L. M. Babcock and G. E. Streit, J. Chem. Phys., 75, 3864 (1981).

APPENDIXES

TABLE A1

A Compilation of k_{obs} vs. (He) for $BF_3 + F^-$

Temperature: 409 K

P, torr	(He)	k_{obs}, 10^{-11}
0.325	0.77	6.6
0.400	0.94	7.4
0.401	0.95	7.7
0.500	1.18	7.9
0.600	1.42	9.0
0.600	1.42	9.0
0.700	1.65	10.0
0.800	1.89	10.6
0.801	1.89	10.8

Temperature: 348 K

P, torr	(He)	k_{obs}, 10^{-10}
0.300	0.83	1.0
0.401	1.11	1.1
0.400	1.11	1.0
0.500	1.39	1.2
0.600	1.66	1.3
0.700	1.94	1.4
0.799	2.22	1.5
0.801	2.22	1.4

TABLE A1 continued,

Temperature: 298 K

P, torr	(He)	k_{obs}, 10^{-10}
0.300	0.97	1.4
0.351	1.14	1.4
0.405	1.31	1.4
0.405	1.31	1.4
0.509	1.65	1.5
0.510	1.65	1.6
0.601	1.95	1.7
0.601	1.95	1.7
0.701	2.27	1.8
0.826	2.68	1.9

Temperature: 248 K

P, torr	(He)	k_{obs}, 10^{-10}
0.300	1.17	2.2
0.300	1.17	2.1
0.400	1.56	2.2
0.400	1.56	2.2
0.500	1.95	2.3
0.600	2.33	2.8
0.700	2.72	2.9
0.800	3.11	3.0
0.801	3.11	3.0

TABLE A1 continued,

Temperature: 219 K

P, torr	(He)	k_{obs}, 10^{-10}
0.300	1.32	2.6
0.300	1.32	2.5
0.400	1.76	2.7
0.401	1.77	2.6
0.500	2.20	3.3
0.500	2.20	3.3
0.600	2.65	3.5
0.700	3.09	3.7
0.801	3.53	3.7
0.801	3.53	3.7

(He) units: 10^{16} molec cm^{-3}

k_{obs} units: cm^3 $molec^{-1}$ s^{-1}

TABLE A2

A Compilation of k_{obs} vs. (He) for

$BF_3 + Cl^-$

Temperature: 348 K

P, torr	(He)	k_{obs}, 10^{-12}
0.400	1.11	5.0
0.401	1.11	5.1
0.500	1.39	5.3
0.600	1.66	5.4
0.601	1.67	5.3
0.700	1.94	5.5
0.800	2.22	5.8
0.800	2.22	6.0
0.800	2.22	5.9

Temperature: 298 K

P, torr	(He)	k_{obs}, 10^{-12}
0.300	0.97	5.6
0.403	1.30	6.9
0.403	1.30	7.2
0.501	1.62	8.0
0.600	1.94	7.7
0.701	2.27	8.1
0.800	2.59	9.6
0.801	2.59	10.5

TABLE A2 continued,

Temperature: 248 K

P, torr	(He)	k_{obs}, 10^{-11}
0.299	1.16	0.9
0.300	1.17	0.9
0.407	1.58	1.0
0.500	1.95	1.3
0.600	2.33	1.4
0.701	2.73	1.5
0.800	3.11	1.6
0.800	3.11	1.7

Temperature: 219 K

P, torr	(He)	k_{obs}, 10^{-11}
0.200	0.88	1.0
0.300	1.32	1.3
0.300	1.32	1.3
0.403	1.78	1.6
0.500	2.20	1.9
0.500	2.20	1.8
0.600	2.64	1.9
0.700	3.08	2.1
0.801	3.53	2.2
0.801	3.53	2.3

(He) units: 10^{16} molec cm^{-3}

k_{obs} units: cm^3 $molec^{-1}$ s^{-1}

TABLE A3

A Compilation of k_{obs} vs. (He) for $BF_3 + Br^-$

Temperature: 219 K

P, torr	(He)	k_{obs}, 10^{-12}
0.300	1.32	4.9
0.400	1.76	6.0
0.400	1.76	5.5
0.500	2.20	5.8
0.600	2.65	5.9
0.700	3.09	5.9
0.800	3.53	6.8
0.802	3.54	6.7

(He) units: 10^{16} molec cm^{-3}

k_{obs} units: cm^3 $molec^{-1}$ s^{-1}

TABLE A4

A Compilation of k_{obs} vs. (He) for

$BCl_3 + Cl^-$

Temperature: 410 K

P, torr	(He)	k_{obs}, 10^{-11}
0.300	0.71	3.0
0.300	0.71	3.2
0.400	0.94	3.3
0.500	1.18	3.3
0.600	1.41	3.1
0.700	1.65	3.1
0.701	1.65	3.0
0.801	1.89	3.2
0.802	1.89	3.1

Temperature: 348 K

P, torr	(He)	k_{obs}, 10^{-11}
0.300	0.83	3.4
0.400	1.11	3.9
0.402	1.11	4.2
0.403	1.12	3.8
0.501	1.39	4.2
0.600	1.66	4.4
0.700	1.94	5.0
0.700	1.94	4.9
0.800	2.22	4.9

TABLE A4 continued,

Temperature: 298 K

P, torr	(He)	k_{obs}, 10^{-11}
0.250	0.81	5.1
0.402	1.30	6.2
0.402	1.30	6.6
0.400	1.29	6.0
0.550	1.78	7.0
0.702	2.27	7.4
0.851	2.76	7.9

Temperature: 248 K

P, torr	(He)	k_{obs}, 10^{-11}
0.210	0.82	7.7
0.210	0.82	8.2
0.300	1.17	9.1
0.400	1.56	9.7
0.400	1.56	10.3
0.500	1.95	10.3
0.550	2.14	10.8
0.600	2.33	11.6
0.700	2.72	13.0
0.800	3.11	13.6
0.800	3.11	14.0

TABLE A4 continued,

Temperature: 219 K

P, torr	(He)	k_{obs}, 10^{-10}
0.300	1.32	1.2
0.300	1.32	1.3
0.400	1.76	1.4
0.400	1.76	1.3
0.500	2.20	1.4
0.600	2.64	1.6
0.700	3.08	1.7
0.800	3.52	1.9
0.800	3.52	1.8

(He) units: 10^{16} molec cm^{-3}

k_{obs} units: cm^3 $molec^{-1}$ s^{-1}

TABLE A5

A Compilation of k_{obs} vs. (He) for

BCl_3 + Br-

Temperature: 410 K

P, torr	(He)	k_{obs}, 10^{-11}
0.300	0.71	2.2
0.400	0.94	2.3
0.400	0.94	2.3
0.500	1.18	2.2
0.600	1.41	2.1
0.700	1.65	2.0
0.801	1.89	2.2
0.802	1.89	2.2

Temperature: 348 K

P, torr	(He)	k_{obs}, 10^{-11}
0.300	0.83	3.0
0.301	0.83	2.8
0.400	1.11	3.1
0.402	1.11	3.1
0.500	1.39	3.2
0.600	1.66	3.2
0.600	1.66	3.3
0.704	1.95	3.5
0.800	2.22	4.0
0.800	2.22	3.9

TABLE A5 continued,

Temperature: 298 K

P, torr	(He)	k_{obs}, 10^{-11}
0.250	0.81	4.0
0.300	0.97	3.9
0.402	1.30	4.5
0.500	1.62	4.8
0.600	1.94	5.4
0.700	2.27	5.8
0.801	2.59	5.6
0.802	2.60	5.7

Temperature: 248 K

P, torr	(He)	k_{obs}, 10^{-10}
0.225	0.87	0.6
0.300	1.17	0.6
0.400	1.56	0.7
0.400	1.56	0.7
0.500	1.95	0.9
0.600	2.33	0.9
0.650	2.53	1.0
0.700	2.72	1.1
0.700	2.72	1.1
0.800	3.11	1.1
0.800	3.11	1.1

TABLE A5 continued,

Temperature: 219 K

P, torr	(He)	k_{obs}, 10^{-10}
0.300	1.32	0.8
0.400	1.76	1.1
0.400	1.76	1.1
0.500	2.20	1.2
0.600	2.64	1.2
0.600	2.64	1.2
0.700	3.08	1.3
0.800	3.53	1.4
0.800	3.53	1.4

(He) units: 10^{16} molec cm^{-3}

k_{obs} units: cm^3 $molec^{-1}$ s^{-1}

TABLE A6

A Compilation of k_{obs} vs. (He) for

$SiF_4 + F^-$

Temperature: 408 K

P, torr	(He)	k_{obs}, 10^{-10}
0.325	0.77	8.9
0.350	0.83	9.3
0.400	0.95	9.8
0.400	0.95	9.2
0.450	1.06	9.3
0.500	1.18	9.2
0.500	1.18	9.4
0.600	1.41	9.5
0.700	1.66	9.5
0.700	1.66	9.2
0.800	1.89	9.2
0.800	1.89	9.9

Temperature: 348 K

P, torr	(He)	k_{obs}, 10^{-9}
0.400	1.11	1.1
0.500	1.39	1.0
0.600	1.66	1.0
0.700	1.94	1.1
0.800	2.22	1.0
0.800	2.22	1.0

TABLE A6 continued,

Temperature: 298 K

P, torr	(He)	k_{obs}, 10^{-9}
0.301	0.97	1.1
0.405	1.31	1.1
0.405	1.31	1.1
0.506	1.64	1.1
0.650	2.11	1.2
0.806	2.61	1.1

Temperature: 248 K

P, torr	(He)	k_{obs}, 10^{-9}
0.400	1.56	1.3
0.550	2.14	1.5
0.700	2.73	1.3
0.700	2.73	1.7
0.800	3.12	1.3
0.800	3.12	1.3

Temperature: 219 K

P, torr	(He)	k_{obs}, 10^{-9}
0.400	1.76	1.3
0.400	1.76	1.6
0.500	2.21	1.6
0.700	3.09	1.5
0.800	3.53	1.5

(He) units: 10^{16} molec cm^{-3}

k_{obs} units: cm^3 $molec^{-1}$ s^{-1}

TABLE A7

A Compilation of k_{obs} vs. (He) for

$SiF_4 + Cl^-$

Temperature: 408 K

P, torr	(He)	k_{obs}, 10^{-11}
0.375	0.89	1.5
0.460	1.09	1.4
0.460	1.09	1.5
0.500	1.18	1.6
0.600	1.42	1.6
0.600	1.42	1.5
0.700	1.66	1.5
0.800	1.89	1.6
0.808	1.89	1.7

Temperature: 348 K

P, torr	(He)	k_{obs}, 10^{-11}
0.300	0.83	2.4
0.300	0.83	2.2
0.400	1.11	2.6
0.400	1.11	2.7
0.500	1.39	2.8
0.600	1.66	3.0
0.700	1.94	3.4
0.800	2.22	3.4
0.800	2.22	3.4

TABLE A7 continued,

Temperature: 298 K

P, torr	(He)	k_{obs}, 10^{-11}
[a] 0.304	0.99	2.8
[a] 0.401	1.30	4.1
[b] 0.501	1.62	3.5
[c] 0.550	1.78	5.0
[b] 0.601	1.95	5.7
[b] 0.650	2.11	6.6
[a] 0.700	2.27	5.8
[a] 0.800	2.59	7.0
[b] 0.900	2.92	8.3
[b] 1.000	3.24	8.7

[a] AFGL SIFT-LSU FA Average

[b] LSU FA only

[c] AFGL SIFT only

TABLE A7 continued,

Temperature: 248 K

P, torr	(He)	k_{obs}, 10^{-11}
0.225	0.88	6.6
0.300	1.16	7.6
0.400	1.56	8.5
0.400	1.56	8.2
0.500	1.95	9.7
0.600	2.34	10.4
0.600	2.34	10.9
0.700	2.73	11.6
0.800	3.12	12.3
0.800	3.12	12.8

Temperature: 219 K

P, torr	(He)	k_{obs}, 10^{-10}
0.200	0.88	1.0
0.300	1.32	1.2
0.300	1.32	1.2
0.400	1.76	1.2
0.400	1.76	1.4
0.500	2.21	1.7
0.600	2.65	1.9
0.700	3.09	2.1
0.800	3.53	2.1
0.800	3.53	2.4

(He) units: 10^{16} molec cm^{-3}

k_{obs} units: cm^3 $molec^{-1}$ s^{-1}

TABLE A8

A Compilation of k_{obs} vs. (He) for

$SiF_4 + Br^-$

Temperature: 248 K

P, torr	(He)	k_{obs}, 10^{-11}
0.400	1.56	0.8
0.400	1.56	1.0
0.500	1.95	0.8
0.500	1.95	1.0
0.600	2.34	1.0
0.700	2.73	1.1
0.800	3.12	1.1
0.800	3.12	1.0

Temperature: 219 K

P, torr	(He)	k_{obs}, 10^{-11}
0.300	1.32	1.0
0.300	1.32	1.0
0.400	1.76	1.3
0.500	2.20	1.5
0.500	2.20	1.6
0.600	2.65	1.5
0.700	3.09	1.8
0.800	3.53	1.8
0.800	3.53	1.8

(He) units: 10^{16} molec cm^{-3} k_{obs} units: cm^3 $molec^{-1}$ s^{-1}

TABLE A9

A Compilation of k_{obs} vs. (He) for

$SF_4 + F^-$

Temperature: 408 K

P, torr	(He)	k_{obs}, 10^{-10}
0.325	0.77	5.0
0.400	0.95	4.8
0.400	0.95	4.8
0.500	1.18	5.2
0.500	1.18	5.4
0.600	1.42	5.3
0.700	1.66	5.5
0.700	1.66	5.7
0.800	1.89	5.8
0.800	1.89	6.3

Temperature: 348 K

P, torr	(He)	k_{obs}, 10^{-10}
0.300	0.83	7.4
0.400	1.11	7.6
0.400	1.11	7.5
0.500	1.39	7.9
0.500	1.39	7.7
0.600	1.66	7.9
0.700	1.94	8.2
0.800	2.22	8.7
0.800	2.22	8.8

TABLE A9 continued,

Temperature: 298

P, torr	(He)	k_{obs}, 10^{-10}
0.300	0.97	8.1
0.300	0.97	8.1
0.301	0.97	9.0
0.300	0.97	8.9
0.325	1.05	8.7
0.350	1.13	8.7
0.400	1.29	8.4
0.400	1.29	8.9
0.400	1.29	9.0
0.453	1.47	8.9
0.500	1.62	9.0
0.650	2.10	8.8
0.700	2.27	9.1
0.801	2.59	9.1

Table A9 continued,

Temperature: 248

P, torr	(He)	k_{obs}, 10^{-9}
0.300	1.17	1.2
0.300	1.17	1.2
0.400	1.56	1.3
0.500	1.95	1.3
0.500	1.95	1.3
0.600	2.34	1.4
0.700	2.73	1.5
0.700	2.73	1.2
0.800	3.12	1.3
0.800	3.12	1.6

Temperature: 219 K

P, torr	(He)	k_{obs}, 10^{-9}
0.300	1.32	1.5
0.300	1.32	1.5
0.400	1.76	1.5
0.600	2.65	1.5
0.800	3.53	1.5
0.800	3.53	1.5

(He) units: 10^{16} molec cm^{-3}

k_{obs} units: cm^3 $molec^{-1}$ s^{-1}

Table A10

A Compilation of Polarizabilities* of Neutral Species Used in This Study

Neutral Specie	α , $\mathring{A}^3$
He	0.204956
Ar	1.6411
N_2	1.7403
CH_4	2.593
CO_2	2.911
CF_4	3.838
BF_3	3.31
BCl_3	9.47
SiF_4	5.45
SF_4	6.02

*T.M.Miller, "CRC Handbook of Chemistry and Physics"(1984).

Table A11

A Compilation of Langevin and ADO Rates for the Halide Ion-Lewis Acid Systems

Reacting System	k_L, cm^3 $molec^{-1}$ s^{-1}	
$BF_3 + F^-$	1.11×10^{-9}	
$BF_3 + Cl^-$	8.83×10^{-10}	
$BF_3 + Br^-$	7.04×10^{-10}	
$BCl_3 + Cl^-$	1.38×10^{-9}	
$BCl_3 + Br^-$	1.05×10^{-9}	
$SiF_4 + F^-$	1.36×10^{-9}	
$SiF_4 + Cl^-$	1.06×10^{-9}	
$SiF_4 + Br^-$	8.13×10^{-10}	
$SF_4 + F^-$	1.58×10^{-9}	(ADO)*
$SF_4 + Cl^-$	1.23×10^{-9}	(ADO)
$SF_4 + Br^-$	9.37×10^{-10}	(ADO)

*All ADO rate coefficients calculated at 298 K.

Table A12

A Compilation of Collision Rates for Excited Complex/Third-Body Couples

Couple	k_s, cm^3 $molec^{-1}$ s^{-1}
BF_4^-/He	5.42×10^{-10}
BF_4^-/N_2	6.71×10^{-10}
BF_4^-/CH_4	1.02×10^{-9}
BF_4^-/CF_4	6.94×10^{-10}
BF_3Cl^-/He	5.40×10^{-10}
BF_3Cl^-/N_2	6.58×10^{-10}
BF_3Cl^-/CO_2	7.19×10^{-10}
BF_3Cl^-/Ar	5.59×10^{-10}
BCl_4^-/He	5.37×10^{-10}
BCl_4^-/N_2	6.35×10^{-10}
BCl_4^-/CO_2	6.84×10^{-10}
SiF_5^-/He	5.38×10^{-10}
SiF_4Cl^-/He	5.37×10^{-10}
SiF_4Br^-/He	5.36×10^{-10}

VITA

Charles R. Herd was born January 13th, 1960 in Baton Rouge, Louisiana. He graduated from Captain Shreve High School in Shreveport, Louisiana in 1978 and received a B.S. in Chemistry from Lousiana State University of Shreveport in May, 1982. He began graduate school at Louisiana State University in the Fall of 1982. Future plans include postdoctoral research for two years and then the pursuit of a career in the field of Chemistry.

DOCTORAL EXAMINATION AND DISSERTATION REPORT

Candidate: Charles R. Herd

Major Field: Chemistry

Title of Dissertation: A Study of the Temperature Dependence of Ion-Molecule Association Reactions. Halide Ion Addition to a Selected Group of Lewis Acids.

Approved:

Major Professor and Chairman

Dean of the Graduate School

EXAMINING COMMITTEE:

Date of Examination:

May 1, 1987